FACULDADE DE ENGENHARIA DA UNIVERSIDADE DO PORTO

Sensorization Module for Diagnostic Instruments

Luisa Dias Martins

Mestrado em Engenharia Biomédica

Supervisor: Prof. Hélio Mendes de Sousa Mendonça

Co-Supervisor: Cláudia Daniela Costa Rocha

July 13, 2024

© Luisa Dias Martins, 2024

Abstract

The field of endoscopy has witnessed significant advances, with a focus on integrating sensor technology to improve diagnostic accuracy and patient safety. Given its impact, it is crucial to ensure safe real-time observation to diagnose and treat various conditions. This dissertation presents a comprehensive study on the development of a sensorization module for gastroendoscopic instruments, aimed at providing real-time data to healthcare professionals during procedures. The proposed system integrates orientation and pressure sensors embedded in a biocompatible coating attached to the endoscope tip, meeting the need for detailed information to improve diagnostic results and mitigate risks associated with insufficient data.

The research involved an extensive review of existing technologies, leading to the selection of suitable sensors with the aim of being integrated via a communication protocol. The study focused on the limitations of current endoscopic systems, particularly the lack of certain variables and, in turn, the challenge of achieving biocompatibility. To address these issues, the dissertation explores the potential of coating electronic components with biocompatible materials as an effective and economically viable solution. This approach aims to increase the safety and functionality of the endoscope without compromising its operational integrity. A detailed analysis of various commercial sensors and microcontrollers was carried out to determine their specifications and suitability for the proposed system. The research included the development of a sensing system that improves the diagnosis of gastroendoscopic examinations by providing additional variables, such as pressure and orientation data. The integration of these sensors offers a more comprehensive understanding of gastrointestinal conditions, allowing accurate visualization of the mucosa and the detection of lesions. The development of the system involved 3D modeling of the endoscope, selection of materials and the creation of a graphical interface for data visualization. Experimental validation of the prototype demonstrated its ability to provide critical diagnostic information in real time, supporting the potential for further advances in medical diagnostics through sensorized endoscopy.

In conclusion, this dissertation emphasizes the potential of integrating sensor technology into gastroendoscopic instruments to improve diagnostic accuracy and patient safety. The proposed sensing system offers a significant improvement over traditional endoscopes by providing real-time data on pressure and orientation. Future research should focus on refining the integration of these sensors, exploring wireless communication options and expanding the range of detectable variables to further support healthcare professionals in the diagnosis and treatment of gastrointestinal conditions. The results highlight the importance of continuous innovation in medical technology to achieve better outcomes for patients.

Resumo

A área da endoscopia tem testemunhado avanços significativos, com um foco na integração da tecnologia de sensores para melhorar a precisão diagnóstica e a segurança do paciente. Dada a sua importância, é crucial garantir a observação segura em tempo real para diagnosticar e tratar diversas condições. Esta dissertação apresenta um estudo abrangente sobre o desenvolvimento de um módulo de sensor para instrumentos gastroendoscópicos, com o objetivo de fornecer dados em tempo real aos profissionais de saúde durante os procedimentos. O sistema proposto integra sensores de orientação e pressão embutidos num revestimento biocompatível acoplado à extremidade do endoscópio, atendendo à necessidade de informações detalhadas para melhorar os resultados diagnósticos e mitigar os riscos associados a dados insuficientes. A pesquisa envolveu uma revisão extensa das tecnologias existentes, levando à seleção de sensores adequados com o objetivo de serem integrados através de um protocolo de comunicação. O estudo focou-se nas limitações dos sistemas endoscópicos atuais, particularmente a falta de determinadas variáveis e, por sua vez, o desafio de alcançar a biocompatibilidade. Para resolver essas questões, a dissertação explora o potencial de revestir componentes eletrónicos com materiais biocompatíveis como uma solução eficaz e economicamente viável. Esta abordagem visa aumentar a segurança e funcionalidade do endoscópio sem comprometer a sua integridade operacional. Foi realizada uma análise detalhada de vários sensores comerciais e microcontroladores para determinar as suas especificações e adequação ao sistema proposto. A pesquisa incluiu o desenvolvimento de um sistema de sensores que melhora o diagnóstico de exames gastroendoscópicos ao fornecer variáveis adicionais, como dados de pressão e orientação. A integração destes sensores oferece uma compreensão mais abrangente das condições gastrointestinais, permitindo uma visualização precisa da mucosa e a deteção de lesões. O desenvolvimento do sistema envolveu a modelação em 3D do endoscópio, a seleção de materiais e a criação de uma interface gráfica para visualização de dados. A validação experimental do protótipo demonstrou a sua capacidade de fornecer informações diagnósticas críticas em tempo real, apoiando o potencial de novos avanços nos diagnósticos médicos através da endoscopia sensorizada.

Em conclusão, esta dissertação enfatiza o potencial da integração da tecnologia de sensores em instrumentos gastroendoscópicos para melhorar a precisão diagnóstica e a segurança do paciente. O sistema de sensores proposto oferece uma melhoria significativa em relação aos endoscópios tradicionais, fornecendo dados em tempo real sobre pressão e orientação. Pesquisas futuras devem focar-se no aperfeiçoamento da integração destes sensores, explorando opções de comunicação sem fios e expandindo a gama de variáveis detetáveis para apoiar ainda mais os profissionais de saúde no diagnóstico e tratamento de condições gastrointestinais. Os resultados destacam a importância da inovação contínua na tecnologia médica para alcançar melhores resultados para os pacientes.

Acknowledgments

This effort and dedication are dedicated to my family, who have shown me what true unity means. To my mother, who has taught me and continues to teach me what it means to have willpower and never give up. She has shown me how to put difficulties into perspective and enjoy the little things that we often take for granted. To my father, who has always demonstrated what it means to be a Superwoman, teaching me the values of integrity and respect, and making me feel that I can achieve anything I set my mind to with discipline and responsibility. To the rest of my family, who have shown me from a young age what joy is and how we can use it as a refuge during the most challenging times. To my friends, for their companionship. In particular, to my friend Alice Araújo, who dedicated some of her time and resources to help develop the 3D printing of the prototype.

To my co-supervisor, Cláudia Rocha, for welcoming me so naturally, making this journey a bit easier with her kindness and constant availability, and for never letting me falter. And finally, to my supervisor, Professor Hélio Mendonça, who helped me from start to finish in navigating this complex phase, guiding me and advocating for my interests. A special thanks for your concern and care, which went beyond what we might consider the usual "duties of a supervisor/co-supervisor."

Luisa Martins

"The task is not so much to see what no one has seen, but to think what no one has yet thought about what everyone sees."

Arthur Schopenhauer

Contents

1 Introduction **1**
- 1.1 Context . . . 1
- 1.2 Motivation . . . 2
- 1.3 Objectives . . . 5
- 1.4 Document Planning . . . 5
- 1.5 Document Outline . . . 6

2 Background on Endoscopy **7**
- 2.1 Gastrointestinal Tract Anatomy . . . 7
- 2.2 Endoscope . . . 8
- 2.3 Endoscope Structure . . . 8
- 2.4 Endoscopy Procedure . . . 11
- 2.5 New Endoscopic Techniques . . . 12
- 2.6 Capsule Endoscopy . . . 14
- 2.7 Conclusions . . . 15

3 State-of-the-art on Hardware for endoscopy **17**
- 3.1 Integrated Circuits . . . 17
  - 3.1.1 Fundamentals . . . 17
  - 3.1.2 Communication Protocols . . . 18
  - 3.1.3 Microcontrollers . . . 20
  - 3.1.4 PCBs development . . . 21
- 3.2 Sensing Systems . . . 22
  - 3.2.1 Pressure and Temperature Sensor . . . 22
  - 3.2.2 Proximity Sensor . . . 25
  - 3.2.3 Distance Sensor . . . 26
  - 3.2.4 Orientation Correction Sensor . . . 28
  - 3.2.5 PH Sensor . . . 31
  - 3.2.6 Other Sensors . . . 33
- 3.3 Conclusions . . . 37

4 Methodology **39**
- 4.1 System architecture . . . 39
- 4.2 Sensors . . . 40
- 4.3 Microcontrollers . . . 43
- 4.4 PCB development . . . 44
- 4.5 3D Modelling . . . 45
- 4.6 Graphical interface . . . 46

4.7 Conclusions 47

5 System implementation **49**
5.1 Prototype Implementation 49
5.2 3D Modelling 54
5.3 Software 56
5.3.1 Firmware 57
5.3.2 Graphical interface 58
5.4 Conclusions 61

6 Experimental Results **63**
6.1 ADXl345 Sensor Results 63
6.2 BME280 Sensor Results 67
6.3 Results Discussion 71

7 Conclusion and future Work **73**
7.1 Conclusions 73
7.2 Future Work 74

References **77**

List of Figures

1.1 Timeline of the history of endoscopy. . . . 3
1.2 In 2018, the rate of gastrointestinal cancers was examined in relation to the global number of cancer cases. . . . 4
1.3 Number of new cancer cases in Portugal in 2020, both sexes, all ages. . . . 4
1.4 Gantt Chart. . . . 6

2.1 Gastrointestinal tract: (a) upper and (b) lower tracts. . . . 8
2.2 Endoscope Structure: (a) connector section; (b) control section; (c) insertion section; (d) tip section. . . . 9
2.3 Conector Section. . . . 9
2.4 Control Section. . . . 10
2.5 Insertion Section. . . . 11
2.6 Tip Section. . . . 11
2.7 Endoscopy Procedure. . . . 12
2.8 Capsule endoscopy. . . . 15

3.1 UART Protocol. . . . 18
3.2 I2C Protocol. . . . 19
3.3 SPI Protocol. . . . 19
3.4 Microcontroller system. . . . 21
3.5 Printed circuit board. . . . 21
3.6 Pressure sensor embedded in a endoscopic hood. . . . 23
3.7 Fully wireless pressure sensor. . . . 24
3.8 Motility pressure sensor. . . . 24
3.9 Proximity sensor for an endoscope to determine axial and radial distance. . . . 26
3.10 Actively shielded capacitive proximity sensor. . . . 26
3.11 Fiber-based distance sensor. . . . 27
3.12 Fiber-Optic distance sensor. . . . 28
3.13 Endoscopic orientation. . . . 29
3.14 Block diagram of rotation correction. . . . 29
3.15 Axes for accelerometer and axes for gyrosensor, respectively. . . . 30
3.16 Diagram of the image orientation correction system. . . . 30
3.17 Ingestible pH sensing system. . . . 31
3.18 Iridium oxide-based capsule system. . . . 32
3.19 Prototype assembling: (a) Frontal setup; (b) Lateral setup. . . . 35

4.1 Architecture diagram. . . . 39
4.2 PCB A to PCB B connection diagram. . . . 45
4.3 3D modelling of the endoscope. . . . 45

4.4 Mockup interface prototype. 47

5.1 Breadboard: (a) ESP32 microcontroller; (b) BME280 sensor; (c) ADXL345 sensor. 50
5.2 PCB A. 52
5.3 PCB B. 53
5.4 New 3D prototype of the endoscope. 54
5.5 Cover attached to the tip of the endoscope. 54
5.6 Cover with PCB attached. 55
5.7 Cover with fixed PCB coated with biocompatible film. 56
5.8 3D printing of the endoscope prototype. 56
5.9 Micropython Editor. 58
5.10 Interface developed in python. 59
5.11 Roll and Pitch angle demonstration. 60

6.1 Setup for vertical measurements. 64
6.2 Graph showing acceleration in X and Y coordinates at different inclinations. . . . 66
6.3 Comercial Sensors. 68
6.4 Temperature measurements graph. 69
6.5 Humidity measurements graph. 71

List of Tables

2.1 Overview of advanced endoscopic imaging techniques. 14

3.1 Comparison of UART, I2C and SPI protocols. 20
3.2 Overview of sensors applied in endoscopy. 36

4.1 Potential sensors for system integration. 42
4.2 Potential microcontrollers for system integration. 43

6.1 Table with acceleration values for different slopes. 65
6.2 Table of temperature values collected from the sensors (ºC). 69
6.3 Table of humidity values collected from the sensors (%). 70

Abbreviations

ADC	Analog-to-Digital Converter
CAN	Controller Area Network
CCD	Charge-coupled device
CE	Chromoendoscopy
CLE	Confocal laser endomicroscopy
CPU	Central processing unit
DALYs	Disability-Adjusted Life Years
FICE	Flexible spectral imaging color enhancement
FMCW	Frequency Modulated Continuous Wave
GI	Gastrointestinal
I2C	Inter-Integrated Circuit
ICs	Integrated circuits
IMU	Inertial Measurement Unit
LIN	Local Interconnect Network
MCU	Microcontroller Unit
MEMS	Micro-electromechanical systems
MISO	Master In Slave Out
MOSI	Master Out Slave In
NBI	Narrow-band imaging
PCB	Printed Circuit Board
SCK	Serial Clock
SPI	Serial Peripheral Interface
SS	Slave Select
UART	Universal asynchronous receiver/transmitter
USB	Universal Serial Bus
VCSEL	Vertical Cavity Surface Emitting Laser

Chapter 1

Introduction

The aim of this chapter is to present the work developed in this dissertation. This chapter is organized into four distinct sections. Section 1.1 provides a contextualization of the thesis topic, emphasizing its application in current scenarios. Following this, Section 1.2 presents the definition of the problem and the associated difficulties that led to the thesis. Section 1.3 details the objectives set for the dissertation. In Section 1.4, the Gantt chart is introduced as a crucial tool for planning, scheduling, and monitoring the progress of activities over time. Lastly, Section 1.5 provides a brief overview of the structure adopted in this work.

1.1 Context

For centuries, physicians have attempted to investigate the cavities of the human body and their contents to advance their knowledge of diseases. The ability to examine less visible areas of the body has been increasing since the 1970s. However, technological advances have accelerated in recent years, transforming image quality and allowing endoscopes to reach previously inaccessible organs. As a result, endoscopy has become a powerful and frequent diagnostic tool and is the only modern imaging technique that allows direct observation of the inside of an organ in a minimally invasive way [1][2].

Endoscopies are divided into categories based on the area of the body to be examined. The American Cancer Society (ACS) provides a brief overview of the most common types of endoscopy and what they are used for. A colonoscopy (lower endoscopy) is mainly performed to examine the inside of the large intestine, which includes the colon, rectum and anus. The procedure can detect polyps and cancers at different stages. In addition, upper endoscopy allows examination of the inner lining of the esophagus, stomach and duodenum. Bronchoscopy is a diagnostic test that examines the trachea, bronchi and part of the lungs, allowing the doctor to look directly at the airways. Another type of endoscopy that is widely used is cystoscopy, where the scope is passed through your urethra to look at it and your bladder. Other types of endoscopy include laparoscopy (abdominal or pelvic), arthroscopy (joints), hysteroscopy (inside the uterus), among others [3] [4].

Through this diverse set of evidence, it has become clear that endoscopy is an incredibly versatile and valuable tool in the field of medicine. The case study of this dissertation focuses on gastrointestinal endoscopy. Gastrointestinal endoscopy is a diagnostic and therapeutic procedure that allows one to image, assess, and treat GI illnesses. Gastrointestinal endoscopy can be categorized as upper or lower endoscopy depending on whether the upper GI tract (esophagus, stomach, duodenum, jejunum) or lower GI tract (rectum, colon, and terminal ileum) is examined [5]. In this procedure, instruments such as an endoscope are used to obtain an examination of the digestive tract and to provide doctors with a detailed view of the areas being examined. In addition, the fact that it is minimally invasive offers patients the hope of a faster and less painful recovery [6].

The development of flexible endoscopy has completely transformed routine clinical practice as well as research in gastroenterology [7]. However, as shown in the Figure 1.1, endoscopy has had to go through an evolutionary process involving three major eras to reach its current state. The first era involved the illumination of cavities through the reflection of natural light or the use of a dark chamber, which is known as the era of the natural light source. Over the years, discoveries were made leading to the era of the reflected or distal artificial light source. This period went through several phases of development. The first phase consisted of an open tube system, advancing to the instrumentation phase of rigid telescopes. This was followed by the appearance of semi-flexible instruments and finally, due to the difficulty of navigating the endoscope through anatomical curves, a last phase emerged: flexible instruments, which are still used today. This progress led to the emergence of the era of the external artificial light source [1]. Taking flexible endoscopy as a starting point, the most important advance was probably the invention of the charge coupling device (CCD). This endoscope does not require a coherent fiber bundle to transmit light from the tip to the end of an endoscope. Instead, the CCD sensor at the tip directly converts the optical image into digital signals that can be transmitted through the endoscope shaft to the processing and display devices on the outside [6]. The continuous enhancement of accessory technologies and endoscopes also allows for the rapid growth in the number and complexity of endoscopic procedures, which results in a new era of modern diagnostics and the emergence of endoscopy for therapeutic purposes [1].

Due to this technological advancement, endoscopy has now been employed to explore nearly the entire accessible human anatomy, allowing for the observation of various conditions. Furthermore, many diseases can be treated through endoscopy, utilizing specialized instruments and high-definition imaging. The widely recognized advantages of smaller or nonexistent scars, reduced morbidity (screening and early detection of possible indications), and faster recovery, compared to open methods in procedural medicine and surgery, have led to endoscopy completely or partially supplanting the role of open methods in numerous areas [6].

1.2 Motivation

Endoscopy is a crucial practice in global health, as more than 250 million endoscopies are performed worldwide every year. In 2021, the worldwide market for endoscopy devices reached a

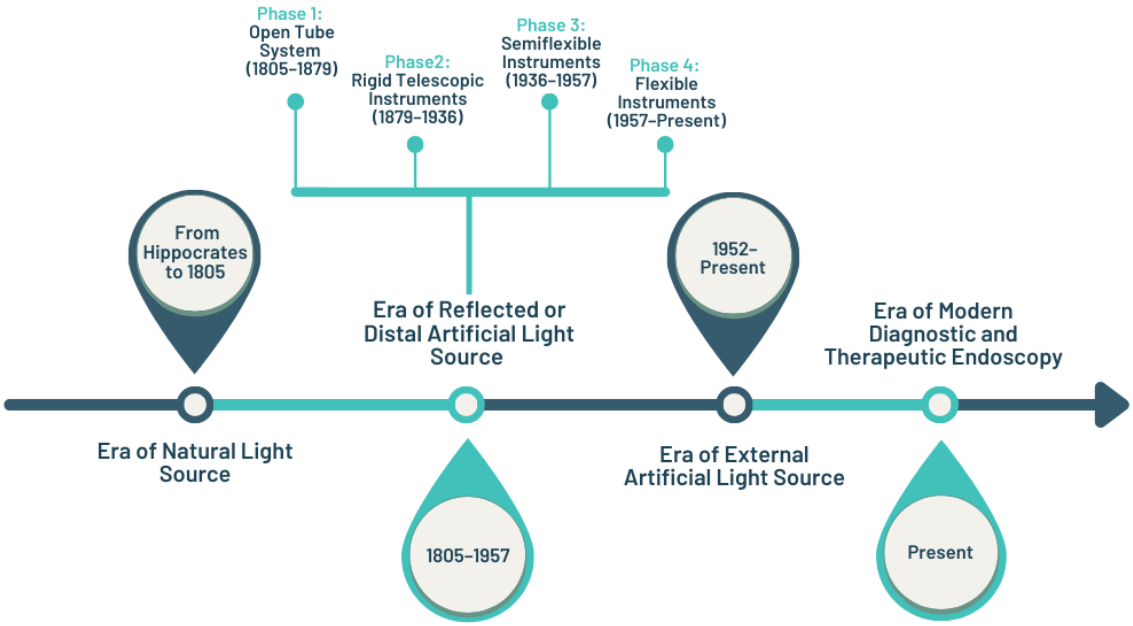

Figure 1.1: Timeline of the history of endoscopy adapted from Lau *et al.* [1].

value of 30.3 billion dollars and is anticipated to grow to 56.2 billion dollars by 2030, according to forecasts [8]. This rapid expansion is attributed to several factors, including the increased occurrence of cancer, a growing elderly population, and the advantageous position of endoscopy device manufacturers [8]. Gastrointestinal diseases seriously affect human health. As the elderly are more exposed to chronic and acute illnesses, the senior population is more likely to use endoscopy procedures. According to the Administration of Community Living (ACL), the number of people aged 65 and over in the United States was 54.1 million in 2019 and is expected to grow to around 94.7 million in 2060 [8]. Digestive diseases accounted for 2276 million estimated prevalent cases, 2.56 million deaths, and 88.99 million DALYs (Disability-Adjusted Life Years) globally in 2019 [9]. In addition, there is a growing global incidence of gastrointestinal tumors, which are characterized by high morbidity and mortality. Gastrointestinal cancers (GI) are responsible for 1 in 4 cancer cases and 1 in 3 cancer deaths. In 2018, there were an estimated 4.8 million new cases of gastrointestinal cancers and 3.4 million related deaths worldwide, as shown in the Figure 1.2 [10]. Regarding Portugal, GLOBOCAN recorded a total of almost fifteen thousand new cases of colorectum and stomach cancer as can be observed in the Figure 1.3 [11]. Therefore, considering all these data, it is evident that gastrointestinal cancers pose a significant challenge to public health. Prevention and diagnostic measures remain the most important tools to control this group of malignancies.

With the increasing incidence of chronic diseases, it is expected that endoscopic technology will follow this development. As a result, endoscopy has an important role to play in the prevention, diagnosis, and treatment of a variety of diseases, particularly those that affect the gastrointestinal tract [12]. Early diagnosis significantly increases survival rates, offering patients better prospects for treatment [13].

In an effort to prevent all the risks and complications associated with endoscopic diagnosis in the detection of gastrointestinal diseases, the development of new technologies represents a crucial advance in medicine, providing a powerful guarantee for the accurate diagnosis of gastrointestinal diseases [14]. These innovations not only improve diagnostic accuracy but also lead to safer, less invasive and more efficient procedures [14]. The addition of a sensing module at the tip of an endoscope, thus creating sensory endoscopy, is one of the recent technologies that offers several significant advantages for medical practice, and will be discussed in more detail in chapter 3 of the study. There is therefore a need to understand which sensor is most suitable and accurate for analysis during an endoscopy diagnosis. With this in mind, this dissertation aims to develop a system architecture that incorporates a sensing module to provide the healthcare professional with data during an endoscopy diagnosis.

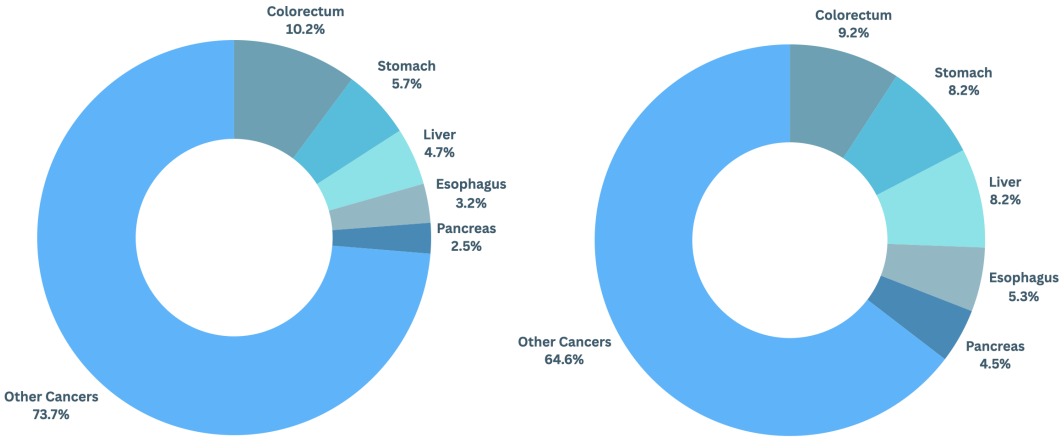

Figure 1.2: In 2018, the rate of gastrointestinal cancers was examined in relation to the global number of cancer cases, with a focus on both the incidence (a) and mortality (b), adapted from Arnold *et al.* [10].

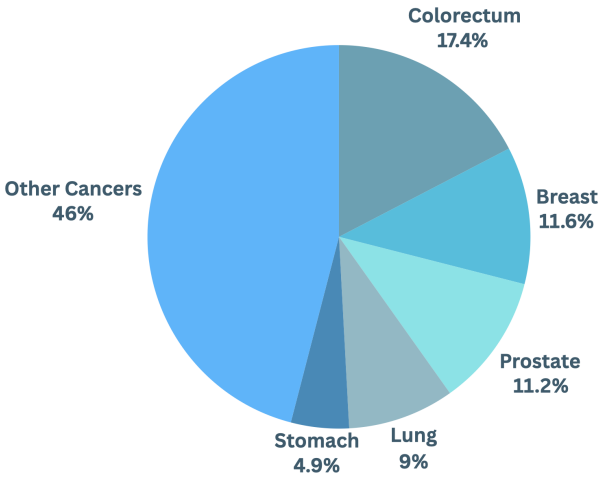

Figure 1.3: Number of new cancer cases in Portugal in 2020, both sexes, all ages adapted from GLOBOCAN [11].

1.3 Objectives

Considering the context and motivation described in the previous sections, the main objective of this dissertation is to explore, study, and develop a sensing module applicable to the diagnostic instrument, focusing on adding tools to extend the functionalities to minimally invasive diagnostics. To achieve this main goal, the objectives of this dissertation can be summarised in the following items:

- Research, selection, and acquisition of sensors;
- Biocompatibility study of materials;
- Development of a sensing system to improve the diagnosis of the examination performed;
- Development and 3D modeling of a device for coupling the sensing module to the endoscope tip;
- Development of an application that enables visualization of the data collected during the examination using the developed sensor.

1.4 Document Planning

The Gantt chart illustrated in Figure 1.4 provides a clear and organized visual tool for tracking the various stages of the project. Firstly, the Introduction phase stands out, covering the initial research carried out to establish the context, motivation, objectives, and outline of the document. This is followed by the Background to Endoscopy phase, which highlights the time spent studying the fundamentals of the dissertation, such as the anatomy of the GI tract, the concept of an endoscope and its structure, the procedures involved, new techniques related to image enhancement and capsule endoscopy technology. The state of the art in endoscopy hardware is a phase that begins with the study of integrated circuits, accompanied by a literature review that includes an analysis of existing technologies and relevant studies. This is followed by the development phase, which is considered to be the longest in the process and includes the overall system architecture, microcontroller programming, printed circuit board development, 3D modeling of a coupling device, and application development. After this phase, there is a significant period of integration and testing to assess the system's viability. Finally, the Conclusion phase will conclude the project. The document writing accompanies the entire process from the introduction to the conclusion.

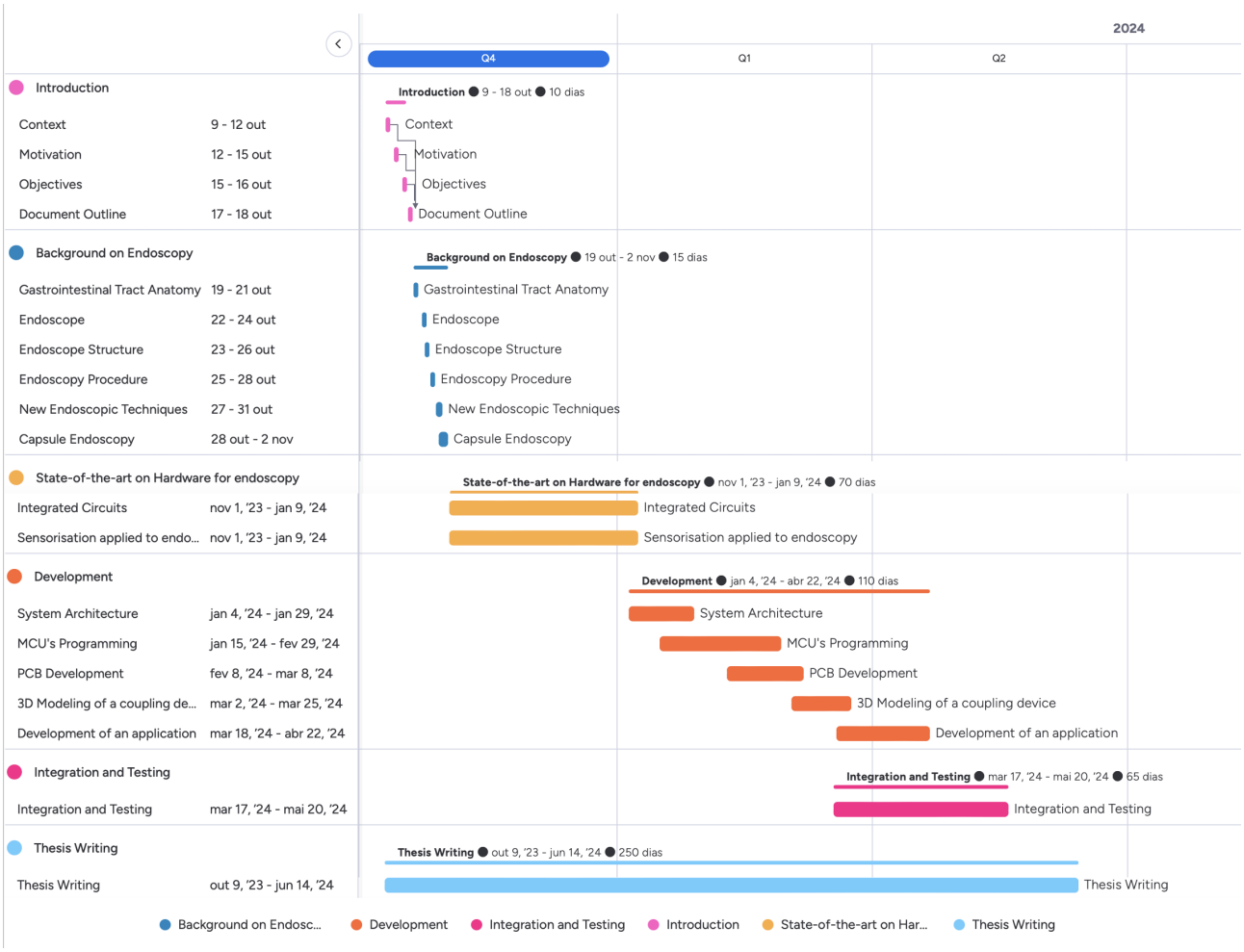

Figure 1.4: Gantt Chart. Q stands for Quarter.

1.5 Document Outline

Besides the Introduction, the remainder of this document is structured as follows: Chapter 2 presents the background theory necessary to understand the following chapters. In this chapter, the concept of the endoscope is introduced, as well as its structure and composition. It also reviews the new endoscopy techniques currently available and discusses the concept of the endoscopic capsule. Chapter 3 begins with an overview of integrated circuits, communication protocols, and microcontrollers. It then provides a state-of-the-art review of the strategies used, with special emphasis on the main types of sensors that can be used in conjunction with the endoscope. It presents an overview of the different techniques and approaches that have been investigated. Some of them have already been tested and are expected to be improved in the future. Additionally, common characteristics of the tools studied are highlighted. Finally, concepts considered of interest in the context of this thesis are listed. The following is Chapter 4, which describes the methodology used, as well as the components and data employed in this project.

Chapter 2

Background on Endoscopy

This chapter aims to provide the reader with a comprehensive explanation and description of the theoretical background needed throughout this document. With this aim in mind, this chapter is divided into seven sections. Section 2.1 offers a brief introduction to the fundamental concepts of gastrointestinal tract anatomy. Section 2.2 introduces the concept of the Endoscope diagnostic instrument. Subsequently, Section 2.3 explores the structure and composition of the flexible endoscope. Section 2.4 then explains the entire procedure behind the endoscopic diagnosis. In addition, Section 2.5 explores the new endoscopic techniques currently on the market, based on image processing to achieve better resolution, and finally, Section 2.6 gives a brief introduction to the topic of capsule endoscopy, which will serve as the basis for a clearer interpretation of Chapter 3. Finally, Section 2.7 presents some brief conclusions on some of the topics covered throughout Chapter 2.

2.1 Gastrointestinal Tract Anatomy

The human GI tract, as illustrated in Figure 2.1, comprises a variety of organs and can be categorized into two main sections: the upper and lower gastrointestinal tract. The upper gastrointestinal tract includes the mouth, esophagus, stomach, duodenum, jejunum, and ileum, while the lower tract is made up of the colon, rectum, and anus. [15]. The GI tract's primary function is to carry out the complex processes of digestion of ingested nutrients. This involves the secretion of enzymes and the absorption of essential nutrients. To perform these processes smoothly and safely, the gastrointestinal tract has a complex multilayered structure, including the inner mucosal layer, sub-mucosal layer, smooth muscle layer and outer serosal layer. This digestion is facilitated by the movement of luminal contents along the gastrointestinal tract, driven by the peristaltic motion of smooth muscles [15].

Given that the digestive system is primarily responsible for obtaining the necessary nutrients for the body through the ingested food, it is recognized that the health and well-being of the digestive system are essential for a good quality of life and survival [15].

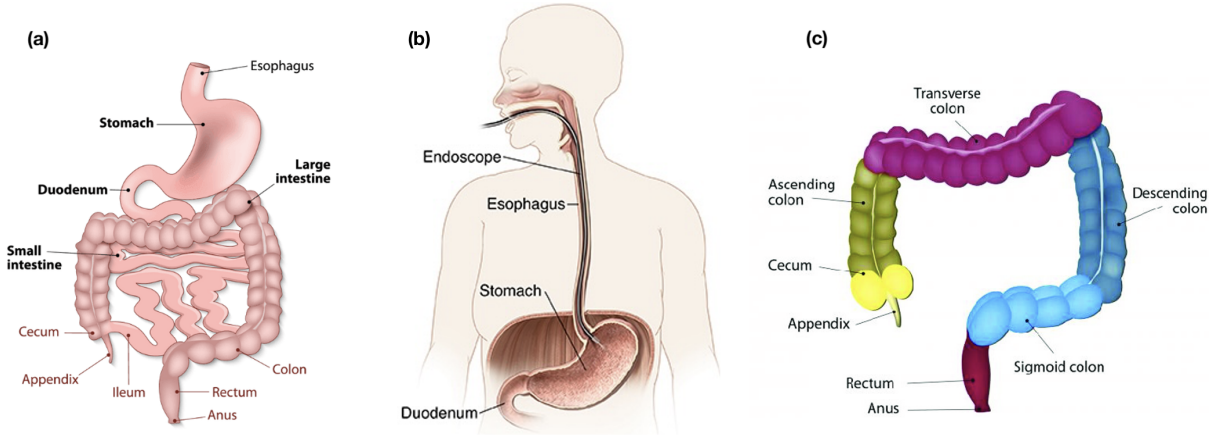

Figure 2.1: Gastrointestinal tract [16]: (a) upper [17] and (b) lower tracts [18].

2.2 Endoscope

Flexible endoscopes are a remarkable innovation in modern medicine, which allows doctors to visualize the inside of inaccessible areas with greater precision. These instruments have become an indispensable tool in diagnosing and treating many gastrointestinal (GI) tract diseases, thanks to their diverse range of applications. Endoscopes enable doctors to assess the GI mucosa, visualize and remove polyps, take tissue samples from extra-luminal organs, and screen for pre-malignant conditions [19].

With the development of new endoscopes, it is now possible to provide high-definition, high-resolution images that can be magnified to selectively highlight vascular structures or enhance the appearance of the mucosa. This has significantly improved the accuracy of diagnoses and the effectiveness of treatments [19].

The use of endoscopes plays a crucial role in carrying out less invasive diagnostic and therapeutic procedures. This not only reduces the discomfort and pain experienced by patients but also significantly improves their quality of life [7].

2.3 Endoscope Structure

Flexible endoscopes are complex medical devices that must function optimally under all circumstances to ensure accurate diagnoses and safe procedures. To achieve this, the user must possess a in-depth understanding of the instrument's structure and operation. Although the basic composition and structure of an endoscope can vary depending on the area being examined, most endoscopes are made up of essential components that are quite similar [20].

The endoscope shown in Figure 2.2 consists of four basic parts: the connector section, control section, the insertion tube and the tip of the endoscope.

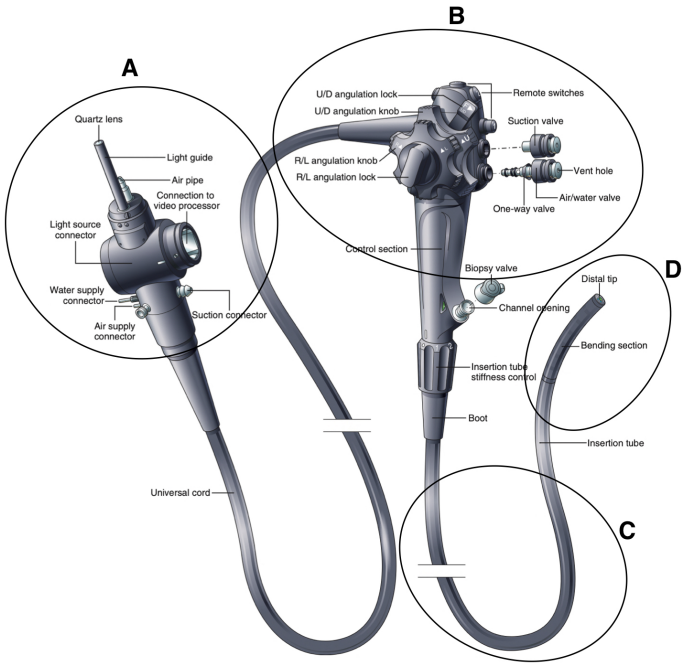

Figure 2.2: Endoscope Structure: (a) connector section; (b) control section; (c) insertion section; (d) tip section [19].

- **Connector Section (A)**

  The connection section is responsible for linking the endoscope to the centre of the video system using the universal cable. As shown in Figure 2.2 in section A and in Figure 2.3, this connection also allows for the supply of water from the water tank and air via the ventilation connector [21]. The light guide connector connects to the endoscope socket on the processor. In addition, there is a suction connector [22].

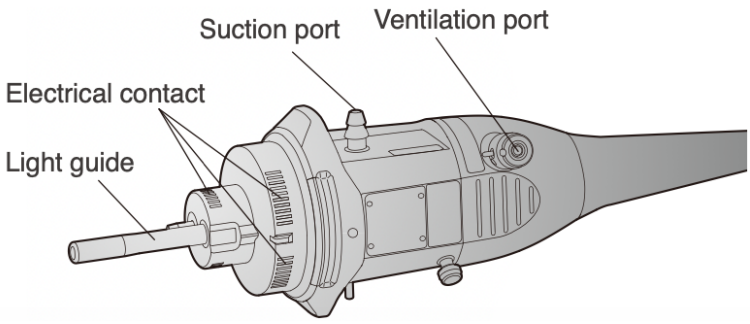

Figure 2.3: Conector Section [21].

- **Control Section (B)**

  The control section, illustrated in Figure 2.2 in section B and in Figure 2.4, is the most versatile part of the endoscope. It is used by the specialist to maneuver the endoscope and insert accessories [19]. The angulation knob on the control section is connected to

the endoscope tip by a series of wires, which allows the tip to be maneuvered resulting in easier insertion into the body and better visualization inside body cavities [21]. During an endoscopic procedure, the doctor is responsible for ensuring a clear view of the area being examined. To achieve this, there are two buttons on the front of the control section that are used. One of these buttons applies suction to clear any fluids that may be obstructing the view of the tissue. The second button has a dual function of blowing air and washing the camera lens [19]. The control section is connected to the insertion tube, and through the instrument channel, endotherapy devices can be used to perform endoscopic biopsies and other treatments [19] [21].

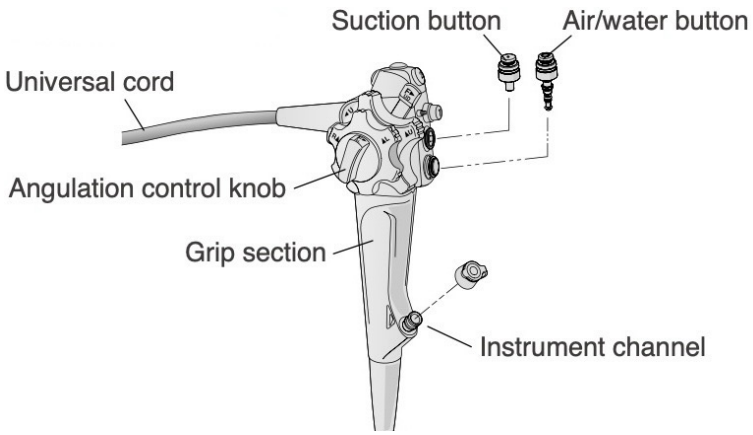

Figure 2.4: Control Section [21].

- **Insertion Tube (C)**

The insertion tube of an endoscope must be durable and flexible to ensure safe and effective insertion into the body, including flexion and retroflexion of the tip. In this section, there are four main components. The objective lens and image sensor work together to provide a wide view of tissue at once. Additionally, some endoscopes come with an optical zoom feature that allows for a more detailed examination of tumor tissue. This section also includes the light guide fiber bundles that transmit light from the external light source through the endoscope to light up the body cavities. Furthermore, the insertion tube has an instrument channel outlet where endotherapy devices can be inserted and removed for procedures such as tissue sampling (biopsy), tumor removal, among others. Finally, there is the water and air supply nozzle, which is used to clean the lens and possible debris and expand the body cavities through air insufflation, as already mentioned [19][21].

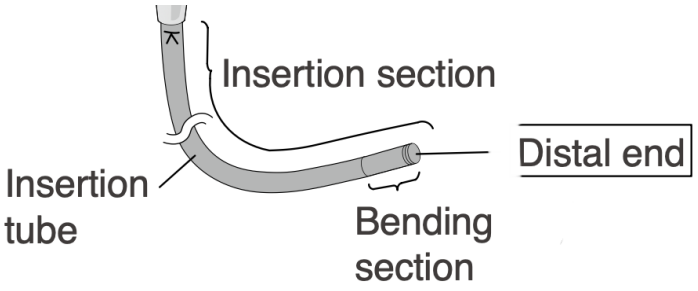

Figure 2.5: Insertion Section [21].

- **Tip of the Endoscope (D)**

  All this structure and composition of the insertion tube mentioned above is important for establishing a strong connection to the endoscope tip since this refers to the distal part of the insertion tube, as represented in Figure 2.2 in section D and in Figure 2.6. The endoscope's tip has an objective lens that can be adjusted as required. Adjacent to the lens is the nozzle which blows air and directs a jet of water. In addition, the lighting system transmits light into the field of vision, but the largest opening in the endoscope is a hole for endoscopic accessories. The tip of the endoscope contains a CCD that works together with the objective lens to form an integrated system. This system allows for the continuous transmission of images from the tip of the endoscope to the processing unit through a connector via the insertion tube. The electronic images are then sent in real-time to a monitor, enabling the doctor to analyze them immediately. [19].

  When planning complex endoscopic interventions, it is important to consider the spatial orientation of endoscope ports and components as they are capable of performing diagnostic and therapeutic procedures with precision [19].

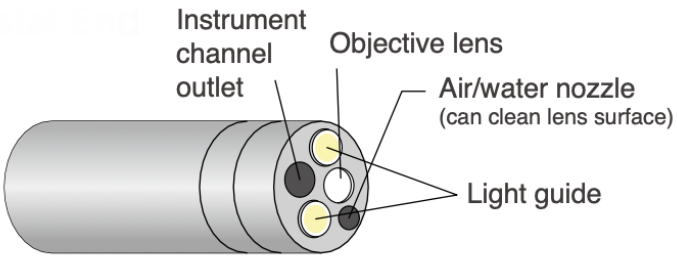

Figure 2.6: Tip Section [21].

2.4 Endoscopy Procedure

Although gastrointestinal endoscopy has been established for over 30 years, it can be technically challenging and carries a small but real risk of major complications [2]. Therefore, it

is essential to have a good, careful technique combined with a sound knowledge of diagnostic procedures.

In order for the diagnosis to occur as stably as possible, the endoscope should be held in the left hand to control the buttons, while the right hand is used to advance and retract the instrument from the cavity, illustrated in Figure 2.7. To avoid patient discomfort, the patient is rolled into the left side, and local anesthetic is applied. If the patient chooses to be sedated, intravenous access is obtained. After the operator has ensured that the endoscope is in good condition, it is inserted through the mouth and carefully navigated through the esophagus, stomach, and duodenum. To facilitate organ visualization, gentle insufflation of air through the endoscope is done to allow it to slide more easily into the stomach. With gentle force, the endoscope flexes along the greater curve of the stomach, allowing the pylorus to be reached, and through air insufflation, passes into the duodenal bulb. Due to the angulation of the duodenum, the control section wheels are used to achieve the view [2] [23].

After completing the procedure, the instrument is gradually removed from the body, and the mucosa is carefully inspected for any signs of abnormalities. If any pathology is noticed, photographs are taken, which in turn are visualized and analyzed by a specialist on a monitor during the diagnostic procedure. In more advanced cases, biopsies and therapy are usually performed during the withdrawal. There are risks of complications associated with diagnostic endoscopy, including process failure, missed pathology resulting in disease progression, reaction to sedation, aspiration, bleeding, and perforation [2]. The knowledge and practice of the points described above can form the basis for greater success and qualitative improvements in the endoscopy procedure.

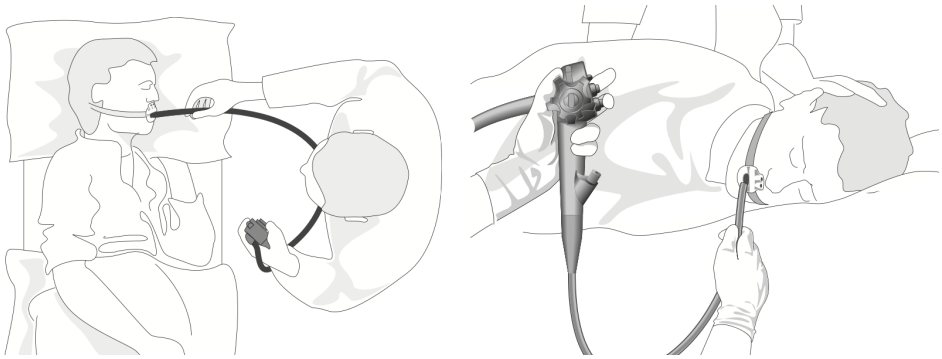

Figure 2.7: Endoscopy Procedure [23].

2.5 New Endoscopic Techniques

Endoscopy is a growing field in medicine, with new technologies and techniques constantly emerging. As image processing technologies advance with better image resolutions, new methods for the early diagnosis of digestive tract diseases are being developed. Some of the techniques developed are described below and summarised in Table 2.1.

- **Chromoendoscopy (CE) -** Chromoendoscopy is a technique that involves using biocompatible dyes on the surface during an endoscopy procedure. The colour helps the doctor to characterise and differentiate the tissues, detecting if there is anything abnormal in the gastrointestinal lining [14][24].

- **Narrow-Band Imaging (NBI) -** Narrow-band imaging is a technique where light of specific blue and green wavelengths is used to enhance the detail of certain aspects of the mucosal surface, focusing especially on the network of capillaries. A special filter is activated electronically by a switch on the endoscope leading to the use of ambient light of wavelengths 415 nm (blue) and 540 nm (green) [14].

- **Flexible Spectral Imaging Color Enhancement (FICE) -** The FICE technology was developed to real-time change the colors of endoscopic images using a filter-free software system, unlike NBI. In this method, spectral images of different wavelengths are generated from conventional endoscopic images. Subsequently, three of these spectral images are selected and assigned to the red, green, and blue color channels, creating new images. The colors in the original image are modified using the light's absorption and emission properties. By enhancing the contrast difference, fine details of the mucosa are highlighted, resulting in a sharper image [25].

- **i-Scan -** The I-Scan technology is another software-based processing technique. This approach digitizes endoscopic images, generating contrasts that enable better visualization and identification of previously invisible lesions. I-Scan comprises three distinct image algorithms that can be adjusted to optimize image effectiveness. Surface Enhancement (SE) enhances mucosal details. Tone Enhancement (TE) improves the identification of small structures and color changes. And finally, Contrast Enhancing (CE) uses blue light for highlighting [25].

- **Confocal Laser Endomicroscopy (CLE) -** CLE is an endoscopic technique developed to achieve high magnification and image resolution. It uses a low-power laser to illuminate the tissue and then detects the fluorescence signal through a pinhole. In order to enhance spatial resolution, only the returning light is detected [14].

Table 2.1: Overview of advanced endoscopic imaging techniques adapted from Li *et al.* [14].

Techniques	Technology	Tissue targe	Limitions
Chromoendoscopy (CE)	Use of biocompatible dyes to highlight any lesions in the mucosa	Surface enhancement due to staining	Prolonged duration of the procedure; Problems related to the use of dyes; Operator experience required.
Narrow-band imaging (NBI)	Light of specific blue and green wavelengths are used to improve the details of certain aspects of the mucosal surface	Improved vascular contrast of capillaries and submucosal vessels	Limited resolution Inability to detect; lesions at the cellular level; Prone to false negatives.
Flexible spectral imaging color enhancement (FICE)	From conventional endoscopic images, a spectral image is generated for each wavelength; Selection of three spectral images, assigned to channels, creates new images	Mucosal surface enhancement; Improving the contrast	More clinical data required for demonstration of clinical availability.
i-Scan	Three image algorithms that optimize image effectiveness by enhancing contrast	Structure and vascular enhancement with different modes	More clinical data required for demonstration of clinical availability.
Confocal laser endomicroscopy (CLE)	Low-power laser to illuminate the tissue, to achieve high magnification and image resolution	Image resolution improvement and cellular structure observation	Professional training required for accurate diagnosis.

2.6 Capsule Endoscopy

Real-time observation of the digestive system in a safe and comfortable way is crucial for the diagnosis and treatment of various medical conditions [26]. Despite the many advantages of using conventional flexible endoscopes (endoscopy, colonoscopy, among others), these have certain limitations, such as being minimally invasive and in some cases not being able to examine certain hard-to-reach parts of the gastrointestinal tract [27].

Capsule endoscopy is a wireless, simple, non-invasive, anesthesia-free endoscopy technique that was originally developed to examine areas of the small intestine inaccessible to conventional methods. However, it can now be used to examine and diagnose conditions throughout the gastrointestinal tract [28][29]. These benefits have made this method increasingly popular, with more than two million capsule examinations performed worldwide [30]. There are different capsules available for diagnosis, such as PillCam SB3 [31], Olympus Endocapsule 10 [32], OMOM [33], among others. These non-invasive capsules typically consist of a camera for capturing images of the interior of the tract and subsequent evaluation, a battery responsible for providing energy throughout the procedure, a light source to improve visibility, an image transmitter for medical

analysis, an antenna that aids in efficient data transmission, and an external encapsulation with biocompatible and non-degradable material, as shown in Figure 2.8 [26][28].

However, the role of endoscopic capsules has some limitations due to the large area of the stomach which makes it difficult to control the movement of the capsule within the body, the inability to inflate/aspirate, the lack of therapeutic capabilities, and the inability to perform biopsies. To overcome these limitations, developments in endoscopic capsule technology and even new devices to control the movement of the capsule are expected [29][30].

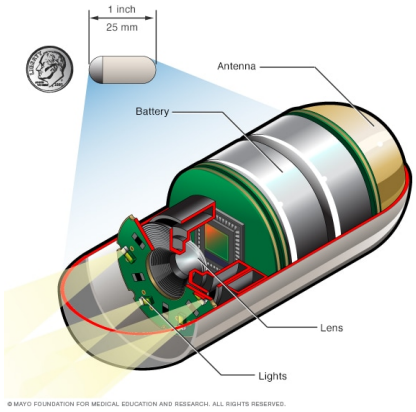

Figure 2.8: Capsule endoscopy [34].

2.7 Conclusions

Based on the previous information, it can be concluded that endoscopy is a highly sought-after field in medicine, whose main function is to examine the interior of the gastrointestinal tract. Therefore, knowledge of the tract is crucial to diagnose and, at times, treat diseases detected during the examination. In addition, healthcare professionals performing endoscopies must be familiar with the specific characteristics of the device to ensure that the endoscopy procedure occurs effectively, ensuring patient safety. However, there are regions along the digestive system that are challenging to access. Through the use of an endoscopic capsule, valuable information about critical areas can be obtained without the need for more invasive procedures. However, they present a significant limitation due to the lack of manipulation capability, resulting in complications for the analysis of specific areas. In this context, the constant evolution of the endoscope plays a crucial role in improving diagnostic accuracy.

Chapter 3

State-of-the-art on Hardware for endoscopy

Following the context provided by Chapter 2, the objective of this chapter is to provide an overview of the current state of the art in detection systems applied to the tip of endoscopes. Chapter 3 begins with Section 3.1, which is divided into three subsections. Subsection 3.1.1 explains the concept and importance of integrated circuits, serving as a basis for Subsection 3.1.2, which explores some of the existing communication protocols. Subsection 3.1.3 covers the concept of microcontrollers and how information is processed. Finally, Subsection 3.1.4 explores the importance and certain characteristics of developing a printed circuit board. Following, Section 3.2 is structured into subsections, each focusing on a specific type of sensor implemented applied to endoscopy. In this section, a review of the studies conducted in this field is presented, highlighting the main challenges that still persist for future research, thus guiding the work carried out in this dissertation. To conclude this chapter, the studies covered in this review are summarized, along with their results and limitations. Finally, in Section 3.3, some brief conclusions are presented on the current state of the art and research opportunities.

3.1 Integrated Circuits

3.1.1 Fundamentals

Integrated circuits (ICs) have undergone significant developments in complexity and performance in the field of electronics, becoming an integral part of most devices [35]. An IC is a miniaturized semiconductor-based circuit composed of various interconnected electronic components such as transistors, diodes, capacitors, resistors, and others. Through a complex network of paths, and depending on how they are connected, electrical signals are transmitted, allowing actions to be performed [36].

There is a wide variety of ICs, of which analog circuits are among the most fundamental. This is due to their operation, where inputs and outputs can take on a continuous range of values, with the output typically proportional to the input. In addition, digital circuits form another category,

characterized by the inclusion of circuits in which the input and output voltages are limited to two possible levels: low or high [35][37]. This fundamental distinction between analog and digital is marked by the continuous or discrete nature of the manipulated signals, which influences the applications and characteristics of the respective integrated circuits [36].

In order to carry out these tasks, it is important to establish a means of communication between the components. Communication between microcontrollers and various peripheral devices, such as sensors, requires some form of communication protocol to facilitate the exchange of data [38]. The way devices coordinate data transfer can be done asynchronously or synchronously. The difference lies in the fact that in asynchronous communication, devices do not share a common clock; they need to agree on the number of bits per second to send/receive. In the case of synchronous communication, there is already a shared clock line, allowing for higher speeds [39][40]. Some types of communication protocols are presented in Subsection 3.1.2.

3.1.2 Communication Protocols

Universal asynchronous receiver/transmitter (UART)

UART is a serial asynchronous communication protocol between devices, enabling data transmission. With only two wires, one for receiving (RX) and the other for transmitting (TX), the protocol achieves simultaneous full-duplex communication [40]. UART operates asynchronously, where the transmitter generates bits based on its clock signal, and the receiver uses its own clock signal to collect data. Synchronization is maintained by the same transmission rate. The transmitting UART sends data in parallel to the line using a control bus, transmitting them serially to the receiving UART. Each byte includes data, a start bit, and one or more stop bits [39][41]. The transmission speed must be configured equally on both devices. However, in demanding environments, UART may have optimization limitations due to its configurable speed [41].

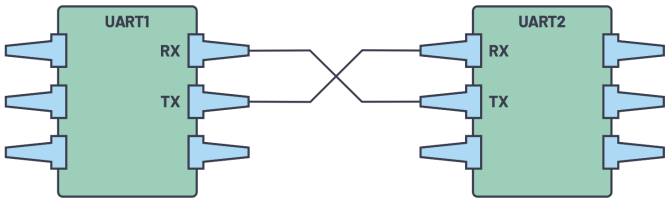

Figure 3.1: UART Protocol [40].

Inter-Integrated Circuit (I2C)

I2C is a synchronous, simple and low-speed serial communication protocol. It is used to connect controller devices with target peripherals [38]. I2C is a protocol that uses only 2 lines for communication, which are shared by all devices on the bus. The first line is a serial clock (SCL) and the second line is serial data (SDA). I2C uses the concept of a master/slave relationship between devices, where the master is responsible for initiating and controlling data transfer by providing the clock signal, while the slaves respond to the master's requests. Data transfer is bidirectional via the serial data line [42]. I2C communication is considered semi-duplex because

only a single controller or target device is sending data on the bus at any one time, in other words, it has a unique address. This allows the I2C protocol to support multiple control and target devices on a single bus, as shown in Figure 3.2. It is worth noting that all connections to the bus are made through open-drain outputs, meaning that they require pull-up resistors to a common voltage source [38][39][42].

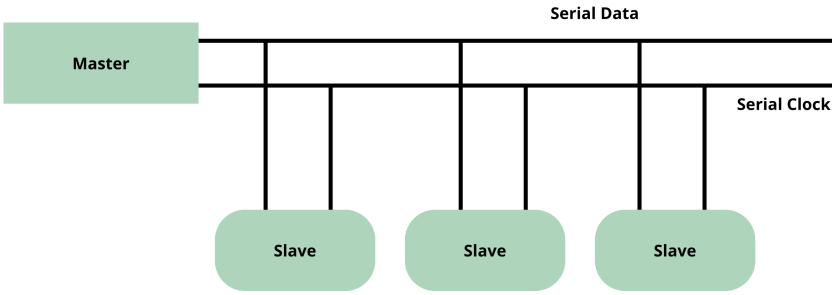

Figure 3.2: I2C Protocol adapted from Lynch *et al.*.

Serial Peripheral interface (SPI)

SPI is a high-speed, short-range, synchronous serial communication protocol. This protocol uses four wires responsible for establishing communication between the device and external peripherals [38][43]. Although it follows the master/slave concept, in SPI there is a master that controls the communication and one or more slave devices, as shown in Figure 3.3. SPI is a protocol that works through four main communication lines: MOSI (Master Out Slave In), responsible for transporting data from the master to the slave(s); MISO (Master In Slave Out), which carries data from the slave(s) to the master; SCK (Serial Clock), controlled by the master; and SS (Slave Select), which selects the device the master intends to communicate with. The SPI protocol provides full-duplex communication, meaning the slave can transmit data to the master at the same time as the master is transmitting data to the slave, which contributes to the efficiency and speed of communication [42][43].

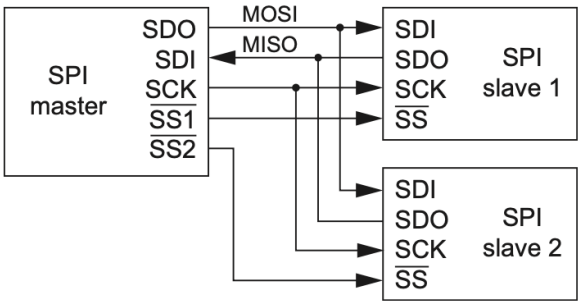

Figure 3.3: SPI Protocol [43].

Besides serial communication protocols such as UART, I2C, and SPI, there are several other options in the market, each designed to meet specific needs. Examples include CAN (Controller

Area Network), LIN (Local Interconnect Network), USB (Universal Serial Bus), among others. The choice often depends on the complexity of certain protocols, which ultimately influences the development cost. Furthermore, some protocols are designed for specific applications, such as automotive systems, and do not represent a general-purpose use of the protocol.

In the following Table 3.1, a comparative analysis of communication protocols (UART, I2C, and SPI) is presented. It includes information on the number of wires used, the type of transfer and interface utilized, as well as the quantity of masters and slaves used. It also indicates the speed, power consumption, and compares the cost of each approach.

Table 3.1: Comparison of UART, I2C and SPI protocols.

Parameter	UART	I2C	SPI
Number of Lines	2 (TX, RX)	2 (SDA and SLC)	4 (MOSI, MISO, SS and SCL)
Transfer Type	Full-duplex	Half-duplex	Full-duplex
Interface Type	Serial and Asynchronous	Serial and Synchronous	Serial and Synchronous
Master/Slave	Single-Master Single-Slave	Multi-master Multi-Slave	Single-Master Multi-Slave
Velocity	Slowest (Baud Rate)	Moderate	High
Energy consumption	Low	High	Medium
Cost	Low	Medium	High

Regarding the communication protocols UART, I2C, and SPI, it is concluded that they play crucial roles in connecting devices in electronic systems. UART stands out for its simplicity and point-to-point communication. On the other hand, I2C offers an efficient approach, using only two wires and supporting multiple devices on a single bus. Meanwhile, SPI stands out for its fast data transfer and versatility, making it ideal for dynamic communication between devices. The choice between protocols will depend on the specific requirements of the system, considering factors such as speed, complexity, and efficiency in resource utilization.

3.1.3 Microcontrollers

Microcontrollers (MCUs) are fundamental electronic components found in a wide range of devices. It is a miniaturised processor embedded in an integrated circuit whose main function is to optimise the processing and control of tasks for specific applications. It is considered a programmable single-task processor, consisting of a central processing unit (CPU), input/output (I/O) ports, a memory unit, serial communication through communication protocols, and other peripherals, all on a single chip, as shown in Figure 3.4. In addition to hardware features, it is essential for any microcontroller to be accompanied by software resources to control its operations and determine its functionalities [44][45]. Many microcontrollers have integrated communication peripherals. As the MCU has a limited number of ports, parallel data transfer is quite limited. However, serial communication, where data is sent bit by bit, is more effective over long distances.

Communication protocols are used to establish this type of communication, depending on the application [44][46]. In conclusion, these compact integrated circuits, combined into a single unit, provide critical control and data processing capabilities for a wide range of applications [44].

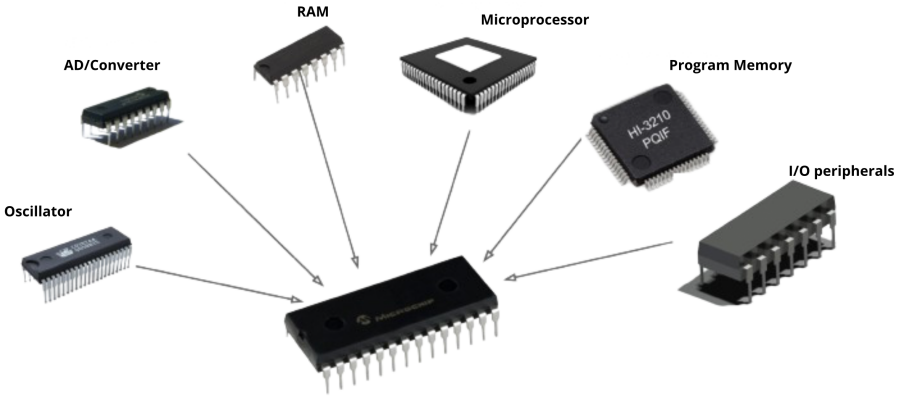

Figure 3.4: Microcontroller system adapted from [47].

3.1.4 PCBs development

The printed circuit board (PCB), as shown in Figure plays a crucial role in facilitating electrical connections among electronic components. This component employs electronic printing techniques to record circuits on the surface of a substrate coated with copper, insulated, and non-conductive, enabling electrical connections between components. Depending on the desired configuration, the PCB can be classified as a Single-sided PCB substrate (only one layer), Double-sided (2 layers), or Multilayer PCB plate (more than 3 layers). However, the substrate can be rigid in nature, providing mechanical resistance, flexible substrate, composed of soft materials that allow shaping depending on the installation, and rigid-flex substrate, which is a combination of the two. In future developments, a reduction in size, high density, precision, reliability, fast transmission, and optimized thickness are expected in the manufacturing process [48].

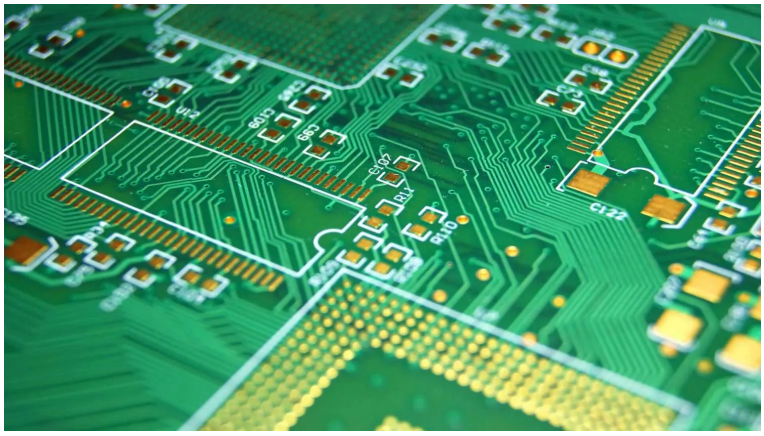

Figure 3.5: Printed circuit board[49].

3.2 Sensing Systems

Endoscopes are instruments designed to provide the doctor with detailed information about the area being examined, in this case, the gastrointestinal tract. They play a crucial role in medicine, allowing the less invasive diagnosis and treatment of digestive diseases, as well as screening of at-risk patients and the general population. Since gastrointestinal endoscopy is one of the most commonly performed tests in the world, there has been a great deal of interest in the field of endoscopic development in recent years, as it is responsible for increasing services for the prevention and early detection of diseases and, consequently, their treatment, which reduces the risk of complications [50] [51].

However, there are still failures in the detection of diseases, leading to more serious cases of cancer development. This failure refers to the fact that the doctor is not able to obtain sufficient information, except for visual information, and it takes some time to interpret the images and determine the seriousness of the abnormalities diagnosed. This results in a certain limitation of the information available to the doctor [52] [53].

New technologies are being investigated to overcome this limitation and provide increasingly accurate diagnoses. One of these technologies is the development of sensor devices attached to the tip of the endoscope, whose main function is to provide the doctor with more diagnostic parameters of the environment during the examination itself. The following sub-sections describe some of the sensors that have already been studied and explain their system architecture [52].

3.2.1 Pressure and Temperature Sensor

Monitoring intraluminal pressure and temperature has become one of the important diagnostic parameters resulting from an endoscopic examination. One reason for its relevance is that, depending on the existing intraluminal pressure, it is possible to accurately determine the size of a cancerous tumour. Another factor is that during endoscopy, in order to facilitate the insertion and curvature of the endoscope inside the cavity, air is introduced for insufflation. By monitoring this parameter, it is possible to avoid abdominal distension and discomfort by controlling the pressure so that it is not excessive (21 kPa) [52] [54] [55].

One of the main contributions to the pressure and temperature sensor was made by Maeda *et al.* [52] in 2015 with their original work on the development of a microsensor integrating an intraluminal pressure and temperature sensor for application in the field of flexible endoscopic surgery [52]. The proposal involves the use of a MEMS (Micro-Electro-Mechanical Systems) sensor composed of a silicone diaphragm, a pressure chamber formed by SU-8 (photoresists), and an integrated circuit of piezoresistance. The change in resistance in the piezoelectric circuit detects pressure, while temperature is detected by a change in the respective resistance. To avoid compromising the camera's view and disturbing the endoscope's operation, the sensor is small in size and is incorporated into the endoscopic bell. Additionally, the back of the diaphragm has a chromium layer that serves as protection against the LED light from endoscopy. This study was

tested in a dog, and the device was embedded in acid-resistant polymers to ensure resistance to acidic solutions present in the stomach [52].

The use of the MEMS sensor incorporated into an endoscopic bell, as shown in Figure 3.6, resulted in real-time monitoring of intraluminal pressure and temperature caused by the supply and exhaust of CO2 during the examination. Maeda *et al.* [52] mentions that the studies met expectations, however, this sensor has some limitations. Its dependence on wires may increase the risk of disconnection, leading to potential restrictions on the movements of the endoscope [52].

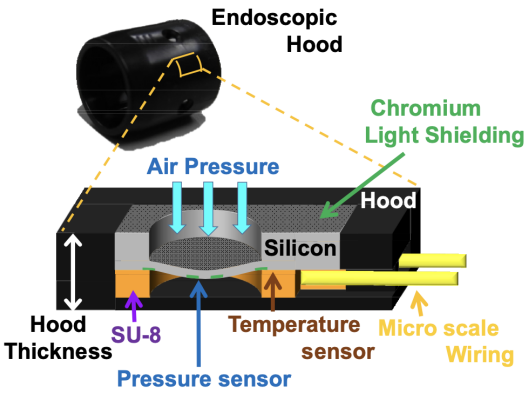

Figure 3.6: Pressure sensor embedded in a endoscopic hood [52].

Despite the overlap of applications and to overcome these limitations, Maeda *et al.* [54] proposed in 2018 a wireless pressure sensor based on endoscopic imaging technologies for application in endoscopic surgeries, as illustrated in Figure 3.7 [54]. This sensor represents an evolution of the MEMS sensor used in the previous study [52], aiming to provide greater mobility and a more comprehensive image analysis. Similar to the previous study [52], this miniaturized sensor is embedded in the endoscopic bell made of plastic to avoid obstructing the camera's view [54].

The sensor used in this project consists of a silicone diaphragm, a structure to detect the use of a chamber to produce structural color, and etched glass to form a narrow vacuum space. The mechanism involves a sensor that reflects structural color, detected only through endoscopic vision. Structural color depends on the applied wavelength, which is altered by air pressure. Thus, the need for electrical wires is eliminated. The final structure of the device with structural color was designed for completely wireless pressure monitoring [54].

Despite the potential interference caused by the absence of wires, the study asserts that the system met the requirements, demonstrating that color changes occur with variations in air pressure through tests conducted in a dog's stomach using an industrial endoscope. This innovative approach is mentioned to address the challenges associated with wired sensors and improve mobility while ensuring effective pressure monitoring in endoscopic applications [54].

Silva *et al.* [55] focused their implementation on the assessment of gastrointestinal motility, i.e., the movements and contractions of the muscles of the digestive system, proposing the development of a pressure sensor applied to flexible endoscopes based on thin-film aluminum strain gauge arrays.

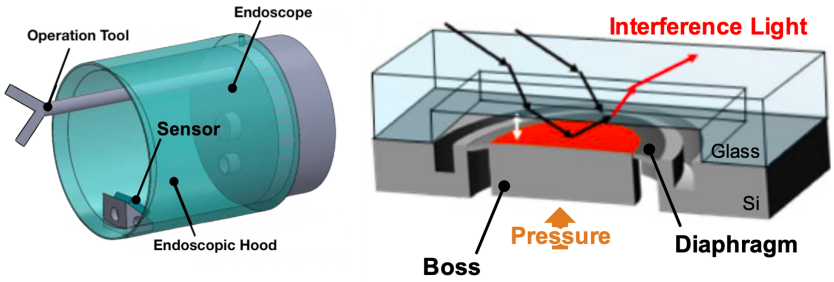

Figure 3.7: Fully wireless pressure sensor adapted from Maeda *et al.* [54].

This method aims to evaluate the pressure within the gastrointestinal tract using a flexible catheter equipped with pressure sensors distributed along its length, efficiently and with high resolution. This proposal is based on the use of strain gauges coated with a Kapton membrane (polyimide film) deposited on a diaphragm made of SU-8. To ensure the necessary biocompatibility, the polymer (PDMS) is used as an encapsulation material. In addition to presenting a high level of integration and ease of fabrication, the fundamental role of these sensors lies in the use of electrical resistance [55]. In simplified terms, pressure causes deformation in the Kapton membrane, which, in turn, alters the electrical resistance of the strain gauges, producing a variation in electrical potential. This change in resistance is measured by the electrical reading system. The signal acquisition is performed by a microcontroller ADC (Analog-Digital Converter). The positioning of the sensors is an important factor to consider, as it influences the increased sensitivity in voltage detection. The developed sensor, shown in Figure 3.8, is thus based on four aluminum strain gauges connected to a fully active Wheatstone bridge, whose output voltage is proportional to the applied pressure [55].

Detecting abnormal pressure patterns facilitates the identification of diseases, supporting the doctor's work. This project mentions observing notable linearity and sensitivity in the sensor; however, it emphasizes the importance of conducting tests in a dynamic configuration, that is, by wrapping the sensor around a catheter, to explore the dynamic response of the sensor and investigate its performance in terms of frequency [55].

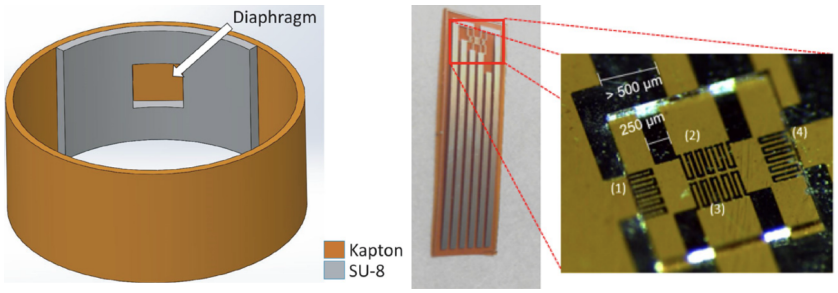

Figure 3.8: Motility pressure sensor [55].

3.2.2 Proximity Sensor

The constant innovation and development of endoscopic techniques to improve the tools currently available is a way of supporting the doctor by providing important information to make a correct diagnosis. In order to maintain accurate navigation, ensure patient safety, minimise collisions and tissue damage, and possible complications during diagnosis, the use of proximity sensors has become a valuable tool. The main utility of this sensor lies in detecting the proximity of surfaces while maintaining an adequate distance between tissues [56] [57].

According to the current state of the art, there are different approaches in flexible endoscopes to detect proximity to the surrounding tissue and derive a position. One option is to use optical fiber sensors; another is to employ image processing, specifically Simultaneous Localization and Mapping (SLAM). However, the development and use of capacitive sensors at the tip of the endoscope represent another way to detect proximity [58].

In 2020, Bințințan *et al.* developed a new inductive proximity switch compatible with laparoscopy to locate intestinal tumors. They used an electromagnetic detection probe and metallic markers fixed to the intestinal mucosa. Experiments conducted on an in-vivo animal model of the small intestine showed effective detection, with the range varying according to the type of marker. The system has the potential to accurately locate digestive tumors laparoscopically, and future work aims to increase its sensitivity and range for full clinical use [59].

In 2022, Calborean *et al.* developed a new instrument to locate tumors in the digestive tract accurately. It consists of an inductive proximity sensor and an electronic block encapsulated in autoclavable stainless steel, working in conjunction with an endoscopic hemostatic clip modified for improved detectability. In experiments on large animals, the modified clips were easily transported and attached to the intestinal mucosa, demonstrating effectiveness. However, the detection range needs to be improved for optimal clinical use [60].

Giacoppo et al. [56] present a prototype based on an optical fiber proximity sensor that is inserted through the working channel of an endoscope. Multiple optical fibers are used to transmit light, and this light is reflected back or absorbed when it reaches an object. Subsequently, the sensor analyzes the amount of light that returns to the detector, interpreting whether there are changes in reflection intensity indicating the distance of the endoscope tip from the tissue, both axially and radially, as depicted in the diagram in Figure 3.9. In terms of electronic materials used, in this prototype, a constant current source (KSQ300) was used to operate the infrared LED diode (ADL-80Y05TL) as an emitter. To measure intensity, a photodiode (BPW 34) is used as a detector. A circuit with a Rail-to-Rail amplifier (MCP6002-I/P) is used to measure the photocurrent. The cutting angle of the sleeve with the fibers was measured in a microscopic image. The angles were determined using ImageJ software. Using a laser triangulator (HL-G112-S-J), the distance was measured. The sensor voltage signal and the distance detection from the laser triangulator were recorded with a microcontroller (Arduino UNO Rev3).

The study mentions that, based on tests conducted with a brass sleeve, the obtained results were considered very interesting, demonstrating the influence of the cutting angle of the fiber at

the distal end of the optical fiber. This allows for a better measurement of the signal in axial and radial directions [56].

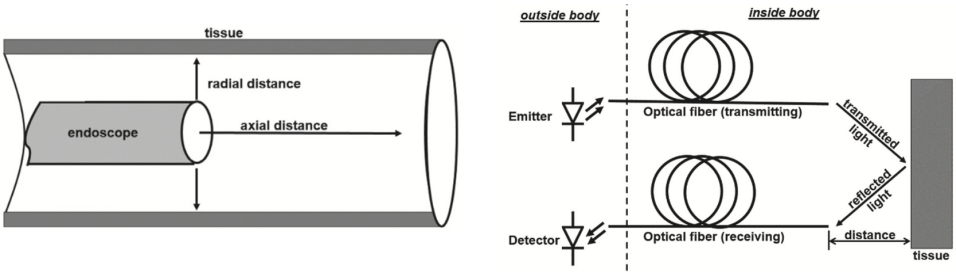

Figure 3.9: Proximity sensor for an endoscope to determine axial and radial distance [56].

In 2023, Giacoppo *et al.* [58] proposed a method using capacitive sensors with active shielding to measure the radial proximity between the endoscope tip and the tissue. To detect this proximity, the sensors emit an electric field from the sensing end. When an object approaches the electric field, the capacitance of the sensor is changed due to electrical interaction with the object. In this study, the sensor consists of four copper foil electrodes connected to a ring with active shielding that prevents certain capacitance variations. The measured capacitance from the four channels passes through a capacitance-to-voltage converter (FDC1004). The data is then transferred via the I2C bus to an Arduino Nano microcontroller (Arduino). The microcontroller is connected to MATLAB, which controls the linear stage. Due to the sensitivity of this method, several factors can affect the proximity measurement, one of which is the effect of the detection angle. To mitigate the effect of the detection angle, prevent capacitance variations, and minimize side effects, two different designs of active shielding were investigated. The results obtained in the study indicate that these designs can effectively reduce the angle and increase the reliability of position measurement [58].

In conclusion, despite certain limitations and the need for further refinement to become fully functional, the study mentioned that the research demonstrates the feasibility of designing a sensor that can be attached to an endoscope for precise proximity measurement to tissue [58].

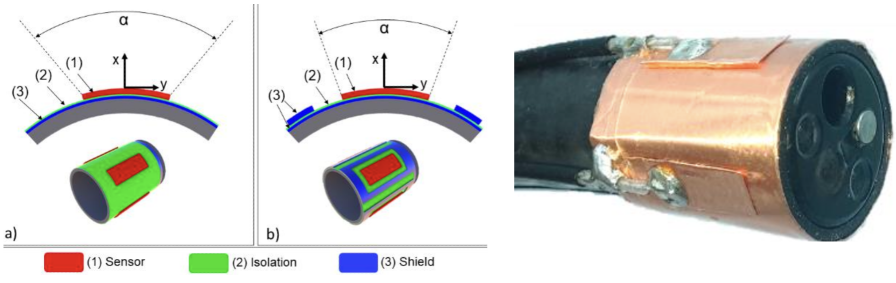

Figure 3.10: Actively shielded capacitive proximity sensor [58].

3.2.3 Distance Sensor

In the field of endoscopy, it is common to confuse proximity sensors with distance sensors,

as both deal with proximity to objects. However, their applications differ significantly. Distance sensors in endoscopy have the ability to measure the distance in real time between the endoscope and the surrounding tissues. This feature is crucial for controlling, optimising and understanding the procedure [61]. One notable application of this technology is to provide endoscopic images that reflect the actual size of anatomical structures, contributing to more accurate prognoses. In addition, this technology can be used to guide catheters, extending its clinical applications [62].

In 2008, Lucesoli *et al.* [63] proposed the implementation of an optical sensor based on low coherence fiber optic interferometry capable of measuring the distance between the tip of the endoscope and the anatomical surface. This system aims to overcome the inability to calibrate images due to the magnification system. This study was tested in pig tracheas, simulating real conditions, demonstrating high sensitivity, and providing correct and repeatable distance measurements [63] [64].

Previous studies utilized distal optics of relatively large sizes, restricting the applicability of the sensor in endoscopes. However, in 2019, Vilches *et al.* [62] introduced an ultra-miniaturized optical fiber implementation for single-point laser distance measurement in endoscopy, illustrated in Figure 3.11. The employed sensor is an interferometric distance sensor. Interferometry involves analyzing interference among reflected light waves to gauge the distance from a surface to an object. Through a GRIN lens and using a beam splitter, the laser-generated light beam is divided into two paths. One path reflects off the surface, while the other reflects off a reference mirror. Both paths converge, and interference analysis determines the distance to the object. In this project, the sensor configuration adopts a common path interferometer, eliminating the need for an additional reference arm to compare with the signal reflected from the target tissues.

The results from tests conducted in this study on ex-vivo tissue indicate the feasibility of performing distance measurements, even in the gastric mucosa. This positions it as an approach of interest for disposable or cost-effective medical devices [62].

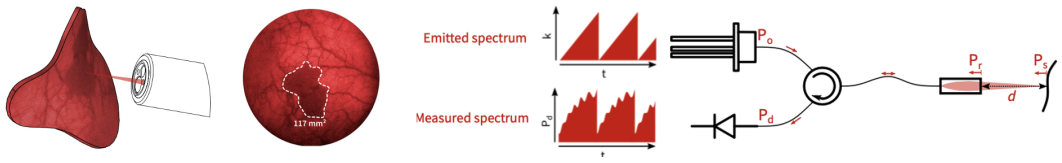

Figure 3.11: Fiber-based distance sensor [62].

Although the previous study by Vilches *et al.* [62] was considered useful and effective in measuring ultra-small distances, it exclusively focused on detecting axial measurements and posed potential risks in diagnosing patients.

Therefore, in 2023, the same author, Vilches *et al.* [65], proposed an innovative multipoint endoscopic sensor based on a microprism array to measure both the distance and orientation of the sensor in relation to the tissue. The approach employs a fiber-based sensor, where multiple beams are split and transmitted using a microprism array to achieve a broad measurement range, as depicted in Figure 3.12. The measurement device with an interferometer is configured using an optical circulator (AC Photonics PIOC). This component directs the beams towards a lens

with a gradient index of focus (GRIN). The scattered light is subsequently detected and analyzed by a laser mediation system based on continuous frequency modulation of the transmitted signal (FMCW). This technique utilizes a vertical cavity surface emitting laser (VCSEL - Seoul Semiconductors RC120001-FFA) [65].

The implemented technology states that the testing of the multipoint sensor demonstrates validity, although precision and algorithms require improvement. Due to its single measurement nature, it is resistant to interference caused by unwanted movements, presenting significant advantages for endoscopic development [65].

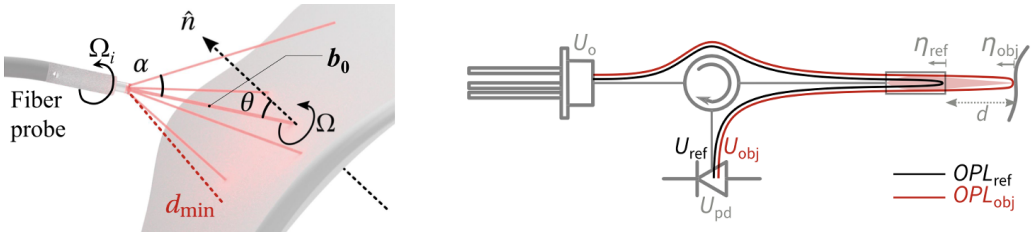

Figure 3.12: Fiber-Optic distance sensor [65].

3.2.4 Orientation Correction Sensor

In order to make the field of endoscopy a safer place, the implementation of new technologies has the potential to make endoscopic procedures more precise, less invasive, and with better clinical outcomes. The guidance and correction of image rotation are among the advancements with the most impact on the diagnosis performed by surgeons and gastroenterologists, given that incompatibilities between the spatial orientations of an endoscopic image and a physician's working environment lead to reduced performance. Furthermore, they assist in the medical interpretation of images obtained by the endoscope. Various approaches have been attempted over the years to track and rectify images; however, real-time calculation and obtaining results have posed a challenge. To overcome these challenges, the use of an inertial sensor at the tip of the endoscope has become a stable and intuitive approach [66] [67].

Holler *et al.* [66] proposed the implementation of a triaxial MEMS inertial sensor positioned at the tip of an endoscope. The sensor's purpose is to measure the impact of gravity in three spatial directions (x, y, z), which can be utilized to correct the image orientation, as depicted in Figure 3.13. In this case, the x-direction is where the endoscope tip points, the y-axis points to the right, and the z-axis points downward in the image.

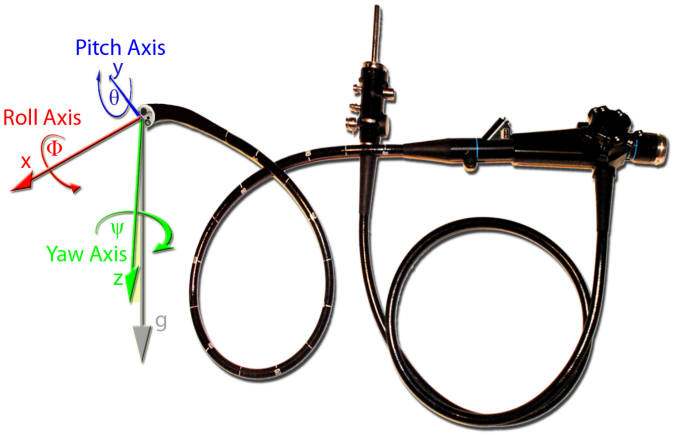

Figure 3.13: Endoscopic orientation [66].

Following data collection, these measurements are transferred through a two-wire I2C communication protocol along the endoscope. Subsequently, the video signal is digitized through a USB video capture device. Then, an analysis of the accelerometer values is carried out via an 8-bit microcontroller, enabling real-time estimation of the rotation angle, as illustrated in the block diagram in Figure 3.14 [66].

This method was investigated and tested in porcine animals to compare the results with and without the final orientation. Holler *et al.* [66] mentioned that with the implemented sensor, greater precision, shorter paths, and almost half the duration were achievable compared to without the sensor. Therefore, providing endoscopic images with a stable horizon proves advantageous for better guidance [66].

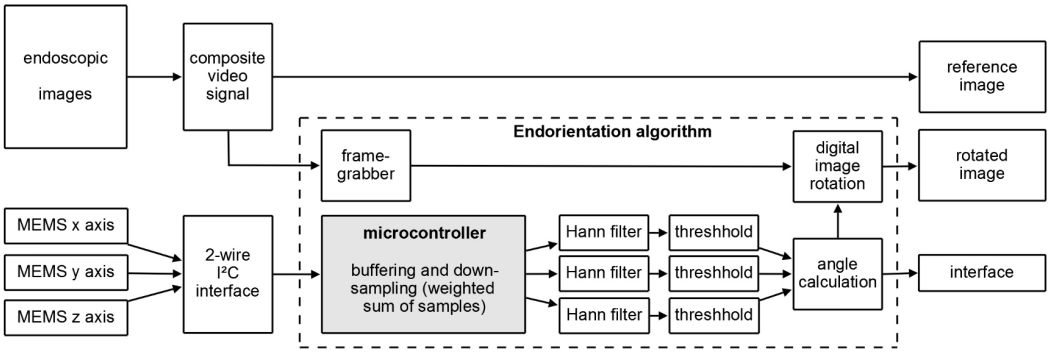

Figure 3.14: Block diagram of rotation correction [66].

The accelerometer method previously proposed by Holler *et al.* [66] used an inertial sensor to correct the orientation of endoscopic images. However, it mentioned the inability to distinguish between translational acceleration and gravity [67].

Therefore, in 2017, Lee *et al.* [67] proposed the implementation of a real-time image orientation correction system using both an accelerometer and a gyroscope. In this study, the accelerometer and gyroscope were attached to the handle of the endoscope to measure acceleration and angular velocity, respectively, as shown in Figure 3.15. The approach is based on the use of

the Bluetooth 3-Space Sensor™, which provides the collected acceleration and angular velocity values and transmits them in real-time to a processing system. The collected values are then used as inputs, and the rotation angle is calculated using a Kalman filter. A charge-coupled device (CCD) camera is used to capture the video. The video is then transferred to a computer, where it is processed and corrected by C++ software. Figure 3.16 represents the diagram of the orientation correction system. The system's effectiveness is analyzed by comparing the optical rotation angle with the angle calculated by the Kalman filter [67].

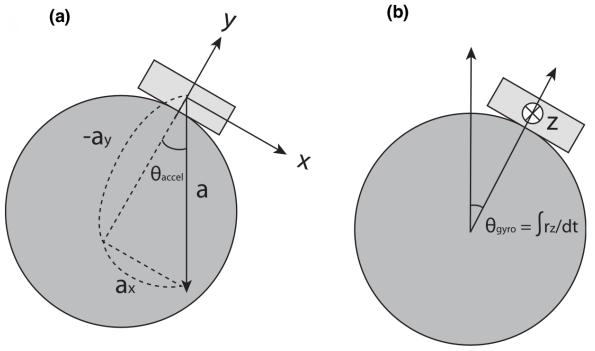

Figure 3.15: (a) Accelerometer (b) Gyrosensor axes [67].

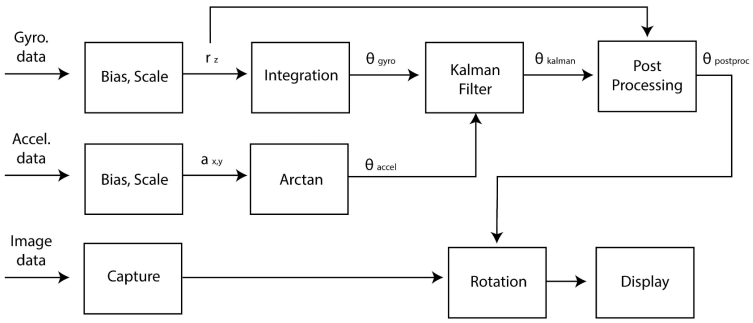

Figure 3.16: Diagram of the image orientation correction system [67].

To demonstrate the importance of this system, tests were conducted with 15 participants during endoscopic examinations with and without the orientation correction system. The results obtained in the study [67] confirmed an improvement in the physician's performance during the examination and the benefit of using the system, as the time was reduced with the use of the correction system. Comparing the use of the accelerometer alone with the simultaneous use of the accelerometer and gyroscope, it was found that the error in correcting the image orientation was significantly reduced [67].

Vedaei *et al.* [68], in 2021, proposed the implementation of four cameras and an Inertial Measurement Unit (IMU) with the aim of locating and orienting the endoscopic capsule. An IMU is a sensor that includes a gyroscope, an accelerometer, and a magnetometer. The following approach utilizes a microcontroller (ATmega32U4) to connect with the entire system through I2C, SPI and UART communication protocols. In order to demonstrate the feasibility of the mentioned

system, Vedaei *et al.* conducted in vitro tests in the swine intestine, stating that the proposed system is capable of accurately locating the capsule.

3.2.5 PH Sensor

In the field of endoscopy, pH analysis is crucial for the diagnosis of gastrointestinal disorders, as abnormalities in the pH of the digestive system can indicate health problems such as peptic ulcer disease, gastro-oesophageal reflux, Crohn's colitis, and others. Throughout the gastrointestinal tract, the intraluminal pH varies according to the environment in which it is found and can vary between one and seven. Taking these differences into account, any abnormality detected during the examination will help the doctor diagnose and subsequently treat the condition [27][69].

Advances in technology have opened the door to the emergence of new devices that can be ingested, most notably the endoscopic capsule methods discussed in section 2.4. Compared to conventional approaches, ingestible sensors offer a non-invasive alternative and provide direct and complete access to the gastrointestinal (GI) system. Recent research into pH detection in the GI tract has mainly focused on the use of metal oxide electrodes, such as iridium oxide, glass membrane electrodes, and ion detection wires with potential applications [27][69].

With the aim of introducing pH monitoring to the market, Asci *et al.* [27] proposed a method in 2022 using an ingestible biosensor capsule for pH detection through wire-based electrochemical sensors. The approach relies on the use of wire-based pH biosensors that generate a voltage signal based on pH levels. A voltage-reading system is then employed to analyze the detected pH. The advanced analog circuit not only measures voltage in an open circuit but also converts the detected value into a digital signal for subsequent processing and storage. Additionally, a microcontroller and EEPROM memory are utilized for data logging, which is then transferred to a computer using the SPI or UART protocol, as depicted in Figure 3.17. The device's biocompatibility is a crucial aspect, achieved through the use of 3D printing technology with biocompatible and photocurable resin [27].

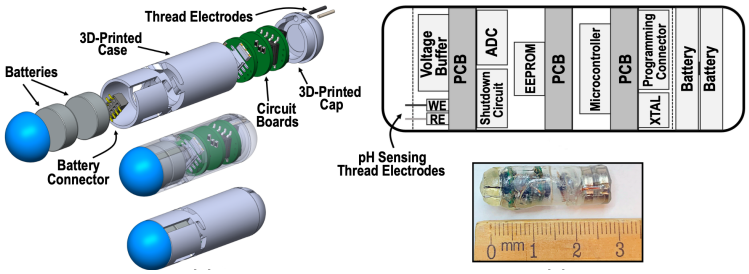

Figure 3.17: Ingestible pH sensing system [27].

Compared to other pH detection methods, the use of detection wires allows the integration of various biochemical sensors into a compact, ingestible, flexible, non-invasive, low-cost, rapidly diagnosable, and easily manufacturable capsule. All these advantages enable achieving high resolution without compromising the measurement. However, the technology mentions the potential

for expansion to other biomarkers in the future by simply adding appropriate detection wires and some additional hardware, potentially transforming it into a multi-sensor system. Moreover, this method holds significant diagnostic potential, as tract analysis can be performed in real-time [27].

Asci *et al.* [27] states that results from a syringe pump system (simulating different gastrointestinal environments) demonstrate accuracy in measurements and sufficient sensitivity to detect pH in the gastrointestinal tract [27].

In 2021, Cheng *et al.* [69] proposed the implementation of a wireless and ingestible capsule system based on yttrium oxide to monitor gastrointestinal pH in real-time. Yttrium oxide, as a sensitive material with greater precision for detecting pH in the gastrointestinal environment, was electrodeposited to form the pH sensor responsible for generating a response signal reflecting the detected pH value in the tract. Connected to the pH sensor is the capsule detection circuit, which receives and sends the signal to the Analog-to-Digital Converter (ADC). Subsequently, the digital voltage signal is read by the microcontroller and transmitted through the Bluetooth module. This digital voltage information is then wirelessly sent to an external receiving device. For the detected pH signal to be transmitted to an external receiving device (computer or smartphone), the use of a wireless auxiliary circuit is necessary to establish the connection between the program and the capsule detection circuit, as illustrated in Figure 3.18. The pH sensor and the capsule detection circuit were both encapsulated in the 3D-printed capsule structure, always considering the importance of the biocompatible encapsulation material, PDMS (polymer), so that the size and shape of the device are suitable for navigating the gastrointestinal tract, avoiding discomfort to the patient [69].

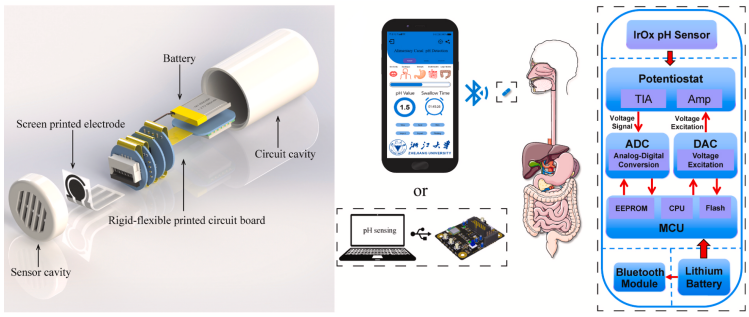

Figure 3.18: Iridium oxide-based capsule system [69].

Despite the need to improve signal transmission and sensitivity in energy reception, the study [69] mentions the potential of this technology in diagnosing gastrointestinal diseases, demonstrated through in vitro tests with artificial digestive fluids and in vivo tests in dogs. This practice revealed that accurate real-time detection of the pH variable in the gastrointestinal tract is possible, always with the perspective of acquiring and enhancing the complex system to meet more advanced needs [69].

3.2.6 Other Sensors

There are other types of sensors implemented in the field of endoscopy, such as pH sensors [70], electrochemical sensors [71],image and physiological sensors [72], ultrasonic sensors [73], antennas [74], and others based on optical fiber [75] and 5-DOF sensor [76]. Additionally, infrared sensors are found incorporated in the core of the endoscopic camera to capture thermal images [77]. The following studies are presented, covering the utilization of these diverse sensors and emphasizing their specific applications and contributions to notable advancements in endoscopy.

In 2008, Roh *et al.* proposed using an in vivo pH sensor, more precisely an Ion-Sensitive Field-Effect Transistor (ISFET), to facilitate the detection of pH in the throat and stomach. In this study, the pH sensor catheter manufactured was tested in vivo on a pig. Positive results were obtained; however, the difficulty of achieving high performance in a small-sized sensor was highlighted [70].

McCaffrey *et al.* [71], in 2015, presented a model of an ingestible wireless endoscopic capsule with a potentiostatic electrochemical sensor. This approach proposes a different analysis of the gastrointestinal tract, intending to electrochemically examine various areas of the tract in real-time through the development of an electrochemical detection system. The tests conducted in this study confirmed that the use of these sensors is a viable diagnostic tool with potential applications. However, there is a need for complete and in vivo clinical trials [71].

Traditional capsule endoscopy can be slightly limited by the resolution of the image sensor and the diversity of tissues in the lesion, so the diagnosis may not be the most obvious. In 2014, Shao *et al.* [72] presented an integrated capsule endoscope with an image sensor and physiological sensor that can diagnose various gastrointestinal diseases. The main function of this study is to develop an integrated system that aims to simultaneously measure morphological and physiological information (pH, pressure, temperature, and impedance) in the gastrointestinal tract to avoid performing many tests [72].

Liang *et al.* [73], in 2022, proposed the use of a laser ultrasound sensor to develop a miniaturized photoacoustic endoscope with optical resolution. The aim is to detect ultrasound waves generated by the absorption of laser pulses by biological tissue, diagnosing conditions such as inflammation, gastrointestinal cancer, among others. In this study, the endoscope is employed to visualize the rectum of a live rat in vivo and observe changes in oxygen saturation during inflammation at optical resolution, highlighting certain limitations in current imaging instrumentation [73].

In certain endoscopic procedures, the need to remove fatty tissue from blood vessels can increase the risk of injury. Therefore, in 2022, Fujimoto *et al.* [74] proposed the use of an antenna sensor in a radio wave endoscope to detect blood vessels covered by fatty tissue. The antenna sensor consists of a transmitting antenna and a receiving antenna. The tests carried out in the study confirmed the detection of a blood vessel at a distance of two mm from the surface of the adipose tissue, both in simulations and in actual measurements [74].

In order to avoid the loss of information during image transmission due to spectral technical limitations, Zaichenko *et al.* [75] proposed a hybrid endoscope for the diagnosis of internal organ

oncology in 2020. The hybrid endoscope involves the transmission of images through both an RGB video camera and a fiber optic-based image sensor, which together provide a comprehensive reflectance spectrum of the lesion in the internal organ. This approach can be used in all areas of endoscopy, as well as in areas where disease diagnosis relies on the provision of video data. Zaichenko *et al.* asserts that in addition to the high spatial resolution provided by the RGB camera, it is possible to obtain maximum spectral information through the sensor used, thus reducing information loss throughout the diagnostic process [75].

In 2023, Li *et al.* [76] proposed a measurement method applied to the monocular endoscope, which incorporates a five-degree-of-freedom (5-DOF) sensor with the primary purpose of obtaining the lens position. Simultaneously with the acquisition of the lens position, a semantic segmentation network is used to segment object masks. The objective dimension is determined by the combination of these two components. Due to the limited availability of visual data in the monocular endoscope for precise measurements, the effectiveness of the proposed sensor was evaluated using an isolated porcine kidney, where several stones of known size were placed for measurement. Based on the tests conducted, the study [76] concludes that the approach is safe and feasible for endoscopy. However, the authors emphasize a future intention to improve dynamic object measurement [76].

In 2022, Scutelnic *et al.* [77] proposed a thermal endoscopy system designed for laparoscopic electrosurgery, based on infrared thermography. The method involves acquiring thermal radiation emitted by bodies at a specific temperature, allowing the calculation of the temperature of anatomical structures by considering emissivity. The approach utilizes Long-Wave Infrared (LWIR) camera cores, such as the Lepton, which are cost-effective and offer good resolution. To overcome dimensional limitations, the study aimed to reduce the size of the electronics. The sensor and the circuit board were integrated into a 3D-printable enclosure, potentially composed of materials like titanium. An optical component in germanium was added. Two PCBs were designed to enable frontal and lateral thermal visualization of the endoscope, as illustrated in the Figure. Data is transmitted to a computer, such as the Raspberry Pi 3, through SPI and I2C interfaces. The SPI protocol is used for transmitting thermal data, while I2C accesses the camera. The Infrared Vision Software is employed for real-time acquisition and visualization of thermal images [77].

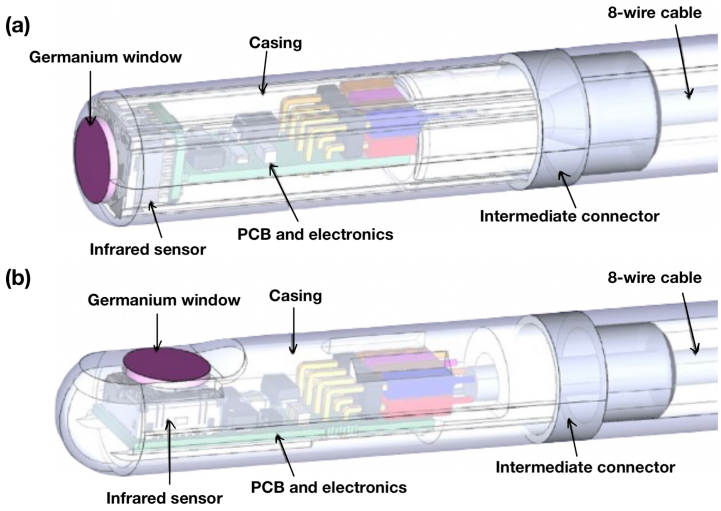

Figure 3.19: Prototype assembling: (a) Frontal setup; (b) Lateral setup adapted from Scutelnic *et al.* [77].

The system was tested on a CO2-rich artificial model to monitor the thermal effects of electrosurgery. Scutelnic *et al.* [77] highlights the success in real-time evaluation of heat propagation in tissues. However, the authors suggest future improvements, including the simultaneous implementation of thermal and visible vision, emissivity correction, and evaluation of the biocompatibility of the materials used in the enclosure and window [77].

In the following Table 3.2, a critical analysis of the works mentioned in the reviewed literature is presented. It contains information about the type of sensor used, its main application, some associated limitations, information about the biocompatibility of the system, and whether any form of communication is established.

Table 3.2: Overview of sensors applied in endoscopy.

Authors	Sensor	Application	Limitations	Communication Protocol	Biocompatibility	Case Study
Giacoppo *et al.* (2023) [58]	Capacitive	Detects targets by emitting an electric field	Sensitive measurement method; Sensing angle; Interference signals.	I2C	NR	Applied to the gastrointestinal tract
Vilches *et al.* (2023) [65]	Fiber-based sensor	Scattered light is detected and analyzed by a laser mediation system	Accuracy and algorithms need improvement.	NR	NR	Laparoscopic
Li *et al.* (2023) [76]	5-DOF Electromagnetic	Measuring object dimensions	Dynamic object measurement.	NR	NR	Tested by measuring kidney stones in a porcine animal
Scutelnic *et al.* (2022) [77]	Long-Wave Infrared (LWIR) camera cores	Calculation of the temperature of anatomical structures	Thermal and visible vision; Emissivity correction.	I2C and SPI	Yes	Laparoscopy
Fujimoto *et al.* (2022) [74]	Antenna sensor	Detect blood vessels covered by fatty tissue.	Longer distances	NR	NR	Proposed for blood vessel detection
Liang *et al.* (2022) [73]	Laser ultrasound	Detect ultrasound waves generated by laser pulses	Imaging instrumentation.	NR	NR	Gastrointestinal Endoscopy
Asci *et al.* (2022) [27]	Electrochemical sensors	pH detection	Expansion to other biomarkers.	SPI or UART	Yes Biosensor and 3D printed device from resin	
Giacoppo *et al.* (2022) [56]	Optical fibers	Transmit light and detect changes in the nearby environment	Impact of the fiber cutting angle; Sensitivity to ambient light.	NR	NR	Inserted through a working channel
Cheng *et al.* (2021) [69]	Electrodeposited iridium oxide	Wireless pH detection	Signal transmission; Sensitivity to energy reception.	NR	Yes (PDMS)	
Vedaei *et al.* (2021) [68]	IMU	Monitor the orientation and travel direction of the capsule.	External magnetic field may affect the IMU sensor.	I2C, SPI and UART	NR	
Calborean *et al.* (2022) [60]	Inductive proximity	Detection of small tumors	Basses collect signal.	NR	Yes (coating with biocompatible materials)	Laparoscopy
Zaichenko and Gurevich (2020) [75]	Fiber optic-based image	Prevents loss of information during image transmission	NR	NR	NR	Can be realised in all possible areas
Bințințan *et al.* (2020) [59]	Proximity	Location of small gastric and colorectal tumors	Low detection range	NR	Yes (coating with biocompatible materials)	Laparoscopy
Vilches *et al.* (2019) [62]	Interferometric	Analyses the interference to measure the distance from a surface to an object	Only detection of axial measurements; Ultra-small distance measurement; Sensitivity to interference.	NR	NR	Guided surgery
Maeda *et al.* (2018) [54]	Silicon MEMS	More detailed information by correlating pressure data with images	Possible Wireless interference; Technical Complexity.	NR	NR	Endoscopic surgery
Lee *et al.* (2017) [67]	3-Space Sensor Bluetooth	Measure acceleration and angular velocity	Accurate and frequent calibration.	NR	NR	Tested in a bronchoscopic exam
McCaffrey *et al.* (2015) [71]	Potentiostatic electrochemical sensor	Electrochemically examine the tract	In vivo tests required.	NR	Yes (PEEK biomaterial)	
Silva *et al.* (2015) [55]	Aluminum thin-film strain-gauge	Evaluate gastrointestinal motility, that is, the movements and contractions of muscles in the digestive system	Explore the dynamic response; Frequency performance.	NR	Yes (PDMS layer)	Applied to the upper gastrointestinal tract
Maeda *et al.* (2015) [52]	Silicon MEMS sensor	Monitor pressure inside the target organ	Difficulty handling the hood during operation; High risk of wire disconnection; Restriction of flexible bending of the endoscope.	NR	NR	Endoscopic surgery
Shao *et al.* (2014) [72]	Image sensor and physiological sensor	Provides morphological and physiological information	Ambient temperature can affect the stability of the output voltage.	NR	NR	
Holler *et al.* (2009) [66]	Triaxial MEMS inertial	Measure the impact of gravity in three direction	Unable to distinguish between translational acceleration and gravity.	I2C	NR	Endoscopic surgery
Lucesoli *et al.* (2008) [63]	Fiber optic	Measure the distance between endoscope and anatomical structure	Basses collect signal.	NR	NR	General endoscopy
Lucesoli *et al.* (2008) [64]	Distance sensor based on FOLCI technique	Measure the distance between endoscope and anatomical structure	Improve the light collected by the probe arm .	NR	NR	General endoscopy
Roh *et al.* (2008) [70]	PH	PH level measuring of the gullet and stomach	Maintain small size performance.	NR	Yes	Gastrointestinal Endosocopy

* NR: Not Reported.

3.3 Conclusions

As a final consideration, the interconnection of microcontrollers with communication protocols plays a crucial role in the efficient integration of sensors into electronic systems. The appropriate selection among protocols, such as UART, I2C, and SPI, is essential to optimize communication between devices, considering factors like speed, complexity, and system efficiency. The microcontrollers' ability to manage various protocols is critical for sensory systems, facilitating the efficient collection and transmission of data. This connection plays a central role in medical applications by enabling the acquisition of precise information.

The state-of-the-art review played a crucial role in providing a comprehensive overview of sensing systems applied to endoscopy. This research allowed for the identification and analysis of various types of sensors, highlighting their characteristics, applications, and performance. By exploring the diversity of available sensory approaches, valuable insights were gained into the current state of technology, assisting in understanding existing options to enhance the efficiency of endoscopic procedures. While analyzing the reviewed sensors, the lack of information on biosensors and material biocompatibility was emphasized, critical aspects to be considered in gastrointestinal endoscopic inspections. Additionally, only the authors Lee *et al.* [67] stood out as tests were conducted on patients, indicating that there is still a long way to go before this set of sensors is implemented in the market. The referenced works present good implementations but lack practical system information, such as materials used, the type of communication established, sensitivity to external factors, among others. Although these methods can offer interesting and potentially effective solutions, a conclusion to be drawn from the literature analysis is the absence of sensors focused on gastrointestinal endoscopy. Most of the works are designed for general endoscopy, sometimes for transluminal surgery (laparoscopy), and endoscopic capsules.

With these considerations in mind, the remainder of this document will describe the work that has been developed to address the identified gaps in the existing literature.

Chapter 4

Methodology

Chapter 4, dedicated to methodology, explores different approaches for project realization. Section 4.1 analyzes the overall structure and interconnection of the components. In Section 4.2, potential commercial sensors for implementation are presented, considering technical and economic criteria. In Section 4.3, potential commercial microcontrollers for implementation are discussed. Following that, in Section 4.4, the selection and analysis of essential software for PCB development are discussed. Following that, in Section 4.5, the 3D modeling of a prototype endoscope in SolidWorks is highlighted. Additionally, the consideration and evaluation of the biocompatibility of the material used to coat the coupling device are addressed. After the 3D modeling, Section 4.6 presents the development of a mockup of the system's graphical interface. Finally, in Section 4.7, some conclusions regarding the system development are presented.

4.1 System architecture

The architecture diagram, shown in Figure 4.1, for the development of a sensing system applied to an endoscope intended for conducting gastroendoscopy examinations is essential for understanding the interconnection and operation among the coupling module, sensors, integrated circuit, and peripheral device.

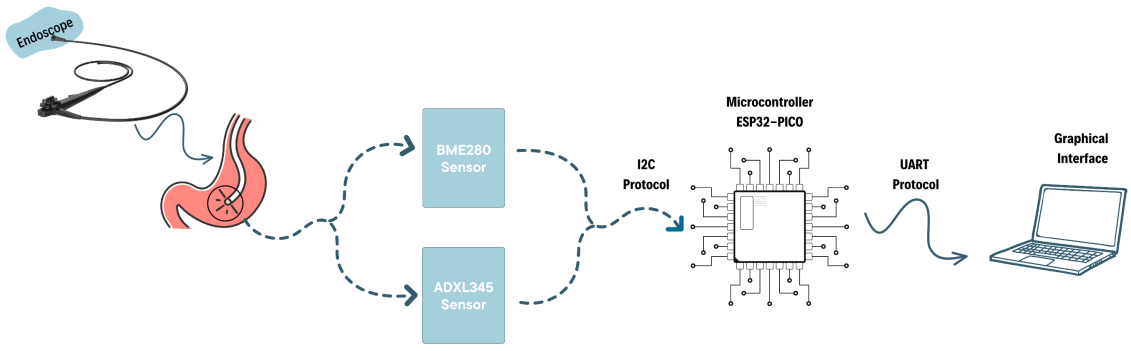

Figure 4.1: Architecture diagram.

The endoscope is equipped with a coupling module, designed and modeled in Solidworks software. This module incorporates two distinct types of sensors, referred to as A and B, located at the tip of the endoscope. Together, these sensors form a crucial detection module for capturing critical variables during the examination. Precise data acquired through the implemented sensors are then transmitted to the integrated circuit using the communication protocol. One of the possible protocols to be used is I2C because it is serial, synchronous, and not too complex. Through the same I2C protocol, this circuit is responsible for transferring the data to the peripheral device, where the doctor can access and interpret the information. These variables are crucial to assisting the doctor in an accurate diagnosis, providing a more comprehensive and detailed understanding of the internal environment during gastroendoscopy. The effective use of these sensors and the communication system significantly contributes to improving the quality and accuracy of medical diagnosis.

4.2 Sensors

In the endoscopic context, the strategic integration of specialized sensors and microcontrollers plays a fundamental role, enabling the acquisition of detailed information about the internal environment of the human body. These hardware components go beyond sensing, playing a crucial role in the dynamic communication of data. Sensors are pivotal in data collection, while microcontrollers act as the system's brain, efficiently coordinating the processing and transmission of this information through communication protocols. This collaboration between hardware and effective communication underscores the essential importance of hardware in the successful implementation of endoscopic systems that provide accurate and real-time information.

Considering that the use of biosensors may not be cost-effective, an overview of some possible commercial sensors for implementation is conducted throughout the thesis. The preferred approach involves selecting a biocompatible coating as an alternative to the use of biocompatible sensors, aiming not only to meet biocompatibility requirements but also to provide a more cost-effective solution for the developing system. The following table, Table 4.1, presents a comparative analysis of some potential sensors for implementation in the sensing system. It includes information about the type of sensor used, the appropriate communication protocol, resolution, dimensions, and specification ranges for each sensor, such as temperature, humidity, pressure, and acceleration, among others.

After studying a variety of commercially available sensors on the market and analyzing the information collected in the state of the art, the proposal is to develop a detection system that integrates an accelerometer and a pressure sensor.The selected sensor is the ADXL345, a 3-axis accelerometer that provides accurate acceleration data. The chosen pressure sensor is the BME280, which offers accurate pressure measurements. This approach aims to provide the physician with precise information about the measured variables, essential for accurate diagnosis in a clinical environment. This strategic choice seeks to maximize the utility of the system, ensuring that the

captured variables are relevant and provide valuable information to the physician during diagnostic procedures in a cost-effective manner.

When analyzing the Table 4.1 and considering the selected sensors, it is noteworthy that the commonly used communication protocol for this type of sensor is I2C.

Table 4.1: Potential sensors for system integration.

Sensor	Sensor Type	Communication Protocol	Resolution (Bits)	Dimensions (mm x mm)	Temperature Range (º C)	Humidity Range (%)	Pressure Range (kPa)	Acceleration Range (g)	Magnetic field range (uT)	Gyro Range (° / s)	Ambient light Range (lx)	Sensing Distance (mm)	Frequency Range (kHz)
TMP102 [78]	Temperature Sensor	I2C, SMBus	12	1.6 x 1.6	-40 to +125	NA	NA	NA	NA	NA	NA	NA	NA
MCP9808 [79]	Temperature Sensor	I2C, SMBus	12	21 x 13	-40 to +125	NA	NA	NA	NA	NA	NA	NA	NA
Si7021 [80]	Humidity and Temperature Sensor	I2C	12 to Humidity 14 to Temperature	3 x 3	-40 to +125	0 to 100	NA	NA	NA	NA	NA	NA	NA
HIH6130 [81]	Humidity and Temperature Sensor	I2C	14	4.9 x 6	-25 to +85	10 to 90	NA	NA	NA	NA	NA	NA	NA
BME280 [82]	Humidity, barometric pressure and ambient temperature	I2C, SPI	NA	2.5 x 2.5	–40 to +85	0 to 100	30 to 110	NA	NA	NA	NA	NA	NA
BMP280 [83]	Barometric Pressure sensor	I2C, SPI	16	2 x 2.5	–40 to +85	NA	30 to 110	NA	NA	NA	NA	NA	NA
MS5611-01BA03 [84]	Barometric Pressure sensor	I2C, SPI	24	5 x 3	–40 to +85	NA	1 to 120	NA	NA	NA	NA	NA	NA
ADXL345 [85]	3-axis accelerometer	I2C, SPI	13	3 x 5	–40 to +85	NA	NA	± 2 ± 4 ± 8 ± 16	NA	NA	NA	NA	NA
LIS3DH [86]	3-axis linear accelerometer	I2C, SPI	16	3 x 3	–40 to +85	NA	NA	± 2 ± 4 ± 8 ± 16	NA	NA	NA	NA	NA
VCNL4010 [87]	Proximity and Ambient light sensor	I2C	16	3.95 x 3.95	–25 to +85	NA	NA	NA	NA	NA	0.25 to 16 383	1 to 200	NA
LDC1614 [88]	Capacitance Proximity Sensor	I2C	28	4 x 4	–40 to +125	NA	NA	NA	NA	NA	NA	NA	1 to 10000
MPU-9250 [89]	IMU (Gyroscope, Accelerometer, and Magnetometer)	I2C, SPI	512	3 x 3	NA	NA	NA	± 2 ± 4 ± 8 ± 16	± 4800	± 250 500 1000 2000	NA	NA	NA
BH1750 [90]	Light intensity sensor	I2C	16	13.9 x 18.5	–40 to +85	NA	NA	NA	NA	NA	0.11 to 100000	NA	NA

* NA stands for Not Applicable.

4.3 Microcontrollers

Considering that the microcontroller acts as the central processing unit of the system, receiving data from sensors, performing processing operations to extract relevant information, and then coordinating the transmission of this data to other components or systems, Table 4.2 presents potential microcontrollers for implementation in the sensing system, along with their respective specifications. This table provides detailed information about the type of microcontroller, communication protocol, ADC resolution, memory size, RAM and ROM capacity, number of I/O ports, dimensions, and operating temperature range. These specifications are crucial for the careful selection of the microcontroller, ensuring its optimal compatibility and performance within the specific context of the sensing system.

Table 4.2: Potential microcontrollers for system integration.

Microcontroller	Communication Protocol	Resolution ADC (Bits)	Memory size (kB)	RAM size (kB)	I/O Number (I/O)	ROM size (kB)	Dimensions (mm) (length x height x width)	Temperature Range (°C)
ATMEGA328-PU [91]	I2C, SPI, UART	10	32	2	23	1	34.79 x 4.57 x 7.49	- 40 to +85
PIC16F877A-I/P [92]	I2C, SPI, UART	10	14	0.368	33	0.256	52.26 x 3.81 x 13.84	- 40 to +85
RP2040 [93]	I2C, SPI, UART, PWM, USB, PIO	12	16384	264	30	16	7 × 0.61 x 7	- 20 to +85
ESP32-PICO-D4 [94]	I2C, SPI, UART, among others	12	4096	520	34	448	7 × 0.94 x 7	–40 to +85
ATTINY85-20PU [95]	SPI	10	8	0.512	6	0.512	9.27 x 3.3 x 6.35	- 40 to +85
MSP430F2418TPM [96]	I2C, SPI	12	0.116	8	48	NR	10 x 1.4 x 10	- 40 to +105
STM32C031K4 [97]	I2C, SPI, UART	12	32	12	45	NR	7 x 7 x 0.5	- 40 to +125
CC2340R5 [98]	I2C, SPI, UART	12	0.512	36	26	12	5 x 5 x 1	- 40 to +125
MKL13Z32VLH4 [99]	I2C, SPI, UART	16	32	4	54	8	10 x 10 x 1.4	- 40 to +105
MKL14Z32VFM4 [100]	I2C, SPI, UART	12	32	4	28	NR	5 x 5 x 1	- 40 to +105

* NR stands for Not Referenced.

After gathering information about various types of commercial microcontrollers from different manufacturers, as presented in Table 4.2, it was observed that the commonly employed communication protocol for sensors of this type is I2C. Faced with this insight, the choice of microcontroller is guided by compatibility with the I2C protocol, considering that the sensors to be used in this prototype also operate through this protocol. This strategic decision ensures efficient integration between the microcontroller and the sensors, optimizing communication and facilitating system development. Taking into account the analysis of different microcontrollers, the microcontroller

to be used is the ESP32-PICO-D4. It is worth noting that, given the prototype phase of the project, future considerations and adjustments may be necessary as the system evolves to fully meet clinical and technical requirements.

In this context, in the development of this detection system, the key components were carefully selected to ensure optimal performance and efficiency. The chosen sensors were the ADXL345 for acceleration and the BME280 for pressure measurement, providing a wide range of essential information for medical diagnosis. In addition to these sensors, the ESP32-PICO-D4 microcontroller was selected due to its compatibility with the I2C protocol, facilitating integration and communication between system components. This combination of sensors and microcontroller not only ensures accuracy but also reliability of measurements.

4.4 PCB development

In order to carry out the development of printed circuit boards, there is a variety of specialized software available. These programs offer a wide range of tools for drawing schematics, routing traces to connect components, placing components, generating manufacturing files, and providing a component library. Some of the available programs include KiCad [1], Altium Designer [2], Eagle [3], and EasyEDA [4], among others. The choice of software depends on user preferences and the specific requirements of the project, as each one has unique production requirements.

In this dissertation, the software chosen is EasyEDA, which allows for easy interaction and understanding of components, operating in a highly intuitive manner. Additionally, it features a library with a diverse range of components, enabling the visualization of schematics in different ways and the development of the Gerber file for subsequent fabrication.

In the development of the PCB, it was decided to divide it into two to facilitate coupling and avoid interference in the insertion of the endoscope due to the size that a single complete PCB could have. Thus, to increase the system's efficiency, the components were distributed across two distinct PCBs, as illustrated in Figure 4.2. PCB A will be attached to the tip of the endoscope, responsible for collecting information through the sensors. Meanwhile, PCB B, installed in the control section of the instrument, receives and processes the data transmitted by PCB A. This includes information from the accelerometer, such as calibration values (x, y, z) and angles (roll, pitch), as well as data from the pressure sensor, including temperature, pressure, and humidity. This approach allows for a more efficient and organized implementation of the system, ensuring that functionalities are properly distributed and operate independently, while also facilitating the coupling and handling of the endoscope during medical procedures.

[1] https://www.kicad.org, accessed on 8/1/2024.
[2] https://www.altium.com/altium-designer, accessed on 8/1/2024.
[3] https://www.autodesk.com, accessed on 8/1/2024.
[4] https://easyeda.com, accessed on 8/1/2024.

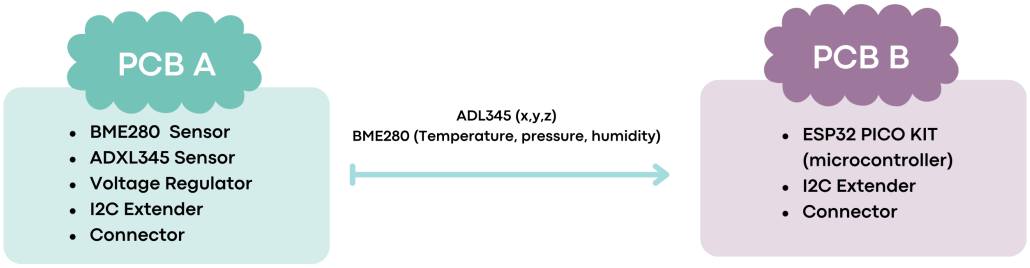

Figure 4.2: PCB A to PCB B connection diagram.

4.5 3D Modelling

From a long-term perspective and aiming to simulate the prototype, a 3D model of a commercial endoscope was developed concurrently, as illustrated in Figure 4.3, using SolidWorks [5]. The modeled endoscope was divided into parts, including the control part with buttons (b), handling pulleys (c), the coated tip of the endoscope (d), among others. Subsequently, the assembly of these parts was carried out, forming the complete product as depicted in (a). The goal is to develop a coupling model that will later be integrated into the sensing model, providing a comprehensive approach for the continuous advancement of the system.

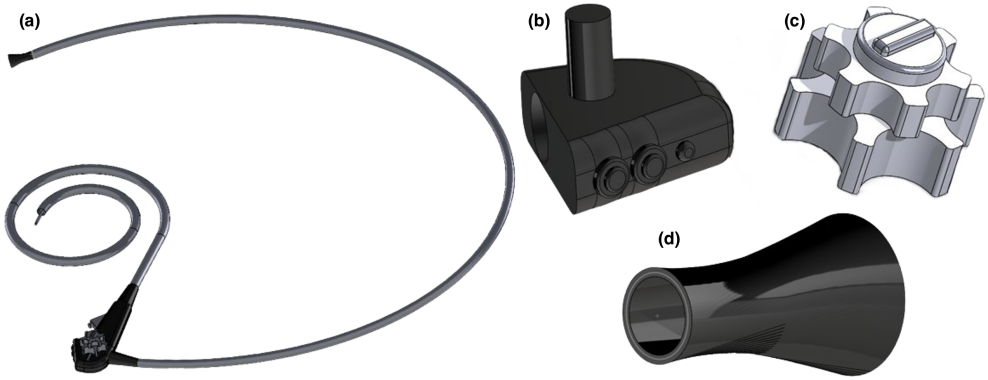

Figure 4.3: 3D modelling of the endoscope : (a) Total Endoscope; (b) Control Section; (c) Handling pulleys; (d) Tip Section.

Biocompatibility

Considering that the endoscope is a medical device that establishes direct contact with the patient's internal tissues and organs during diagnostic procedures, using a biocompatible sensing system coupled to the tip of the endoscope is a crucial factor. Biocompatibility refers to the ability of an implant material to function within the body without triggering adverse local or systemic responses. If the system's materials used in the endoscope are not biocompatible, it can lead to the occurrence of adverse reactions. Biomaterials that provoke little or no response from the organism are considered inert materials [101] [102].

[5] https://www.solidworks.com/, accessed on 27/12/2023.

From a medical standpoint, there are two main options to ensure patient safety when introducing electronic components at the tip of the endoscope. The first is to choose electronic components made of biocompatible materials, such as titanium or medical-grade polymers. The second option involves developing the system first and then coating the components with biocompatible materials, such as medical-grade polymers, to avoid adverse reactions in the patient. Both approaches aim to ensure the biocompatibility of the medical device and minimize any risk of complications during the endoscopic procedure [102]; however, there is the issue that biocompatible coatings are not always feasible. For instance, if a pressure sensor is fully coated, the sensitivity of the sensor membrane is lost. Applying a coating to this membrane can compromise the proper functioning of the system, representing one of its limitations.

4.6 Graphical interface

To develop the graphical user interface code, Python 3 [6] was chosen due to its simplicity and flexibility in creating visual applications. Python 3 offers a wide range of libraries, such as Tkinter, which facilitate the rapid and efficient development of graphical interfaces [103].

In order to facilitate the visualization of the variables collected during the diagnosis of medical endoscopy, the development of a graphic interface is essential to improve the interpretation and analysis of data by health professionals. As already mentioned, during endoscopy, information such as images, videos, and variables are collected, which need to be projected and understood quickly for an accurate diagnosis. A graphical interface allows this data to be presented clearly and intuitively, highlighting areas of interest and possible anomalies that might otherwise go unnoticed. This leads to the possibility of improving diagnosis, reduces human error and facilitates communication between healthcare professionals and patients. Therefore, an effective graphical interface enables a more accurate and efficient diagnosis, improving patient care [104].

In order to illustrate the desired vision for the graphic interface, a mockup was developed. The model shown in Figure 4.4 highlights the layout of the graphic elements and the interaction between the different components. This mockup serves as a visual representation of the proposed design, offering a concrete vision of how endoscopy data can be presented clearly and intuitively to healthcare professionals.

[6] https://www.python.orgch

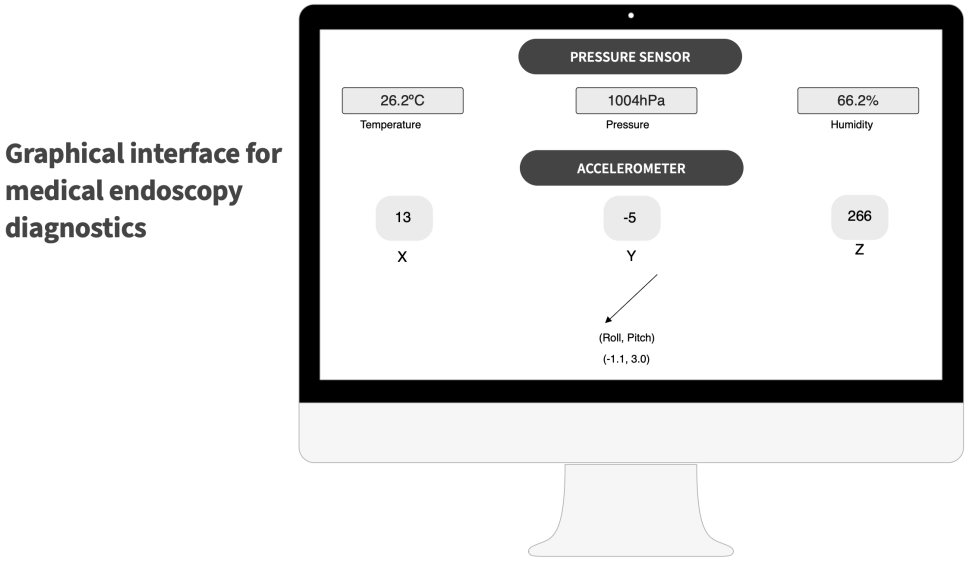

Figure 4.4: Mockup of the graphical interface.

The Figure 4.4 shows the variables collected by the pressure sensor, in the order of temperature, pressure and humidity, with their respective units. Then, the values are shown according the acceleration values along the x, y and z axes. Finally, the roll and pitch angles are shown, which represent the possible variations of the accelerometer. The vector is intended to help you understand the direction the endoscope takes in relation to the x and y axes. This visual representation provides a comprehensive view of the information captured during endoscopy.

4.7 Conclusions

In summary, the detection system developed for a gastroendoscopy endoscope aims to enhance medical diagnosis by capturing crucial variables during examinations. The selected accelerometer and pressure sensors were integrated into the system via an I2C circuit, transmitting data to a peripheral device accessible to healthcare professionals. Although initially prototypical, this approach stands out due to the strategic selection of relevant sensors and the additional consideration of the biocompatibility of electronic components, ensuring their compatibility during clinical procedures.

The software chosen for the development of the printed circuit board (PCB) was EasyEDA, which facilitates schematic design, has an extensive component library, allows component connections through traces, and supports the development of Gerber files for subsequent manufacturing. This versatile tool simplifies the development process and increases the overall efficiency of the project. It was concluded that two PCBs needed to be developed instead of a single PCB, a solution that allowed for the reduction of dimensions, making it possible to implement the PCB containing the sensors at the tip of the endoscope. Using SolidWorks, a 3D prototype of the endoscope was modeled, highlighting components such as the control section, handling pulleys, and the coated tip. Given that the medical endoscope makes direct contact with the interior of the human body, the

study of biocompatibility is essential for the device's proper functioning. Two options were considered, with the most financially viable being the implementation of a cover made of compatible material along with a biocompatible electronic coating film, instead of biocompatible sensors.

To ensure that the information collected during an endoscopic diagnosis is presented more clearly and objectively, a mock-up of the graphical interface was developed, offering a concrete and intuitive visual representation of how endoscopy data can be displayed to healthcare professionals. Accordingly, the proposed sensing system aims to enhance the quality and accuracy of medical diagnosis, adopting an integrated approach to drive the continuous advancement of the system.

Chapter 5

System implementation

Following the methodological proposal, Chapter 5 aims to present and explain the details of the System's implementation. Firstly, Section 5.1 presents the implanted prototype where the initial tests were carried out and then the final configuration of PCB A and PCB B. Next, Section 5.2 presents a new and improved version of the medical endoscope in SolidWorks, as well as the entire process of developing the biocompatible cover and film that will fit the diagnostic instrument. As a final result, a 3D print of the instrument will be presented. Section 5.3 is divided into the Subsection 5.3.1that sets out the initial ideas and considerations for developing a code to collect variables during diagnosis and the Subsection 5.3.2 that explains the development of the interface in MicroPython. Finally, in Section 5.4, final considerations are made about the results presented.

5.1 Prototype Implementation

The breadboard presented in the Figure 5.1, which contains various components such as the ESP32 microcontroller (A), the BME280 pressure sensor (B), and the ADXL345 accelerometer (C), was used as a prototype for the initial tests of the system developed on the PCB. This initial setup allowed for the preliminary tests to be carried out directly on the board, facilitating the development and validation of the code. During this phase, important adjustments were made to ensure the correct integration of the components and the overall functionality of the system. The two developed PCBs were integrated into a single board, which significantly simplified the entire development and testing process, allowing for a more cohesive analysis of the collected data. It is important to highlight that the I2C extender was not used on the breadboard, as there was no need for it in the initial prototyping phase. This resulted in a simpler and more efficient configuration for the initial tests, enabling quick identification and correction of any issues, and providing a solid foundation for subsequent tests with the final printed circuit board.

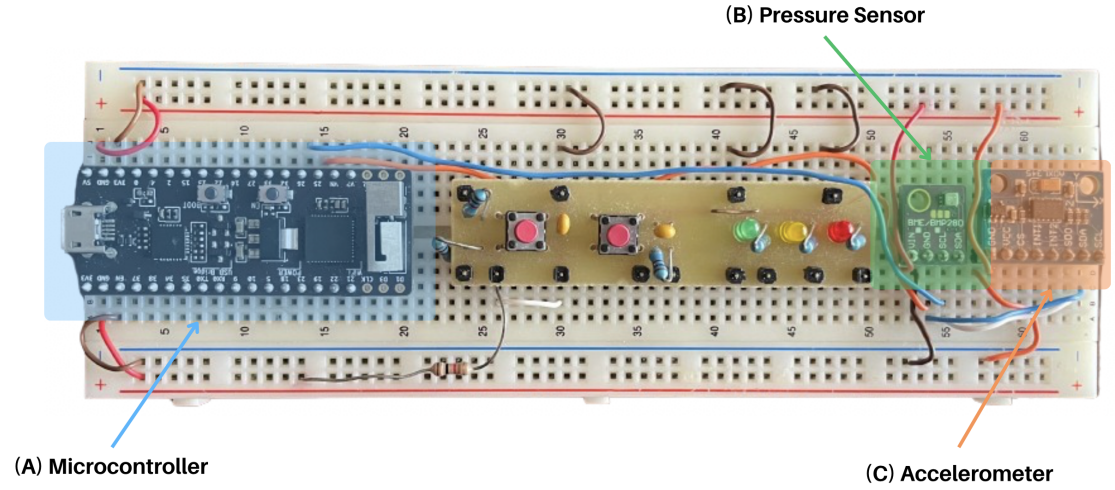

Figure 5.1: Breadboard : (a) ESP32 microcontroller; (b) BME280 sensor; (c) ADXL345 sensor.

By initially testing the components and code integration on the test board, it was possible to make critical adjustments before transferring the design to the final PCBs. Dividing the components into two separate, optimally designed PCBs was a necessary adaptation to meet the strict spatial requirements of the endoscope tip, ensuring that the final device was functional and practical in its intended medical application.

Due to the extremely small dimensions of the cover attached to the tip of the endoscope, the components were divided into two PCBs: one for the endoscope tip (PCB A), depicted in Figure 5.2, and another for the control part (PCB B), illustrated in Figure 5.3. A large rigid PCB would not be feasible for such a small structure. Therefore, the PCB at the endoscope tip was redesigned to optimize space to the maximum, resulting in a layout of 30 mm in length by 8 mm in width. This compact design was essential to accommodate the space constraints imposed by the medical device. PCB A, presented in the various models in Figure 5.2, was carefully sized to ensure its functionality within the physical limitations of the application. In addition to the requirement for small dimensions, even with maximum size reduction, a rigid PCB would still require a larger cover, hindering the entry of the endoscope into the body. To solve this problem, the most effective solution was to make PCB A flexible. The fact that it is flexible and has a rectangular shape allowed it to be adjusted to the internal circular shape of the cover without any issues regarding size or rigid material, ensuring that the PCB could be integrated efficiently and functionally at the tip of the endoscope.

- **PCB A**

  PCB A consists of a BME280 Pressure Sensor, an ADXL345 Sensor (accelerometer), a Voltage Regulator, an I2C Extender, specifically the P82B715 I2C Bus Extender, and a 4-pin connector with a 90-degree angle, as shown in Figure 4.2. The BME280 sensor is an environmental sensor that measures temperature, atmospheric pressure, and humidity. To incorporate this component into the PCB layout, a 4.7uF capacitor was used, as schematized

in the datasheet. The ADXL345 is a three-axis acceleration sensor. To design the schematic of this component, the use of 2 pull-up resistors of 4.7 k was necessary. Additionally, both the datasheet of the BME280 sensor and the ADXL345 sensor presented a voltage regulator, whose main purpose is to control the output voltage of an electrical circuit, ensuring that it remains constant. For this component, 4 capacitors of different capacitances were required. The I2C Extender is a device used to extend I2C communication beyond normal limits, allowing communication over longer distances. In addition to presenting connections for VCC and GND, it has 4 pins (SX/SDA and SY/SCL for data transfer and LX and LY for communication with the other I2C present on PCB B). Finally, the function of the 4-pin connector is to establish connection with the other PCB through pins 2 and 3, while pins 1 and 4 connect to GND and VCC, respectively. This PCB was designed to be incorporated at the tip of the endoscope, responsible for collecting variables through the sensors during the examination and transmitting them via the I2C communication protocol to PCB B. These components were placed on the layout as shown in Figure 5.2 (a), through searching for the component reference in the EasyEDA library. Following the information from the datasheets of each component, the necessary connections were made. As expected, all components were connected to VCC and GND to ensure the proper operation of the circuit.

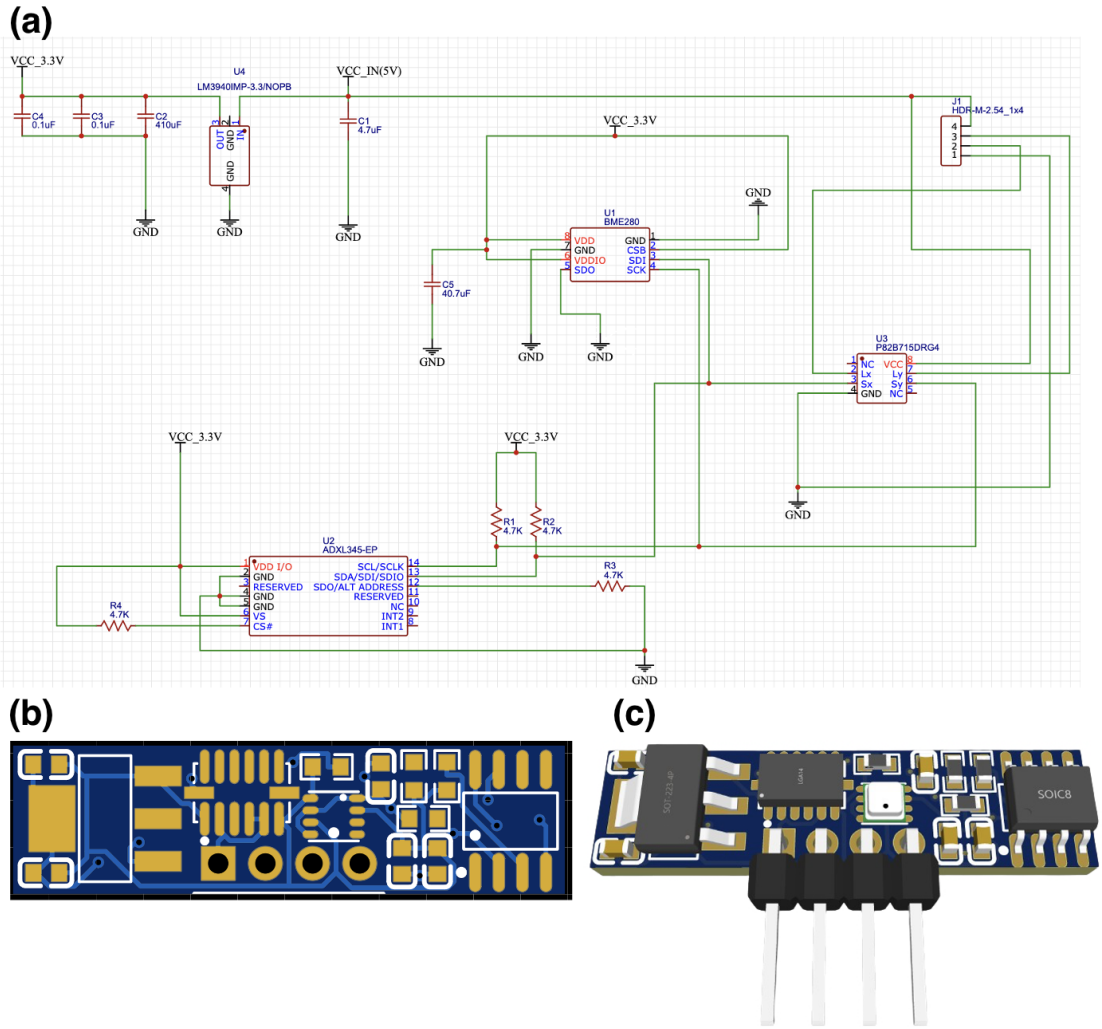

Figure 5.2: PCB A : (a) schematic; (b) 2D model; (c) 3D model.

- **PCB B**

  Based on Figure 4.2, it is possible to observe that the schematic of PCB B was developed incorporating the ESP32 PICO KIT microcontroller, which is a low-cost, low-power development board based on the ESP32, the I2C Extender, specifically the P82B715 I2C Bus Extender, a 4-pin connector, similar to the one on PCB A, and a 20-pin connector. This PCB was designed to be incorporated into the control part of the endoscope, responsible for receiving the data collected and provided by PCB A through the I2C communication protocol. Through searching for the component reference in the library, these components were added to the schematic as shown in Figure 5.3 (a). Analyzing the datasheet of each electronic component, the necessary connections were made. Additionally, two pull-up resistors were added to the output of the data transmission wires of the microcontroller (scl=Pin(25), sda=Pin(26)). Similarly to the previous PCB, all components were connected to VCC and GND to ensure the proper operation of the circuit.

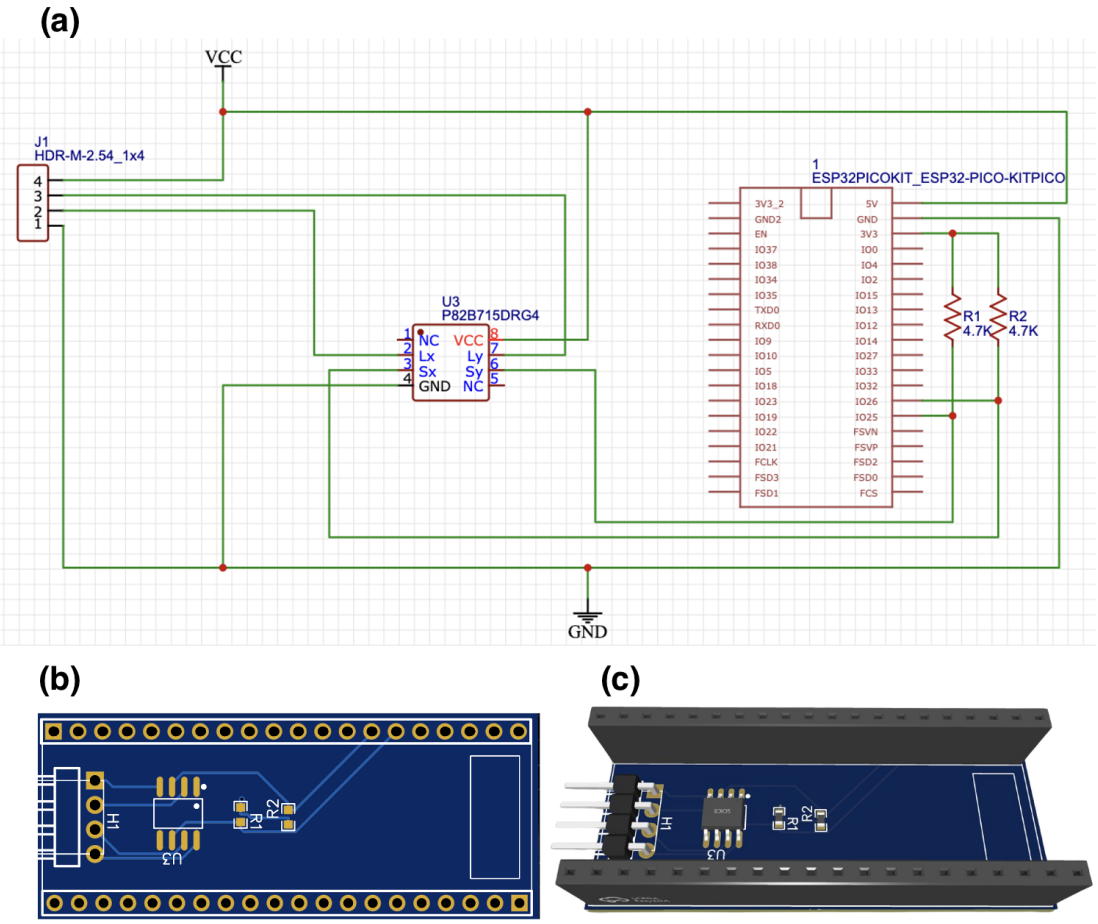

Figure 5.3: PCB B : (a) schematic; (b) 2D model; (c) 3D model.

To make the PCB visualization as realistic as possible, it is possible to switch from a schematic to a 2D view and then to a 3D model in EasyEDA. After creating a new project and designing the circuit shown in Figures 5.2 (a) and 5.3 (a), where components from the library were added and connected, it is important to validate the schematic to ensure that each component is correctly connected and there are no errors. Next, convert the schematic to a PCB using one of the program's features. Considering the desired final prototype, it is necessary to pay attention to the dimensions and placement of the components to maximize space utilization and reduce the final size of the PCB. In the PCB layout, the components are positioned, and the tracks are routed according to the schematic. The 2D visualization tools are then used to visually check the layout, as shown in Figures 5.2 (b) and 5.3 (b). To generate and visualize the 3D model, illustrated in Figures 5.2 (c) and 5.3 (c), a similar process is followed, with the added benefit of being able to interact with the model by rotating, zooming, and viewing the PCB from different angles. This is useful for verifying component placement and getting a more realistic sense of how the final board will look.

5.2 3D Modelling

The development of a new endoscope prototype using SolidWorks software is illustrated in Figure 5.4. This process includes the detailed 3D modeling of the diagnostic instrument's components, aiming to improve functionality and ergonomics compared to the previously presented model. The prototype was designed to optimize integration with advanced detection systems and include a biocompatible cover and film, ensuring both the effectiveness in collecting new diagnostic variables and the safety of the patient.

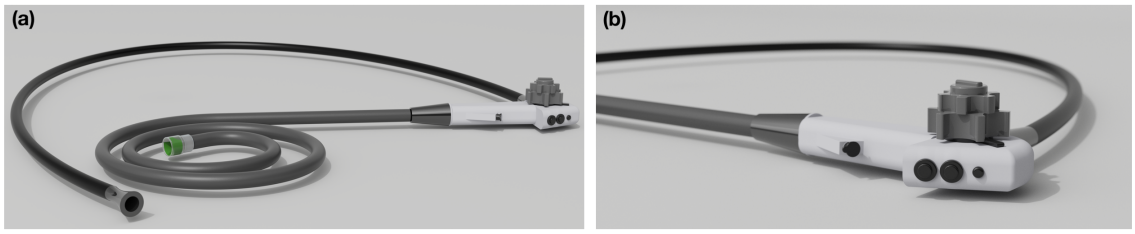

Figure 5.4: New 3D prototype of the endoscope: (a) Total Endoscope; (b) Control Section.

As seen in Figure 5.4 (a), there is a new device attached to the tip of the endoscope. This device is a transparent and biocompatible cover. The transparency allows for clear visualization during the procedure, while the biocompatible material minimizes the occurrence of adverse body reactions, thus reducing any risk of complications during the endoscopic procedure. This ensures patient safety and diagnostic efficacy. The cover is detailed more thoroughly in Figure 5.5.

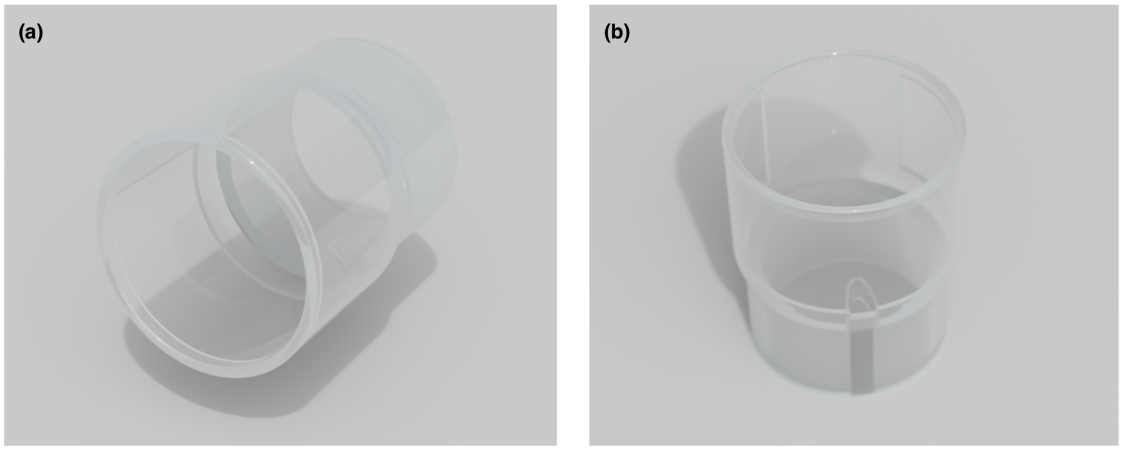

Figure 5.5: Cover attached to the tip of the endoscope : (a) side view; (b) top view.

Following the previously presented images, it can be assured that the main purpose of the cover is to support and protect the electronic components of the endoscope from contact with the human body. To attach the printed circuit board (PCB) to the endoscope cover, it was necessary to use some of the functionalities of the SolidWorks program. To achieve this, the design specifications were first defined through the determination of dimensions and angles. Next, the design

specification was executed using the "extrude" and "fillet" tools to ensure the desired shape of the cover. This resulted in the formation of a groove, using the "extrude" tool again, this time to create a recess in the internal surface of the cover that matches the dimensions of the flexible PCB where it will be secured. Additionally, further cutouts were needed to allow the passage of cables necessary for integration with the detection system, also protected by biocompatible material. This design, presented in Figure 5.6, not only protects the electronic components but also ensures that the integration between the endoscope and the detection system is stable and secure in collecting variables during the procedure.

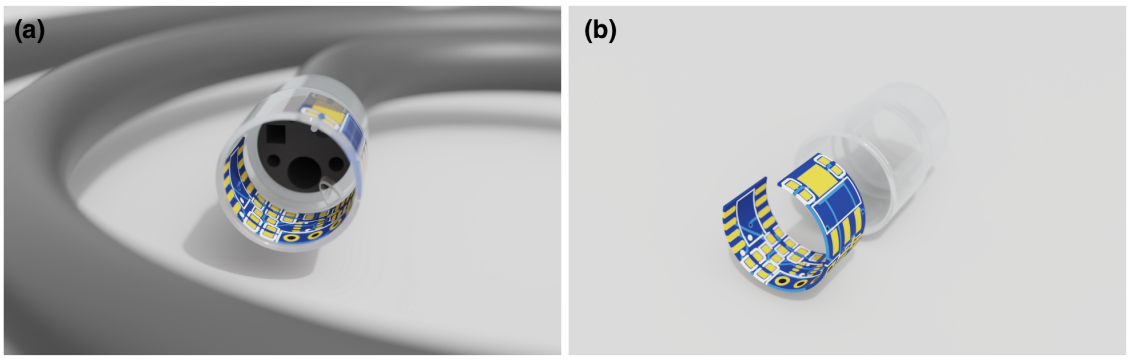

Figure 5.6: Cover with PCB attached : (a) front view; (b) side view.

To protect the electronic components present on the flexible PCB fixed to the cover, a biocompatible film was designed to cover the flexible PCB, avoiding potential adverse reactions from the human body during the endoscopic procedure. In SolidWorks, the design process of this film began with measuring the circumference of the transparent cover. Then, this circumference was drawn, considering the need for it to be slightly smaller than both the cover and the PCB, to ensure a proper fit, and the necessary measurement was removed. Using the "Extrude" tool, an extrusion was created to give thickness to the film, thus providing complete protection to the electronic components. The assembly of the cover with the flexible PCB and biocompatible film can be observed in Figure 5.7 through the side view (a) and top view (b).

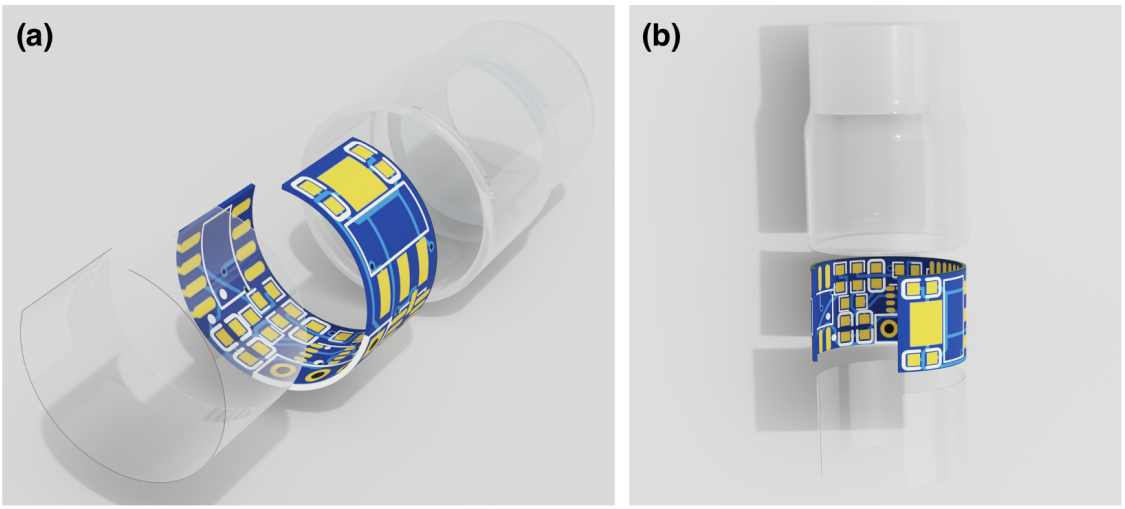

Figure 5.7: Cover with fixed PCB coated with biocompatible film: (a) side view; (b) top view.

As a final outcome, the 3D printing was carried out to validate the concept and demonstrate the feasibility of the solution. This printing was done using resin, providing an accurate physical representation of the developed prototype, including a representation of the flexible PCB inside it. The 3D print can be seen in Figure 5.8, showcasing the final product in detailed three-dimensional view.

Figure 5.8: 3D printing of the endoscope prototype: (a) front view; (b) side view; (c) top view.

5.3 Software

The development of software is a crucial step for the efficient integration and operation of the system's components. This section addresses aspects related to firmware and the graphical interface, both essential for the collection, processing, and presentation of sensor data during a medical diagnosis. The choice of tools and the implementation of the code are detailed to ensure robust performance and effective interaction.

5.3.1 Firmware

The integration of components is essential for the development of a system capable of providing accurate and relevant information during medical diagnosis, ensuring the effectiveness of data collection and proper processing of sensor variables for subsequent medical analysis. The code developed in this section represents a crucial component of the integration system, playing a fundamental role in gathering variables from the sensors during diagnosis, facilitating communication between the physical components of the system, the sensors, and the processing unit.

To develop the firmware code, the MicroPython [1] was chosen due to several advantages. Firstly, the Micropython language is clear and easy to use, facilitating development. In addition, MicroPython's real-time execution capability enables fast responses in embedded systems, which is crucial for efficiency and performance. Another significant advantage is the wide range of libraries available, which simplifies the implementation of advanced features. MicroPython is a compact implementation of Python 3, designed specifically to work on microcontrollers and more basic systems, providing direct and efficient integration with various components, such as sensors and actuators. It is therefore the ideal choice for projects that require speed, efficiency and ease of development [105] [106].

The code developed in MicroPython, as shown in the Figure 5.9, is used to collect sensor variables during a diagnosis, utilizing the ADXL345 and BME280 libraries, which were previously downloaded. The code begins by importing the necessary libraries for I2C communication, pin manipulation, UART communication, and timing. Next, the I2C communication is configured at a frequency of 100 kHz, using pins 25 (SCL) and 26 (SDA). To establish communication between the microcontroller and the sensors, instances of the BME280 and ADXL345 sensors are created, associating them with the configured I2C bus. Within an infinite loop, the code performs several operations every second. First, it reads the data from the BME280 sensor, which includes values for pressure, temperature, and humidity, and the data from the ADXL345 sensor, which provides acceleration values along the X, Y, and Z axes. Using these values, the code calculates the rotation and inclination (roll and pitch) using a specific function from the ADXL345 library. Finally, it combines all the read and calculated data into a single list and prints it. The loop repeats every second (‘sleep(1)‘).

The connection between the microcontroller and the developed interface is important for receiving, processing, and displaying data more clearly. This connection allows the microcontroller to receive information from the sensors, process it, and then send it to the interface for presentation. The goal of this integration is to facilitate the users' role, enabling them to see data in real-time, interact with the system, and make decisions based on this information. This bidirectional communication establishes a bridge between the sensors and the user, enabling faster and more informed decision-making, as well as facilitating remote monitoring.

[1] https://micropython.org language, accessed on 28/5/2024.

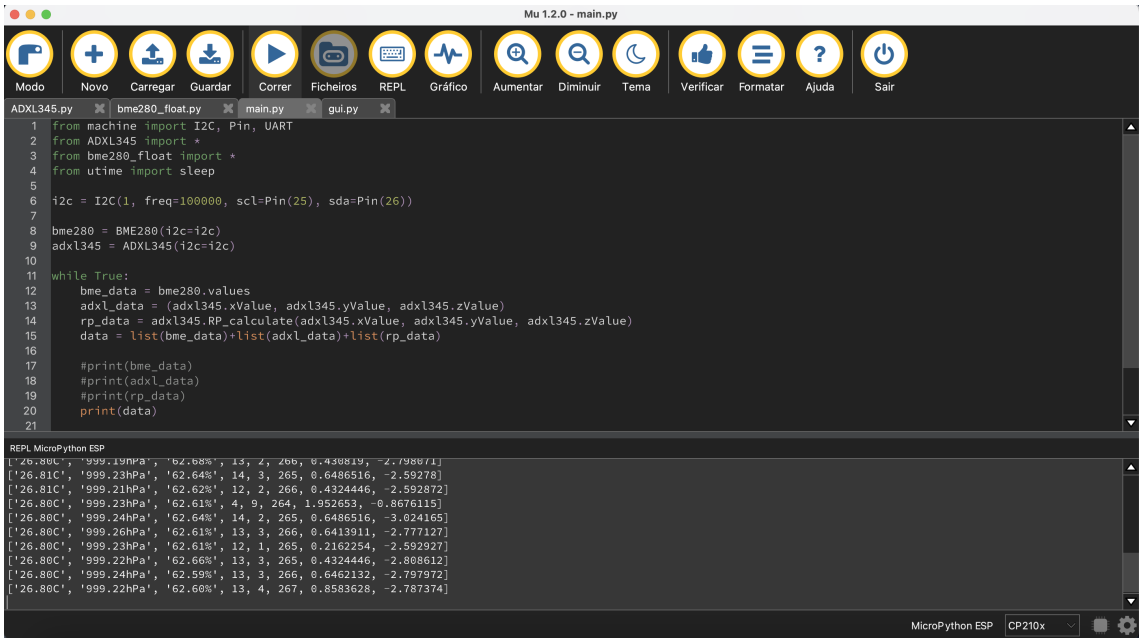

Figure 5.9: Micropython Editor.

5.3.2 Graphical interface

To recreate a graphical interface similar to the one illustrated in Figure 4.4, a Python code was developed using the Tkinter library, which was previously downloaded. This code displays real-time sensor data. Communication with the BME280 sensors (pressure, temperature, and humidity) and ADXL345 sensors (acceleration on the X, Y, and Z axes) is done through a serial port. First, the code imports the necessary libraries and configures serial communication with the specified port, through which sensor data is sent to the computer. In the interface, various labels are created to present the sensor readings. The ‘Vector‘ class is defined to perform operations used to calculate and display the roll and pitch based on the ADXL345 data. In the main loop (‘main‘), data is continuously read from the serial port, decoded, and separated into different variables for each sensor. These data are then displayed in the graphical interface on the corresponding labels, and the roll and pitch directions calculated from the ADXL345 data are visually updated. Additionally, the ‘GetCoords‘ function is used to calculate the acceleration values to draw a direction line based on the roll and pitch data.

Finally, the Python-developed interface, shown in Figure 5.10, is configured to update every second continuously, ensuring that sensor data is presented in real-time and dynamically. This code allows for the monitoring and display of sensor data during a diagnosis, providing a visual interface that facilitates the analysis and interpretation of the collected data.

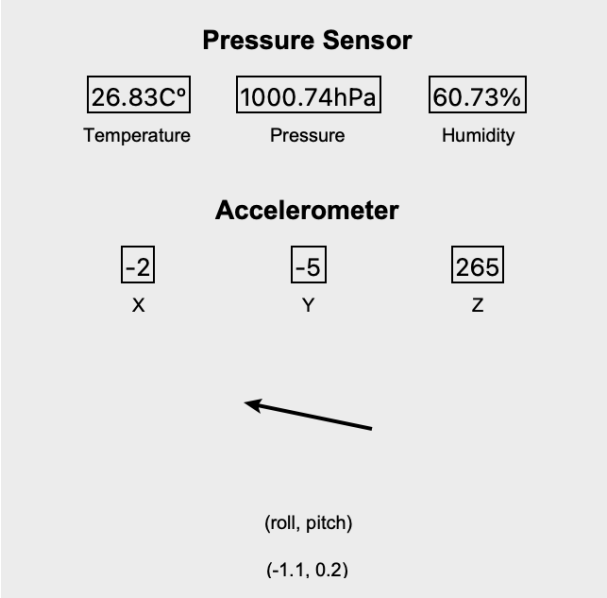

Figure 5.10: Interface developed in python.

From the variables presented in the graphical interface in Figure 5.10, the user can perform a clearer and more detailed analysis of the environment where the diagnosis is made. However, it is important to understand the meaning of these variables and their true functions in an endoscopy environment.

The pressure sensor provides three values:

- **Temperature: 27.14°C** - The temperature in the diagnostic environment allows for the detection of infections and ensures the safety of the procedure. It is essential to adhere to the manufacturer's temperature specifications to avoid improper disinfection and burns [107].
- **Pressure: 999.89 hPa** - This pressure is slightly below the standard atmospheric pressure (1013.25 hPa). It may indicate that the equipment is being used in a slightly elevated area. This variable is crucial for detecting anomalies, obstructions, and unwanted gas insufflations [107].
- **Humidity: 46.50%** - Adequate humidity levels help maintain patient comfort, image quality, and sensor performance [107].

The accelerometer provides calibration values for each axis (x, y, z). The units of these values are digital, binary, which were later converted to G's:

- **X: 8** - The X value indicates a slight horizontal tilt. In this case, it is almost aligned with the horizontal line, which is good for stability.
- **Y: -182** - The Y value suggests a significant tilt along the vertical axis, indicating that the equipment is tilted backward or downward.

- **Z: 191** - The high Z value indicates a strong acceleration along the vertical axis, possibly suggesting that the device is tilted.

The calculation of "roll" and "pitch" is a way of describing the orientation of an object in three dimensions. As shown in Figure 5.11, these values are used to determine the angle of inclination along the lateral axis, Y axis (pitch) and the angle of rotation along the longitudinal axis, X axis (roll) of an object such as a sensor in relation to the horizontal and vertical axes. The roll and pitch values are calculated using the accelerometer readings in the three axes (x, y, z). The mathematical expressions are based on trigonometric functions derived from the components of the acceleration vectors. The value $\frac{180}{\pi}$ is used in both expressions to convert the result from radians to degrees.

- **Roll**

$$\phi = \arctan\left(\frac{y}{z}\right) \times \frac{180}{\pi}$$

The angle Roll calculated from the accelerometer data is:

-44.2 - The negative roll indicates that the device is tilted to the left at a significant angle. In an endoscopy, this may mean that the device is being maneuvered into a curve or angle to visualize or reach a specific area.

- **Pitch**

$$\theta = \arctan\left(\frac{-x}{\sqrt{y^2+z^2}}\right) \times \frac{180}{\pi}$$

The angle Pitch calculated from the accelerometer data is:

-1.7 - The negative pitch indicates a slight downward tilt, which may be necessary to navigate through a cavity during the endoscopic procedure.

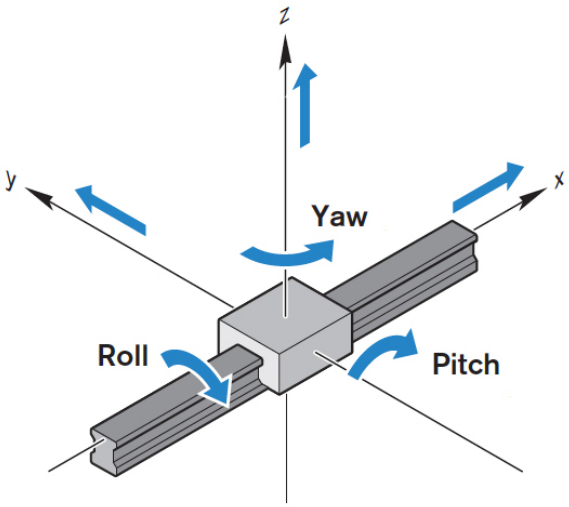

Figure 5.11: Roll and Pitch angle demonstration [108].

Finally, the directional arrow pointing to the left may indicate the current direction of movement or orientation of the endoscopic device. This is useful for the operator to understand the direction of insertion or maneuvering of the endoscope more perceptibly.

The acceleration values and the directional arrow provide information about the stability and direction of the device. Adequate temperature and humidity indicate that the equipment is operating in a controlled environment. These variables are fundamental to avoid damage and maintain safety during medical procedures. Therefore, the data provided in the image offer a comprehensive view of the environmental conditions and orientation of the endoscopic device, ensuring a more accurate and safe diagnosis.

The code provided reads data from a sensor via a serial port and displays this data in a graphical interface built with Tkinter. The temperature, pressure, and humidity data are displayed as strings with units, while the acceleration values along the axes (x, y, z) and angles (roll, pitch) data are displayed as numerical values. The data received through the serial port is processed and formatted for display. Here is an example of the structure of the received data:

['23.01C', '1007.12hPa', '64.86%', 28, 0, 269, 0.0, -5.964926]

The first three values pertain to the BME280 sensor (temperature, pressure, and humidity) and are strings with the corresponding unit. These values are displayed as strings with units to make the interface more readable and intuitive for the user, helping to avoid ambiguity. The remaining values are numerical (integers or floats) and pertain to the ADXL345 sensor, which collects the x, y, and z axis values, as well as the roll and pitch angles. These values are kept as numbers to facilitate further calculations and processing. For example, the roll and pitch values can be used to calculate the direction of a vector.

The difference in the formatting of the data (some as strings with units and others as numerical values) is generally determined by the library used to read the sensors or the way the data is sent by the microcontroller that collects the sensor data.

5.4 Conclusions

In this chapter, experimental results obtained from the development and integration of a new endoscope prototype were presented, aiming to optimize functionality and safety during diagnostic procedures.

Due to the extremely small dimensions of the cover at the tip of the endoscope, the components were divided into two PCBs: one for the endoscope tip and another for the control part. The PCB at the endoscope tip was redesigned to optimize space. To address dimension constraints, PCB A was made flexible, conforming to the internal circular shape of the cover. PCB A, containing pressure and motion sensors (BME280 and ADXL345), a voltage regulator, and an I2C extender, collects variables during examination and transmits them to PCB B via the I2C protocol. PCB B, located in the control part, incorporates an ESP32 microcontroller and receives data collected by PCB A, transmitting it to an external device for visualization. Both PCBs were designed

and validated using EasyEDA, allowing for efficient integration into the endoscopic device. The development of a new endoscope prototype, modeled in 3D using SolidWorks, resulted in significant improvements in functionality and ergonomics. The prototype includes a biocompatible cover and film, optimizing integration with detection systems and ensuring patient safety. The transparent cover allows for clear visualization during procedures and protects electronic components, minimizing adverse reactions. The flexible PCB, mounted at the endoscope tip, is secured to the cover using specific SolidWorks functionalities to ensure a precise fit. Additional cutouts allow for the passage of cables necessary for integration with the detection system, all protected by biocompatible material. To protect electronic components, a biocompatible film was designed to cover the flexible PCB, ensuring complete protection. Concept validation was achieved through 3D printing in resin, demonstrating the feasibility of the proposed solution. To facilitate visualization of variables collected during endoscopic diagnosis, a graphical interface was developed in Python using Tkinter to display data from BME280 and ADXL345 sensors in real-time via serial communication. The interface presents temperature, pressure, humidity, and the roll and pitch angles of the endoscope. The code developed in MicroPython plays a fundamental role in collecting these variables, facilitating communication between physical system components, sensors, and the processing unit. This code, using the ADXL345 and BME280 libraries, enables continuous reading of pressure, temperature, humidity, and acceleration data, calculating rotation and inclination, and presenting this information clearly and objectively to healthcare professionals through the developed interface.

The results obtained demonstrate the effectiveness of the new endoscope prototype, combining compact design, biocompatible materials, and advanced technology to offer safer and more accurate diagnostics.

Chapter 6

Experimental Results

This Chapter 6 presents an analysis of the results obtained in the experiment. In Section 6.1, the experimental results of the ADXL345 accelerometer are presented through the analysis of tilt levels. Section 6.2 presents the experimental results of the BME280 temperature sensor. Finally, in Section 6.3, an analysis and discussion of the results obtained through the comparison between the developed system and the real system are provided.

6.1 ADXl345 Sensor Results

To ensure that the ADXL345 sensor is functioning correctly, an experiment was conducted. Using a compass and a protractor, a circle was drawn on a sheet of paper with angles marked at 15-degree intervals, totaling 360 degrees. After setting up the equipment, the breadboard was positioned at the center of the circle, with the sensor pointing to 0 degrees to start the experiment. The setup involved mounting the ADXL345 sensor on a breadboard and connecting it to a microcontroller, such as the ESP32, using I2C connections for data communication. A program developed in Micropython was used to read and record the sensor measurements. The sensor's position was initially verified to ensure that the acceleration readings were correct when the sensor was at rest. Next, the breadboard was rotated in increments of 15 degrees until a complete rotation was achieved. At each 15-degree increment, the acceleration values along the X, Y and Z axes were recorded on the computer using the Micropython program, which collected the sensor variables in real-time.

To identify variations in the coordinates according to different inclinations (angles) and to ensure the accuracy of the results, the experiment was conducted on the vertical plane. Figure 6.1 shows the setups for the measurements performed. This approach allowed for a detailed analysis of the ADXL345 sensor's behavior in different positions, ensuring its proper functionality.

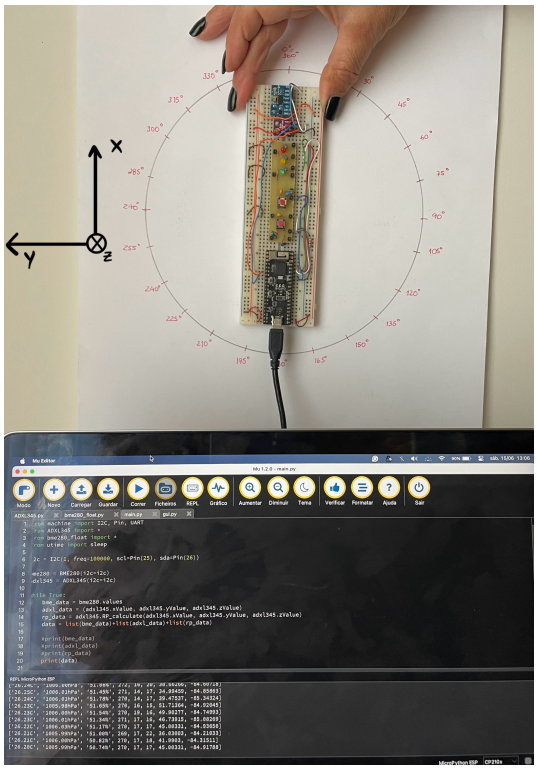

Figure 6.1: Setup for vertical measurements.

- **Vertical measurement**

  To obtain the coordinates in the vertical plane, an experiment was set up on a leveled wall with a mounting board perpendicular to the horizontal plane, rotating it in 15-degree increments as depicted in Figure 6.1. The collected data were processed using a developed program and transferred to Table 6.1, where the X, Y, and Z axis coordinates were recorded.

  The ADXL345 sensor, a three-axis accelerometer, measures acceleration in the X, Y, and Z directions. When placed at the center of a vertically drawn circle on a sheet of paper and rotated, the sensor rotates around its Z-axis. During this rotation, the values of the X and Y coordinates vary following sine and cosine functions of the rotation angle (θ): $X = A \cdot \cos(\theta)$ and $Y = A \cdot \sin(\theta)$, where Arepresents the measured acceleration, typically influenced by gravity. The Z-axis acceleration value should remain constant with low values close to zero, reflecting gravitational acceleration. This value will be positive if the sensor's Z-axis points downward, towards the center of the Earth. Rotation around the Z-axis does not significantly affect the Z-axis reading because it does not alter the gravitational component along that axis. The data collected during the measurements were converted to gravity units (G), as detailed in Table 6.1. The ADXL345 sensor operates with a 10-bit resolution, allowing it to represent acceleration values from 0 to 1024 units along the X, Y and Z axes. According to the sensor's datasheet, configured for a ±2g range, each bit corresponds to approximately 0.004g. Thus, with 10 bits, the sensor can measure up to ±2g, equivalent to 1024 units, implying that 1g of acceleration is approximately 256 units (1024 units / 4g). Converting

the acceleration values along the X, Y and Z axes into units of gravity units (G‘s) facilitates direct interpretation of acceleration relative to standard gravitational force. On a horizontal plane, where the Z-axis shows a consistent reading of about 256 units, close to 1g, this indicates that the sensor predominantly detects gravitational acceleration along this axis. This consistent reading reflects the gravitational force perpendicular to the surface of the horizontal plane.

This conversion to gravity units simplifies the analysis and comparison of data with other measurements, enabling straightforward interpretation of measured acceleration relative to gravity.

Table 6.1: Table with acceleration values for different slopes.

	Vertical measurement					
Angle	**X**	**Y**	**Z**	**X (G)**	**Y (G)**	**Z (G)**
0º=360º	270	9	14	1.055	0.035	0.055
15º	259	78	16	1.012	0.305	0.063
30º	234	136	17	0.914	0.531	0.066
45º	193	189	18	0.754	0.738	0.070
60º	140	229	20	0.547	0.895	0.078
75º	79	255	18	0.309	0.996	0.070
90º	13	262	16	0.051	1.023	0.063
105º	-62	252	17	-0.242	0.984	0.066
120º	-123	222	17	-0.480	0.867	0.066
135º	-173	183	16	-0.676	0.715	0.063
150º	-210	129	16	-0.820	0.504	0.063
165º	-235	69	15	-0.918	0.270	0.059
180º	-243	5	13	-0.949	0.020	0.051
195º	-234	-65	9	-0.914	-0.254	0.035
210º	-205	-128	7	-0.801	-0.500	0.027
225º	-167	-178	5	-0.652	-0.695	0.020
240º	-117	-216	3	-0.457	-0.844	0.012
255º	-49	-245	3	-0.191	-0.957	0.012
270º	19	-253	3	0.074	-0.988	0.012
285º	85	-242	3	0.332	-0.945	0.012
300º	148	-213	4	0.578	-0.832	0.016
315º	202	-170	6	0.789	-0.664	0.023
330º	237	-123	9	0.926	-0.480	0.035
345º	262	-60	14	1.023	-0.234	0.055

From the analysis of the values presented in the Table 6.1, it is confirmed that the measurements of the ADXL345 sensor at different angles show that the X and Y coordinates follow an expected sinusoidal pattern, as illustrated in Figure 6.2, reflecting the variation of gravitational acceleration with the angles of rotation. At 0º to 360º, X is 1.055 G and Y is 0.035 G, indicating the predominance of acceleration along the X axis. At 90º and 270º, Y reaches its peaks (1.023 G and -0.988 G), while X is close to zero, demonstrating the rotation perpendicular to gravity. At 180º, X is -0.949 G and Y is 0.020 G, showing the

opposition to the initial X axis. The Z-axis acceleration value remains almost constant and low, varying between 0.012 G and 0.078 G, which confirms that rotation around the Z-axis does not significantly affect the reading. The values close to zero for the Z-axis acceleration are due to factors such as the sensor not being fully seated on the breadboard and slight tilting, which cause minor deviations from the intended zero value. This reaffirms the precision and functionality of the ADXL345 sensor under different inclinations.

The analysis of the values in Table 6.1 shows that the measurements of the ADXL345 sensor at different angles exhibit an expected sinusoidal pattern for the acceleration values along the X and Y axes, as illustrated in Figure 6.2. This pattern reflects the variation in gravitational acceleration with the angles of rotation. From 0º to 360º, the X acceleration value is 1.055 G, and the Y acceleration value is 0.035 G, indicating predominant acceleration along the X axis. At 90º and 270º, the Y acceleration value reaches its peaks (1.023 G and -0.988 G, respectively), while the X acceleration value is close to zero, demonstrating rotation perpendicular to gravity. At 180º, the X acceleration value is -0.949 G, and the Y acceleration value is 0.020 G, showing opposition to the initial X axis. The Z acceleration value remains almost constant and low, varying between 0.012 G and 0.078 G. This indicates that rotation around the Z axis does not significantly affect its reading. Although a zero value is expected for the Z coordinate, it shows values very close to zero due to some factors. These factors include the sensor not being fully seated on the breadboard, which can cause it to tilt slightly, resulting in small deviations. Thus, instead of an exact zero, the values are very close to zero. Overall, these results reaffirm the precision and functionality of the ADXL345 sensor at different inclinations.

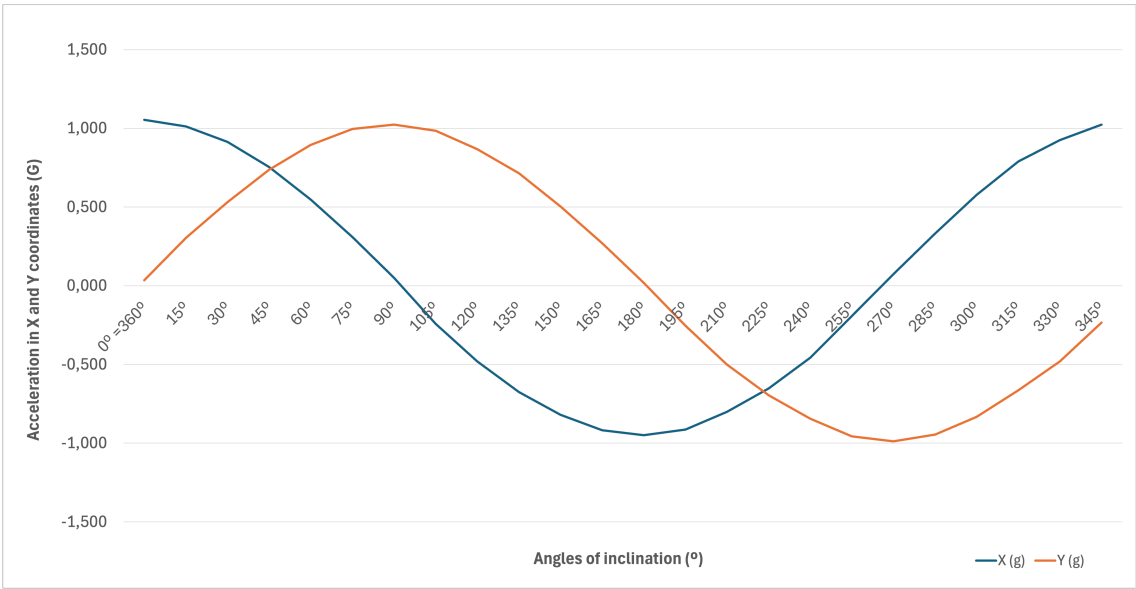

Figure 6.2: Graph showing acceleration in X and Y coordinates at different inclinations.

The graph of acceleration readings on the X and Y axes of the ADXL345 sensor, shown

in Figure 6.2, exhibits sinusoidal patterns when the sensor is rotated around the Z axis, as theoretically expected. On the X axis, acceleration varies from a maximum positive near 1 G at 0º and 360º, decreases to zero at 90º, becomes negative near -1 G at 180º, and returns to zero at 270º. On the Y axis, acceleration starts at zero at 0º, reaches a maximum positive near 1 G at 90º, returns to zero at 180º, becomes negative near -1 G at 270º, and returns to zero at 360º. These patterns reflect the expected behavior for uniform rotational motion. The accuracy of the ADXL345 in measuring gravitational acceleration at different inclinations is affirmed by the clarity of the oscillations in the graph. Additionally, the stability of the readings, not displayed on the Z axis as mentioned, reinforces its ability to maintain consistency even during rotations around the Z axis.

6.2 BME280 Sensor Results

In order to understand and validate the correct operation of the BME280 sensor, a comparative experiment was carried out with two other commercial sensors, illustrated in Figure 6.3. Sensor A used was the Thermometer/Hygrometer EQUATION DIGITAL, capable of measuring both temperature and humidity. Meanwhile, Sensor B, the Thermometer Indoor/Outdoor EQUATION model, measures only temperature with values displayed to one decimal place. All three sensors were subjected to identical environmental conditions and for the same duration, ensuring precise comparison of the collected data. To encompass a wide range of temperature and humidity variations, the sensors were exposed to different locations and conditions throughout the day, including standard ambient temperature, inside a refrigerator, direct sunlight exposure, and outdoor exposure under cloudy and rainy conditions. Each location was chosen to provide varying environmental challenges, enabling a comprehensive assessment of the sensors' measurement capabilities across diverse conditions. The data collection process involved using a breadboard connected to a computer, where the BME280 sensor was interfaced alongside an ESP32 microcontroller. Data were recorded and monitored in real-time using a program developed in Micropython, specifically designed to collect variables from the BME280 sensor, including temperature and humidity.

The experiment was structured to ensure each sensor was placed in its designated location, allowing sufficient time for stabilization before data collection commenced. Following each measurement session, the data were transferred to a table for comparative analysis. This analysis was segmented into temperature and humidity, providing a clear and detailed understanding of the BME280 sensor's performance under different environmental conditions. This systematic approach not only verified the accuracy and performance of the BME280 sensor but also yielded valuable insights into its reliability and applicability across various scenarios, encompassing both temperature and humidity measurements.

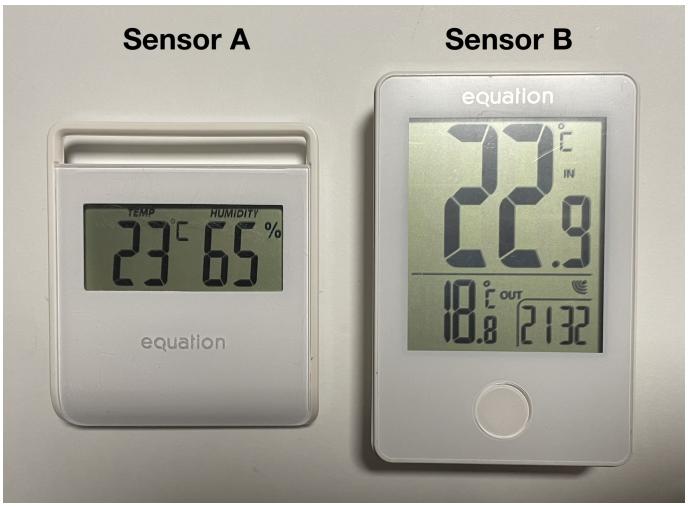

Figure 6.3: Comercial Sensors.

- **Temperature measurements**

  The data presented in Table 6.2 provides a comparison of the temperature measurements between the BME280 sensor and two commercial sensors, Sensor A and Sensor B. It can be seen that the BME280 sensor's measurements are, in most cases, close to the values obtained by the reference sensors, with some variations. To calculate the absolute error in temperature measurement, the readings from Sensor B were taken as the true value because it has one decimal place, making its readings more accurate. It is important to note that the error calculation unit is according to the corresponding quantity, i.e. in the case of temperature, the absolute error is in (ºC), just as the humidity error is in (%). The formula used to calculate the absolute error was:

$$\textit{Absolute Error} = \textit{Real Value} - \textit{BME280 Sensor Value} \tag{6.1}$$

  The following table presents the collected temperature data from the three sensors (BME280, Sensor A, and Sensor B (Real Sensor)) across different samples, along with the calculated absolute error:

  The temperature readings from the BME280 sensor are generally close to those from Sensors A and B, with minor differences in certain samples. The analysis of the absolute error, which represents the difference between the BME280 sensor and Sensor B values, reveals that the most significant variations occur in samples 4 and 6, with errors of 1.02 and 1.40, respectively. These variations can be attributed to rapid environmental fluctuations or the sensor not being properly placed, which could cause a slight tilt and potentially affect the resolution of the results. On the other hand, for samples 2 and 7, the associated error is relatively low, at 0.13 and 0.05, respectively, indicating a high accuracy of the BME280 sensor.

Table 6.2: Table of temperature values collected from the sensors (ºC).

Samples	BME280 Sensor (ºC)	Sensor A (ºC)	Sensor B (ºC)	Absolute Error
1	6.24	6	6.5	0.26
2	6.67	7	6.8	0.13
3	7.56	8	8.3	0.74
4	16.78	17	17.8	1.02
5	24.85	25	25.2	0.35
6	25.3	23	23.9	1.40
7	26.25	26	26.2	0.05
8	35.47	34	34.3	1.17
9	39.93	38	38.7	1.23
10	41.07	40	41.8	0.73

To highlight the data presented in Table 6.2, a scatter plot was created, shown in Figure 6.4, where the X-axis represents the values measured by Sensor B, and the Y-axis represents the values measured by the BME280 sensor. Each point on the graph corresponds to a specific sample.

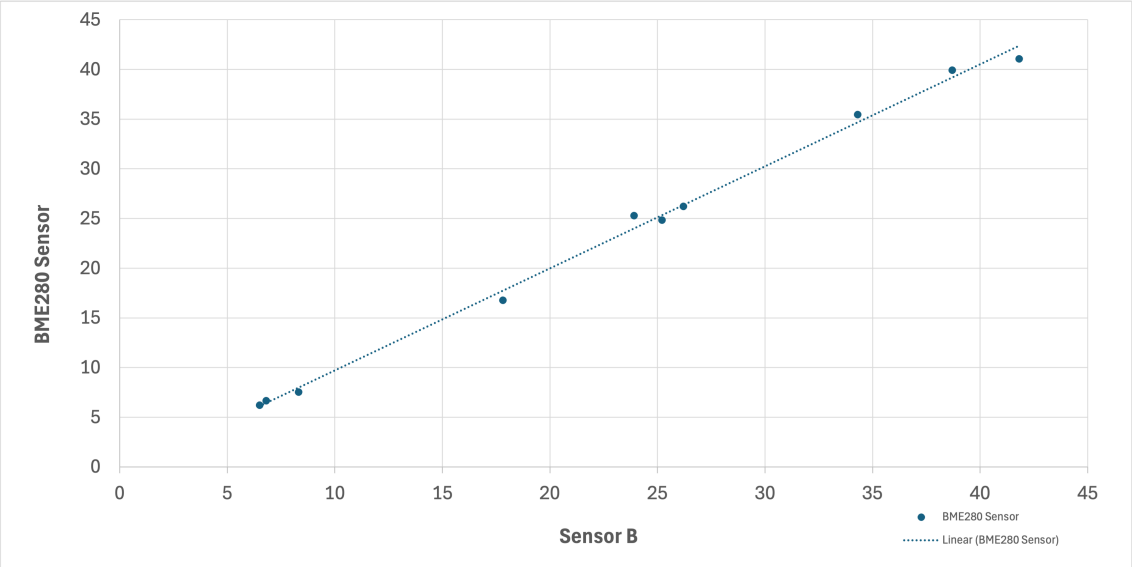

Figure 6.4: Temperature measurements graph.

The scatter plot shown in Figure 6.4 illustrates the relationship between temperature measurements from the BME280 sensor and Sensor B, considered the most accurate. A strong linear correlation between the two datasets is evident, as indicated by the dashed trend line. Most data points align closely around this line, suggesting that temperature readings from the BME280 are closely aligned with those from Sensor B. While there are some minor differences in individual points, particularly at extreme temperatures, the overall consistency of points around the trend line suggests that the BME280 sensor provides accurate and reliable

measurements compared to commercial sensors. This validates the utility of the BME280 for temperature measurements across various conditions. Therefore, the BME280 sensor can be considered a practical and effective tool for applications requiring temperature monitoring.

- **Humidity measurements**

The data presented in Table 6.3 provide a comparison of humidity measurements between the BME280 sensor and Sensor A.

Table 6.3: Table of humidity values collected from the sensors (%).

Samples	BME280 Sensor (%)	Sensor A (%)	Absolute Error
1	27.85	31	3.15
2	32.11	39	6.89
3	33.66	39	5.34
4	39.45	41	1.55
5	38.77	46	7.23
6	52.83	47	5.83
7	36.06	49	12.98
8	61.33	58	3.33
9	64.61	60	4.61
10	87.21	85	2.21

Using Sensor A as the reference to calculate the absolute error, significant variations in the results can be observed. For example, samples 7 and 5 show the highest absolute errors, reaching 12.98 and 7.23, respectively, indicating significant differences between the BME280 and Sensor A measurements in terms of humidity. Samples 2 and 3 also present considerable absolute errors, with values of 6.89 and 5.34, respectively, although lower compared to samples 7 and 5. Conversely, samples 10, 4, and 1 have the lowest absolute errors of 2.21, 1.55, and 3.15, respectively, showing good agreement between the BME280 and Sensor A under these humidity conditions. This highlights the importance of considering the accuracy of the BME280 sensor in different usage contexts to optimize the precision of humidity measurements. To calculate the absolute error in humidity measurements, the same formula mentioned earlier for temperature error calculation was used.

To visualize the data from Table 6.3 more clearly, a scatter plot was created where the X-axis represents measurements from Sensor A, considered as the reference in this case, while the Y-axis represents corresponding measurements from the BME280 sensor for humidity. Similar to the temperature graph, each point on the plot represents a specific sample.

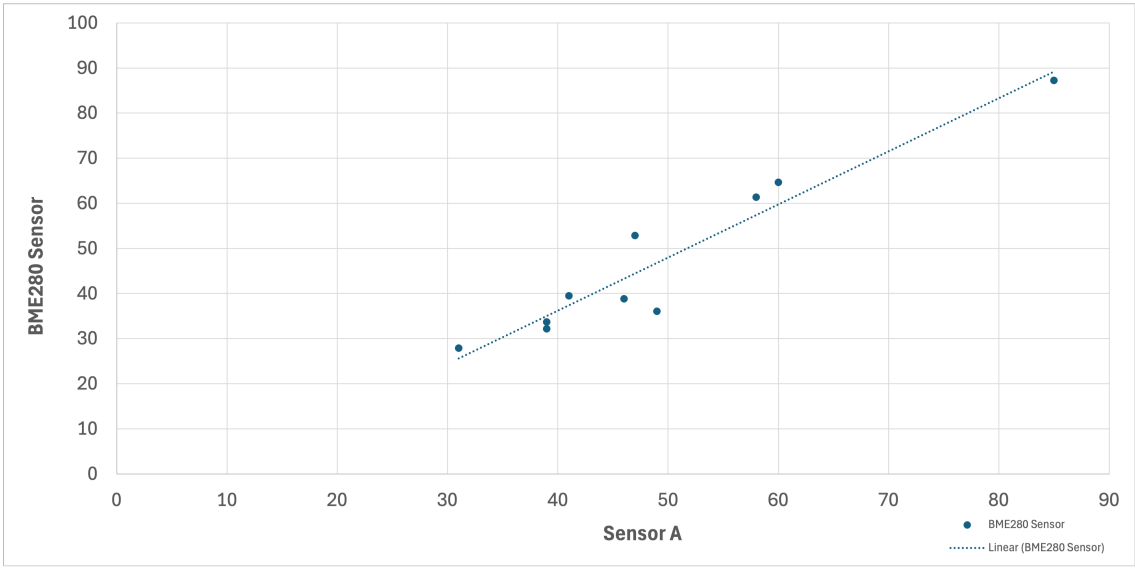

Figure 6.5: Humidity measurements graph.

The graph, represented in Figure 6.5, reveals the relationship between the readings of two humidity sensors. The graph includes a dotted trend line suggesting a positive linear relationship between the measurements of the two sensors. Although the correlation is not perfect, it is generally observed that as Sensor A readings increase, BME280 sensor readings also increase. Most points are distributed along the trend line, indicating that BME280 sensor measurements are often close to Sensor A measurements. Points that deviate more from the trend line may represent samples where larger absolute errors were observed. For instance, samples with higher absolute errors (such as samples 7 and 5 mentioned earlier) can be identified as points that deviate more from the trend line. Despite the minor variations observed in some samples, the accuracy and overall stability of the measurements along the correlation line validate the BME280 as a reliable choice for applications requiring humidity monitoring.

6.3 Results Discussion

The experiments conducted with the ADXL345 sensor in the vertical plane demonstrated its capability to accurately detect and record variations in acceleration along the X, Y, and Z axes. In the vertical plane experiments, the ADXL345 sensor exhibited sinusoidal variations in the values of the X and Y axes depending on the rotation angle, reflecting changes in the gravitational component measured by the sensor. The Z-axis remained stable at low values close to zero, indicating reliable detection of gravitational acceleration. This consistency reinforces the correct functionality of the ADXL345 sensor in detecting acceleration variations across different planes. Regarding the BME280 sensor used for temperature measurements, based on the analysis of the collected

data, it is confirmed that the BME280 sensor exhibits good accuracy and reliability across a variety of measurement conditions compared to commercial sensors. Comparative analyses revealed minimal variations, but the BME280 sensor maintained consistent precision in temperature measurement. In terms of humidity measurement, the BME280 sensor showed greater variability compared to the reference sensor, especially under high humidity conditions. While it demonstrated good accuracy under stable humidity conditions, additional adjustments may be necessary to optimize the precision of the BME280 sensor in different usage contexts.

In conclusion, the results highlight both the ADXL345 and BME280 sensors as effective tools for precise measurements of acceleration, temperature, and humidity under a variety of experimental conditions. These findings underscore the utility and applicability of these sensors in diverse technological and scientific applications.

Chapter 7

Conclusion and future Work

The development of the sensor module for gastroendoscopic instruments represents a significant advancement in the field of medical diagnostics. Chapter 7 addresses the main conclusions of the work conducted in Section 7.1 and presents directions for future research in Section 7.2, with the aim of further enhancing the developed technology and expanding its applications.

7.1 Conclusions

The integration of sensor technology into gastroendoscopic instruments represents a significant advance in medical diagnostics. This dissertation developed a sensorization module that improves the functionality of traditional endoscopes by incorporating pressure sensor and accelerometer. The detailed analysis of commercial sensors and microcontrollers, combined with the rigorous methodology for developing the system, resulted in a prototype capable of providing diagnostic data in real time.

The results of this research underline the potential of sensor endoscopy to revolutionize diagnostic procedures. By offering additional variables, such as pressure and acceleration data, this technology provides medical professionals with a more comprehensive understanding of the gastrointestinal environment. This can lead to more accurate diagnoses, timely interventions and better outcomes for patients. The sensors were integrated into the endoscope with the aim of not compromising its operational integrity or the quality of the visual information, proving that advanced sensor modules can coexist with existing endoscopic functionalities. Experimental validation confirmed the system's effectiveness in improving the accuracy and safety of gastroendoscopic procedures. The pressure sensor reliably detected variations in gastric pressure, which can indicate disturbances, while the accelerometer ensured accurate visualization of the gastrointestinal mucosa, helping to detect lesions. These capabilities highlight the importance of real-time data acquisition to increase diagnostic accuracy and reduce the risk of complications. The biocompatibility of the materials used to encapsulate the sensors was another critical aspect addressed in this dissertation. Ensuring that electronic components do not induce adverse reactions when in contact with body tissues is fundamental to patient safety. The study concluded that coating electronic

components with biocompatible materials offers an effective and economically viable solution, avoiding the need for inherently biocompatible sensors; however, this research has also identified several limitations and areas for future work. One significant limitation is the system's reliance on wired connections, which can restrict the mobility of the endoscope and pose a risk of disconnection. Future research should explore wireless communication options to improve the flexibility and reliability of the system. The potential of sensor endoscopy extends beyond gastroenterology. Similar sensor modules could be adapted for use in other types of endoscopic procedures, such as bronchoscopy, cystoscopy and laparoscopy, broadening the impact of this technology in various medical fields. This adaptability underlines the versatility of sensor technology in medical diagnostics.

In conclusion, this dissertation highlights the substantial benefits of integrating sensor technology into endoscopic instruments. The proposed sensor system not only increases the accuracy and safety of gastroendoscopic procedures, but also paves the way for future innovations in medical diagnostics. Continued research and development in this field is essential to realize the full potential of sensor endoscopy, ultimately leading to better care and outcomes for patients. This paper advocates the continued advancement and adoption of innovative technologies in medical practice to keep pace with evolving healthcare needs.

7.2 Future Work

The prototype developed in this dissertation achieved its objective by providing the development of an endoscope that includes different variables, which served to analyze and improve the performance of a diagnosis made by a specialist doctor during an endoscopy in everyday scenarios.

That said, there is room for improvement. To make the prototype more immersive and realistic, there are several aspects that can be enhanced in the future. Optimizing the underlying code is crucial for improving the graphical interface with the variables presented to the specialist. By improving the interface, the results obtained during the medical diagnosis will become more intuitive and easier to read, enhancing the overall experience for doctors and providing a more realistic and precise analysis. The use of smaller electronic components or even the implementation of biosensors would also improve this experience, increasing the sense of safety and simplifying its implementation. To evaluate the endoscope's performance in a real-world setting, it is important to apply it to patients and conduct assessments. The integration of new sensors in the sheath that will be attached to the endoscope's tip, coated with biocompatible material, will allow the collection of additional crucial variables for the diagnosis. These sensors will provide important information to the doctor during the diagnosis, such as temperature, pressure, and humidity, as well as the acceleration and orientation of the endoscope tip relative to the walls of the examined organ.

There are more critical situations that occur in real life that were not evaluated and could be designed to improve this experience. The incorporation of specific scenarios that simulate different clinical conditions, such as the presence of lesions or obstructions, and the implementation of a

controlled environment where factors such as time and precision are essential, are examples of new critical situations that can be explored to enhance the performance of the endoscope.

References

[1] W.Y. Lau, M.D., C.K. Leow, and Arthur K.C. Li. History of endoscopic and laparoscopic surgery. *WO R L D Journal of SURGERY*, pages 444–453, 1997. URL: https://link.springer.com/article/10.1007/PL00012268#citeas.

[2] Timothy Keen and Corinne Brooks. Principles of gastrointestinal endoscopy. *Surgery (Oxford)*, 41(2):100–105, 2023. URL: https://www.sciencedirect.com/science/article/pii/S026393192200237X, doi:https://doi.org/10.1016/j.mpsur.2022.11.005.

[3] American Cancer Society. Endosocpy. https://www.cancer.org/cancer/diagnosis-staging/tests/endoscopy.html. Online; accessed 1 May 2023.

[4] Axel Boese, Cora Wex, Roland Croner, Uwe Bernd Liehr, Johann Jakob Wendler, Jochen Weigt, Thorsten Walles, Ulrich Vorwerk, Christoph Hubertus Lohmann, Michael Friebe, and Alfredo Illanes. Endoscopic imaging technology today, 5 2022. doi:10.3390/diagnostics12051262.

[5] Marcia Irene Canto, Marcia Cruz-Correa, and Dayna Early. *Gender Difference in Gastrointestinal Endoscopy*, volume 1, pages 477–489. Elsevier Inc., May 2007. Copyright: Copyright 2021 Elsevier B.V., All rights reserved. doi:10.1016/B978-012440905-7/50313-3.

[6] Piet C. De Groen. History of the endoscope [scanning our past]. *Proceedings of the IEEE*, 105:1987–1995, 10 2017. doi:10.1109/JPROC.2017.2742858.

[7] Niehls Kurniawan and Martin Keuchel. Flexible gastro-intestinal endoscopy — clinical challenges and technical achievements, 2017. doi:10.1016/j.csbj.2017.01.004.

[8] Strategic Market Research. A Surprising Over 250 million Endoscopies Are Performed Each Year Globally. https://www.strategicmarketresearch.com/blogs/endoscopies-performed-each-year. Online; accessed 1 May 2023.

[9] Anand Krishnan, Zhilin Zeng, Amin Talebi Bezmin Abadi, Decai Zhang, Rui Wang, Zhaoqi Li, and Shaojun Liu. Open access edited by reviewed by global, regional, and national burden of ff digestive diseases in countries and territories from to oooo, 2022. URL: https://www.ncbi.nlm.nih.gov/pmc/articles/PMC10088561/.

[10] Melina Arnold, Christian C. Abnet, Rachel E. Neale, Jerome Vignat, Edward L. Giovannucci, Katherine A. McGlynn, and Freddie Bray. Global burden of 5 major types of gastrointestinal cancer. *Gastroenterology*, 159:335–349.e15, 7 2020. doi:10.1053/j.gastro.2020.02.068.

[11] World Health Organization. Cancer Today. https://gco.iarc.fr/today/online-analysis-pie?v=2020&mode=cancer&mode_population=continents&population=900&populations=620&key=total&sex=0&cancer=39&type=0&statistic=1&prevalence=0&population_group=0&ages_group%5B%5D=0&ages_group%5B%5D=17&nb_items=7&group_cancer=1&include_nmsc=1&include_nmsc_other=1&half_pie=0&donut=0. Online; accessed 1 May 2023.

[12] MEDANTA. Having an endoscopy can have a number of benefits. https://www.medanta.org/patient-education-blog/having-an-endoscopy-can-have-a-number-of-benefits. Online; accessed 1 May 2023.

[13] David Crosby, Sangeeta Bhatia, Kevin M. Brindle, Lisa M. Coussens, Caroline Dive, Mark Emberton, Sadik Esener, Rebecca C. Fitzgerald, Sanjiv S. Gambhir, Peter Kuhn, Timothy R. Rebbeck, and Shankar Balasubramanian. Early detection of cancer, 3 2022. doi:10.1126/science.aay9040.

[14] Hua Li, Xiaohua Hou, Rong Lin, Mengke Fan, Suya Pang, Longjie Jiang, Qian Liu, and Ling Fu. Advanced endoscopic methods in gastrointestinal diseases: A systematic review, 2019. doi:10.21037/qims.2019.05.16.

[15] Beverley Greenwood-Van Meerveld, Anthony C. Johnson, and David Grundy. Gastrointestinal physiology and function. *Handbook of Experimental Pharmacology*, 239, 1 2017. doi:10.1007/164_2016_118.

[16] Birmingham gastroenterology. All About the Upper GI Tract. https://bgapc.com/all-about-the-upper-gi-tract/. Online; accessed 1 May 2023.

[17] Saint Luke‘s. Upper GI Endoscopy. https://www.saintlukeskc.org/health-library/upper-gi-endoscopy-0. Online; accessed 1 May 2023.

[18] Ravindra Kale. Role of short-chain fatty acids in modulation of gut health. *Article in Journal of Food Agriculture and Environment*, 2005. URL: https://www.researchgate.net/publication/364954411, doi:10.1234/4.2022.5605.

[19] Divyanshoo R. Kohli and John Baillie. *How Endoscopes Work*, pages 24–31. Elsevier, 1 2019. doi:10.1016/B978-0-323-41509-5.00003-7.

[20] Pat Holland. Flexible endoscopes: Structure and function. *Gastroenterology nursing : the official journal of the Society of Gastroenterology Nurses and Associates*, 24:116–9, 05 2001. doi:10.1097/00001610-200105000-00003.

[21] Olympus Global. Structure and Components of Endoscopes. https://www.olympus-global.com/ir/data/pdf/ir_medical_2022e_08.pdf. Online; accessed 1 May 2023.

[22] FUJINON. MANUAL DE OPERAÇÃO (Preparação e Operação). https://www.labor-med.com.br/images/produtos/EG-201FP.pdf. Online; accessed 1 May 2023.

[23] Jean Marc Canard, Jean Christophe Létard, and Anne Marie Lennon. *Diagnostic Upper Endoscopy*, pages 84–100. Elsevier, 9 2011. doi:10.1016/B978-0-7020-3128-1.00003-1.

[24] Murat Akarsu and Cevher Akarsu. Evaluation of new technologies in gastrointestinal endoscopy, 1 2018. doi:10.4293/JSLS.2017.00053.

[25] Eduardo Guimarães Hourneaux de Moura. New technologies and techniques in gastrointestinal endoscopy. *Interventions in Obesity Diabetes*, 1, 5 2018. doi:10.31031/iod.2018.01.000517.

[26] Dylan Miley, Leonardo Bertoncello Machado, Calvin Condo, Albert E. Jergens, Kyoung-Jin Yoon, and Santosh Pandey. Video capsule endoscopy and ingestible electronics: Emerging trends in sensors, circuits, materials, telemetry, optics, and rapid reading software. *Advanced Devices Instrumentation*, 2021, 1 2021. doi:10.34133/2021/9854040.

[27] Cihan Asci, Ruben Del-Rio-Ruiz, Atul Sharma, and Sameer Sonkusale. Ingestible ph sensing capsule with thread-based electrochemical sensors. volume 2022-October. Institute of Electrical and Electronics Engineers Inc., 2022. doi:10.1109/SENSORS52175.2022.9967347.

[28] Miguel Muñoz-Navas. Capsule endoscopy, 4 2009. doi:10.3748/wjg.15.1584.

[29] Basil Akpunonu, Jeannine Hummell, Joseph D. Akpunonu, and Shahab Ud Din. Capsule endoscopy in gastrointestinal disease: Evaluation, diagnosis, and treatment. *Cleveland Clinic Journal of Medicine*, 89:200–211, 2022. doi:10.3949/ccjm.89a.20061.

[30] Ana Maria Singeap, Carol Stanciu, and Anca Trifan. Capsule endoscopy: The road ahead, 1 2016. doi:10.3748/wjg.v22.i1.369.

[31] Medtronic. PillCam™ SB 3 Capsule Endoscopy System. https://www.medtronic.com/covidien/en-us/products/capsule-endoscopy/pillcam-sb3-system.html. Online; accessed 13 december 2023.

[32] Olympus. ENDOCAPSULE 10 System . https://www.olympus.pt/medical/en/Products-and-Solutions/Products/Product/ENDOCAPSULE-10-System.html. Online; accessed 13 december 2023.

[33] JINCHAN. OMOM HD Capsule Endoscopy Platform. https://www.jinshangroup.com/solutions/omom-hd-capsule-endoscopy-camera/. Online; accessed 13 december 2023.

[34] Mayo Clinic. Capsule endoscopyt. https://www.mayoclinic.org/tests-procedures/capsule-endoscopy/about/pac-20393366. Online; accessed 1 May 2023.

[35] Vaibhav Gupta and Pooja Sharma. Fundamental of integrated circuit, 2018. URL: https://www.ijltemas.in/DigitalLibrary/Vol.7Issue4/04-06.pdf.

[36] Lenovo. What is an integrated circuit (IC)? https://www.lenovo.com/us/en/glossary/integrated-circuit/?orgRef=https%253A%252F%252Fwww.google.com%252F. Online; accessed 15 december 2023.

[37] Britânica. integrated circuit. https://www.britannica.com/technology/integrated-circuit/The-p-n-junction. Online; accessed 15 december 2023.

[38] Joseph Wu. A basic guide to i 2 c, 2022. URL: https://www.ti.com/lit/an/sbaa565/sbaa565.pdf?ts=1702563469788&ref_url=https%253A%252F%252Fwww.google.com%252F.

[39] Hélio Sousa Mendonça. SPI e I2C. https://paginas.fe.up.pt/~hsm/misc/old/comp/spi-e-i2c/. Online; accessed 15 december 2023.

[40] Kevin M. Lynch, Nicholas Marchuk, and Matthew L. Elwin. *UART*, pages 159–176. Elsevier, 2016. doi:10.1016/b978-0-12-420165-1.00011-1.

[41] Eric Peña and Mary Grace Legaspi. Uart: A hardware communication protocol understanding universal asynchronous receiver/transmitter, 2020. URL: https://www.analog.com/media/en/analog-dialogue/volume-54/number-4/uart-a-hardware-communication-protocol.pdf.

[42] Arnold S. Berger. *Serial communication systems*, pages 239–256. Elsevier, 2020. doi:10.1016/b978-0-12-817811-9.00011-9.

[43] Kevin M. Lynch, Nicholas Marchuk, and Matthew L. Elwin. *SPI Communication*, pages 177–190. Elsevier, 2016. doi:10.1016/b978-0-12-420165-1.00012-3.

[44] Dawound Shenouda Dawound. Digital System Design - Use of microcontroller. https://www.riverpublishers.com/pdf/ebook/RP_E9788793102293.pdf. Online; accessed 20 december 2023.

[45] Microcontroller Division Applications. MICROCONTROLLERS MADE EASY. https://www.st.com/resource/en/application_note/cd00003980-microcontrollers-made-easy-stmicroelectronics.pdf. Online; accessed 20 december 2023.

[46] Alyssa J. Pasquale, Ph.D. Microcontrollers. https://doctor-pasquale.com/wp-content/uploads/2021/02/The-Yellow-Book.pdf. Online; accessed 20 december 2023.

[47] Circuit Basics. Introduction to microcontrollers. https://www.circuitbasics.com/introduction-to-microcontrolleres/. Online; accessed 20 december 2023.

[48] iPCB. What is a PCB Board? https://www.ipcb.com/pcb-board.html. Online; accessed 8 january 2024.

[49] FS Tech. O que é um PCB? https://www.fs-pcba.com/pt/what-does-pcb-mean/. Online; accessed 8 january 2024.

[50] Alexander Meining, Alexander Hann, and Karl Hermann Fuchs. Innovations in gi-endoscopy, 2022. doi:10.1016/j.ajg.2022.06.003.

[51] Rui Li, Gongping Chen, Yu Dai, Yu zhao, Guangming Xia, Jianxun Zhang, Liang Cui, and Xiaotao Yin. Object dimension measurement based on monocular endoscope and 5-dof sensor. *Measurement: Journal of the International Measurement Confederation*, 206, 1 2023. doi:10.1016/j.measurement.2022.112293.

[52] Yusaku Maeda, Kohei Maeda, Hideki Kobara, Hirohito Mori, and Hidekuni Takao. A pressure/temperature sensor embedded in an endoscopy hood for intraluminal monitoring during flexible endoscopic operation. In *2015 IEEE SENSORS*, pages 1–4, 2015. doi:10.1109/ICSENS.2015.7370372.

[53] Hyung Chul Lee, Chul Woo Jung, and Hee Chan Kim. Real-time endoscopic image orientation correction system using an accelerometer and gyrosensor. *PLoS ONE*, 12, 11 2017. doi:10.1371/journal.pone.0186691.

[54] Yusaku Maeda, Hirohito Mori, Tomoaki Nakagawa, and Hidekuni Takao. Fully wireless pressure sensor based on endoscopy images. volume 57. Japan Society of Applied Physics, 4 2018. doi:10.7567/JJAP.57.04FC05.

[55] L. R. Silva, P. J. Sousa, L. M. Goncalves, and G. Minas. Flexible gastrointestinal motility pressure sensors based on aluminum thin-film strain-gauge arrays. *Journal of Micromechanics and Microengineering*, 25, 7 2015. doi:10.1088/0960-1317/25/7/074007.

[56] Giuliano A. Giacoppo, Lena Schunter, and Peter P. Pott. Impact of the fiber cutting angle on fiber optic proximity sensors in endoscopy. *Current Directions in Biomedical Engineering*, 8:37–40, 8 2022. doi:10.1515/cdbme-2022-1011.

[57] Christian Marzi, Hosam Alagi, Olivia Rau, Jochen Hampe, Jan Gerrit Korvink, Bjorn Hein, and Franziska Mathis-Ullrich. Capacitive proximity sensor for non-contact endoscope localization. pages 9614–9620. Institute of Electrical and Electronics Engineers Inc., 2022. doi:10.1109/ICRA46639.2022.9811734.

[58] Giuliano A. Giacoppo, Juliane Mayer, Julien Hartmann, Ada L. Bachmann, and Peter P. Pott. Actively shielded capacitive proximity sensor for endoscopy. *Current Directions in Biomedical Engineering*, 9:93–96, 9 2023. doi:10.1515/cdbme-2023-1024.

[59] Vasile Bințințan, Adrian Calborean, Mihaela Mocan, Sergiu Macavei, Adrian Cordoș, Catalin Ciuce, Adriana Bințințan, Romeo Chira, Georgiana Nagy, Valeriu Surlin, Dan Timofte, Felix Nickel, Beat Mueller, George Dindelegan, Constantin Ciuce, Stelian Brad, Mircea Murar, and Bogdan Mocan. New inductive proximity sensor platform for precise localization of small colorectal tumors. *Materials Science and Engineering C*, 106, 1 2020. DOI: 10.1016/j.msec.2019.110146. doi:10.1016/j.msec.2019.110146.

[60] Adrian Calborean, Sergiu Macavei, Mihaela Mocan, Catalin Ciuce, Adriana Bintintan, Adrian Cordos, Cosmin Pestean, Romeo Chira, Liviu Zarbo, Lucian Barbu-Tudoran, George Dindelegan, Felix Nickel, Bogdan Mocan, Valeriu Surlin, and Vasile Bintintan. Non-invasive laparoscopic detection of small tumors of the digestive tract using inductive sensors of proximity. *Scientific Reports*, 12, 12 2022. DOI: 10.1038/s41598-022-04822-x. doi:10.1038/s41598-022-04822-x.

[61] MaxBotix. Distance Measurement Sensors. https://maxbotix.com/blogs/blog/distance-measurement-sensors. Online; accessed 1 May 2023.

[62] Sergio Vilches, Çağlar Ataman, and Hans Zappe. Interferometric fiber-based real-time distance sensor for endoscopic applications. volume 10868, 2019. Cited by: 1. URL: https://www.scopus.com/inward/record.uri?eid=2-s2.0-85064389048&doi=10.1117%2f12.2507811&partnerID=40&md5=65b04cd549d49d9ced27ea5c85316ad0, doi:10.1117/12.2507811.

[63] Agnese Lucesoli, Luigino Criante, Bruno Farabollini, Floriano Bonifazi, Francesco Simoni, and Tullio Rozzi. Distance optical sensor for quantitative endoscopy. *Journal of Biomedical Optics*, 13:010504, 2008. DOI: 10.1117/1.2870138. doi:10.1117/1.2870138.

[64] Agnese Lucesoli, Luigino Criante, Francesco Simoni, Andrea Di Donato, Tullio Rozzi, Bruno Farabollini, and Floriano Bonifazi. Quantitative endoscopy by folci-based distance sensor. In *SENSORS, 2008 IEEE*, pages 870–873, 2008. DOI: 10.1109/ICSENS.2008.4716579. doi:10.1109/ICSENS.2008.4716579.

[65] Sergio Vilches, Hans Zappe, and Caglar Ataman. Multi-point fiber-optic distance sensor for endoscopic surgery monitoring. *IEEE Photonics Technology Letters*, 35:883–886, 8 2023. doi:10.1109/LPT.2023.3270628.

[66] K Höller, J Penne, A Schneider, J Jahn, J Guttierrez, T Wittenberg, H Feußner, and J Hornegger. Endoscopic orientation correction, 2009. URL: https://link.springer.com/chapter/10.1007/978-3-642-04268-3_57.

[67] Hyung Chul Lee, Chul Woo Jung, and Hee Chan Kim. Real-time endoscopic image orientation correction system using an accelerometer and gyrosensor. *PLoS ONE*, 12, 11 2017. doi:10.1371/journal.pone.0186691.

[68] Seyed Shahim Vedaei and Khan A. Wahid. A localization method for wireless capsule endoscopy using side wall cameras and imu sensor. *Scientific Reports*, 11, 12 2021. doi:10.1038/s41598-021-90523-w.

[69] Chen Cheng, Yue Wu, Xinru Li, Zijian An, Yanli Lu, Fenni Zhang, Bin Su, and Qingjun Liu. A wireless, ingestible ph sensing capsule system based on iridium oxide for monitoring gastrointestinal health. *Sensors and Actuators B: Chemical*, 349, 12 2021. doi:10.1016/j.snb.2021.130781.

[70] Jay Roh, Ji-Hyoung Roh, Kyu-Sik Shin, Nam-Kyu Cho, Don-Haeng Lee, Byung-Moo Moon, and Dae-Sung Lee. A small ph sensor catheter of the endoscope to be used for the acidity test of gullet and stomach, 2008. DOI: 10.18494/SAM.2009.571. doi:10.18494/SAM.2009.571.

[71] C. Mc Caffrey, K. Twomey, and V. I. Ogurtsov. Development of a wireless swallowable capsule with potentiostatic electrochemical sensor for gastrointestinal track investigation. *Sensors and Actuators, B: Chemical*, 218:8–15, 5 2015. doi:10.1016/j.snb.2015.04.063.

[72] Qi Shao, Hao Liu, Hongyi Li, and Yunsheng Yang. Miniature ph sensor for capsule endoscopy with composite diagnosis. In *SENSORS, 2014 IEEE*, pages 339–342, 2014. doi:10.1109/ICSENS.2014.6985003.

[73] Yizhi Liang, Wubing Fu, Qiang Li, Xiaolong Chen, Huojiao Sun, Lidai Wang, Long Jin, Wei Huang, and Bai Ou Guan. Optical-resolution functional gastrointestinal photoacoustic endoscopy based on optical heterodyne detection of ultrasound. *Nature Communications*, 13, 12 2022. doi:10.1038/s41467-022-35259-5.

[74] Takafumi Fujimoto, Syunsuke Yonemitsu, Manaki Sasano, Toshiyuki Tanaka, and Chai Eu Guan. Antenna sensor for radio-wave-type endoscope in real scale mode. volume 2022-December. Institute of Electrical and Electronics Engineers, 2022. doi:10.1109/CAMA56352.2022.10002435.

[75] Kirill V. Zaichenko and Boris S. Gurevich. Hybrid endoscopes applications for internal organs oncology diagnostics. In *2020 Ural Symposium on Biomedical Engineering, Radioelectronics and Information Technology (USBEREIT)*, pages 0066–0068, 2020. doi:10.1109/USBEREIT48449.2020.9117750.

[76] Rui Li, Gongping Chen, Yu Dai, Yu zhao, Guangming Xia, Jianxun Zhang, Liang Cui, and Xiaotao Yin. Object dimension measurement based on monocular endoscope and 5-dof sensor. *Measurement: Journal of the International Measurement Confederation*, 206, 1 2023. doi:10.1016/j.measurement.2022.112293.

[77] Dumitru Scutelnic, Giacomo Marchioro, Salvatore Siracusano, Paolo Fiorini, Riccardo Muradore, and Claudia Daffara. Thermal endoscope based on cost-effective lwir camera cores. *HardwareX*, 11, 4 2022. doi:10.1016/j.ohx.2022.e00300.

[78] Texas Intruments. TMP102 Low-Power Digital Temperature Sensor With SMBus and Two-Wire Serial Interface in SOT563. https://www.ti.com/lit/ds/symlink/tmp102.pdf?ts=1702999202024&ref_url=https%253A%252F%252Fwww.google.com%252F. Online; accessed 20 december 2023.

[79] Microchip. MCP9808. https://ww1.microchip.com/downloads/en/DeviceDoc/25095A.pdf. Online; accessed 20 december 2023.

[80] Silicon Labs. I2C HUMIDITY AND TEMPERATURE SENSOR. https://www.silabs.com/documents/public/data-sheets/Si7021-A20.pdf. Online; accessed 20 december 2023.

[81] Honeywell. Honeywell HumidIcon™ Digital Humidity/Temperature Sensors: HIH6130/6131 Series. https://prod-edam.honeywell.com/content/dam/honeywell-edam/sps/siot/en-ca/products/sensors/humidity-with-temperature-sensors/honeywell-humidicon-hih6100-series/documents/sps-siot-hih6130-6131-install-50061154-3-en-ciid-142166.pdf. Online; accessed 20 december 2023.

[82] Bosch. Humidity sensor BME280. https://www.bosch-sensortec.com/products/environmental-sensors/humidity-sensors-bme280/. Online; accessed 20 december 2023.

[83] Bosch. Pressure sensor BMP280. https://www.bosch-sensortec.com/products/environmental-sensors/pressure-sensors/bmp280/. Online; accessed 20 december 2023.

[84] TE Connectivity. Barometric Pressure Sensor, with stainless steel cap. https://www.analog.com/media/en/technical-documentation/data-sheets/adxl345.pdf. Online; accessed 20 december 2023.

[85] Analog Devices. ADXL345. https://www.te.com/commerce/DocumentDelivery/DDEController?Action=showdoc&DocId=Data+Sheet%7FMS5611-01BA03%7FB3%7Fpdf%7FEnglish%7FENG_DS_MS5611-01BA03_B3.pdf%7FCAT-BLPS0036. Online; accessed 20 december 2023.

[86] STMicroelectronics. MEMS digital output motion sensor: ultra-low-power high-performance 3-axis "nano" accelerometer. https://www.st.com/resource/en/datasheet/lis3dh.pdf. Online; accessed 20 december 2023.

[87] Vishay. Fully Integrated Proximity and Ambient Light Sensor With Infrared Emitter, I2C Interface, and Interrupt Function. https://www.vishay.com/docs/83462/vcnl4010.pdf. Online; accessed 20 december 2023.

[88] Texas Instruments. LDC1612, LDC1614 Multi-Channel 28-Bit Inductance to Digital Converter (LDC) for Inductive Sensing. https://www.ti.com/lit/ds/symlink/ldc1614.pdf?ts=1703083201403&ref_url=https%253A%252F%252Fwww.google.com%252F. Online; accessed 20 december 2023.

[89] TDK InvenSense. Nine-Axis (Gyro + Accelerometer + Compass) MEMS MotionTracking™ Device. https://invensense.tdk.com/products/motion-tracking/9-axis/mpu-9250/. Online; accessed 20 december 2023.

[90] Rohm Semiconductor. Digital 16bit Serial Output Type Ambient Light Sensor IC. https://www.mouser.com/datasheet/2/348/bh1750fvi-e-186247.pdf. Online; accessed 20 december 2023.

[91] Microchip. ATmega48A/PA/88A/PA/168A/PA/328/P. https://ww1.microchip.com/downloads/en/DeviceDoc/ATmega48A-PA-88A-PA-168A-PA-328-P-DS-DS40002061A.pdf. Online; accessed 29 december 2023.

[92] Microchip. 28/40/44-Pin Enhanced Flash Microcontrollers. https://pt.mouser.com/datasheet/2/268/39582C-278080.pdf. Online; accessed 29 december 2023.

[93] RP2040 Datasheet. A microcontroller by Raspberry Pi. https://datasheets.raspberrypi.com/rp2040/rp2040-product-brief.pdf?_gl=1*lpfot5*_ga*MTAzMzg4NTcyNC4xNzA0ODgzMjUy*_ga_22FD70LWDS*MTcwNDg4MzI1Mi4xLjEuMTcwNDg4Mzg1OS4wLjAuMA.. Online; accessed 10 january 2024.

[94] ESP32 PICO Series. Datasheet. https://www.espressif.com/sites/default/files/documentation/esp32-pico_series_datasheet_en.pdf. Online; accessed 10 january 2024.

[95] Atmel. Atmel 8-bit AVR Microcontroller with 2/4/8K Bytes In-System Programmable Flash. https://pt.mouser.com/datasheet/2/268/Atmel_2586_AVR_8_bit_Microcontroller_ATtiny25_ATti-1315542.pdf. Online; accessed 29 december 2023.

[96] Texas Instruments. MSP430F261x, MSP430F241x Mixed-Signal Microcontrollers. https://www.ti.com/lit/ds/symlink/msp430f2618.pdf?HQS=dis-mous-null-mousermode-dsf-pf-null-wwe&ts=1703881915627&ref_url=https%253A%252F%252Fpt.mouser.com%252F. Online; accessed 29 december 2023.

[97] STMicroelectronics. STM32C031K4. https://www.st.com/en/microcontrollers-microprocessors/stm32c031k4.html. Online; accessed 29 december 2023.

[98] STMicroelectronics. CC2340R5 SimpleLinkTM Bluetooth ® 5.3 Low Energy Wireless MCU. https://www.ti.com/lit/ds/symlink/cc2340r5.pdf?ts=1703882236247&ref_url=https%253A%252F%252Fwww.ti.com%252Fproduct%252FCC2340R5. Online; accessed 29 december 2023.

[99] NXP Semiconductors. MKL13Z32VLH4. https://www.nxp.com/docs/en/data-sheet/KL13P80M48SF3.pdf. Online; accessed 30 december 2023.

[100] NXP Semiconductors. MKL14Z32VFM4. https://www.nxp.com/docs/en/data-sheet/KL14P80M48SF0.pdf. Online; accessed 30 december 2023.

[101] M. R. Cohn, A. Unnanuntana, T. J. Pannu, S. J. Warner, and J. M. Lane. *7.16 Materials in fracture fixation*, pages 278–297. Elsevier, 1 2017. DOI: 10.1016/B978-0-12-803581-8.10109-2. doi:10.1016/B978-0-12-803581-8.10109-2.

[102] Adrian Goldis, Ramona Goldis, and Traian V. Chirila. Biomaterials in gastroenterology: A critical overview, 11 2019. DOI: 10.3390/medicina55110734. doi:10.3390/medicina55110734.

[103] About Python. Datasheet. https://www.python.org. Online; accessed 28 may 2024.

[104] Guido Van Rossum and Fred L. Drake. *Python 3 Reference Manual*. CreateSpace, Scotts Valley, CA, 2009.

[105] Hanife Rexhepi. *IMPROVING HEALTHCARE INFORMATION SYSTEMS - A KEY TO EVIDENCE BASED MEDICINE*. PhD thesis, 06 2015.

[106] MicroPython. MicroPython. https://micropython.org. Online; accessed 28 may 2024.

[107] Olympus. Manual do SiSteMa de endoScopia. https://www.olympus-oste.eu/media/contact_and_support/download/system_guides/W7052_805.pdf. Online; accessed 4 june 2024.

[108] Motion basics. How to define roll, pitch, and yaw for linear systems. https://www.linearmotiontips.com/motion-basics-how-to-define-roll-pitch-and-yaw-for-linear-systems/. Online; accessed 21 june 2024.